Role of arylhydrocarbon receptor signalling in reactive gliosis

Marianne Reiser

München, 2019

Aus dem Institut für Stammzellforschung
Helmholtz Zentrum München
und
Aus dem Physiologischen Institut, Lehrstuhl: Physiologische Genomik
der Ludwig-Maximilians-Universität München

Direktorin: Prof. Dr. Magdalena Götz

Role of arylhydrocarbon receptor signalling in reactive gliosis

Dissertation
zum Erwerb des Doktorgrades der Medizin
an der Medizinischen Fakultät
der Ludwig-Maximilians-Universität zu München

vorgelegt von
Marianne Reiser

aus Garmisch-Partenkirchen

2019

Mit Genehmigung der Medizinischen Fakultät
der Universität München

Berichterstatterin:	Prof. Dr. Magdalena Götz
Mitberichterstatter:	Prof. Dr. Antje Grosche Prof. Dr. Martin Kerschensteiner
Mitbetreuung durch den promovierten Mitarbeiter:	Prof. Dr. Jovica Ninkovic
Dekan:	Prof. Dr. med. dent. Reinhard Hickel
Tag der mündlichen Prüfung:	21.11.2019

Table of Content

Abbreviations

AhR	Aryl hydrocarbon receptor
ARNT	Aryl hydrocarbon receptor nuclear translocator
ATP	Adenosine triphosphate
BBB	Blood-Brain-Barrier
BDNF	Brain-derived neurotrophic factor
bHLH	Basic helix-loop-helix
BrdU	Bromdesoxyuridin
cDNA	Complementary deoxyribonucleic acid
CNS	Central nervous system
COX	Cyclooxygenase
CYP	Cytochrome
DAMP	Damage-associated molecular pattern
DAPI	4', 6-Diamidin-2-phenylindol
DCX	Doublecortin
DNA	Deoxyribonucleic acid
dpi	Days post injury
EAE	Experimental autoimmune encephalomyelitis
EGF	Epidermal growth factor
EGFR	Epidermal growth factor receptor
FGF	Fibroblast growth factor
g	Gram
GFAP	Glial fibrillary acidic protein
GLAST	Glutamate aspartate transporter
GLT	Glutamate transporter
GO	Gene Ontology
h	Hour
HAH	Halogenated aromatic hydrocarbons
HBSS	Hank's Balanced Salt Solution
HMGB	High mobility group box
HSP	Heat shock protein
i.p.	Intraperitoneal
Iba1	Ionized calcium-binding adapter molecule 1
Ig	Immunoglobulin
IGF	Insulin-like growth factor
IL	Interleukin
INF	Interferon
kg	Kilogram
KIR	K+ inward rectifier
l	Litre
LPS	Lipopolysaccharide
mg	Milligram
ml	Millilitre
mm	Millimetre
MMP	Matrix metalloproteinase
mol	Mol

NES	Nuclear export signal
NF-κB	Nuclear factor kappa-light-chain-enhancer of activated B cells
NG2	Neural/Glial antigen 2
NGS	Normal goat serum
NLS	Nuclear localization signal
nmol	Nanomol
Olig2	Oligodendrocyte transcription factor 2
PAH	Polycyclic aromatic hydrocarbons
PBS	Phosphate buffered saline
PDL	Poly-D-lysine
PFA	Paraformaldehyde
PLP13	Receptor like protein 13
pmol	Picomol
PORN	Poly-L-Ornithine
qPCR	Quantitative polymerase chain reaction
RMS	Rostral migratory stream
RNA	Ribonucleic acid
RT-PCR	Real time detection polymerase chain reaction
S.E.M.	Standard error of the mean
sec	Second
SEZ	Subependymal zone
SOX2	Sex determining region Y-box 2
SW	Stab wound
TBI	Traumatic brain injury
TCDD	2,3,7,8-Tetrachlorodibenzodioxin
TFA	Trifluoroacetic acid
TLR	Toll-like receptor
TN-C	Tenascin C
TNF	Tumor necrosis factor
Treg	Regulatory T-cell
WHO	World health organization
XRE	Xenobiotic responsive element
µg	Microgram
µl	Microliter
µm	Micrometre

Abstract

Many common neurological disorders like traumatic brain injury (TBI) or stroke cause a loss of functional neurons and trigger a comprehensive response of glial cells, called reactive gliosis. Since reactive gliosis produces a persisting glial scar and since neurogenesis in the adult mammalian brain is insufficient to replace lost neurons, these conditions often compromise cerebral functions and lead to permanent disability with enormous socioeconomic burdens.

In the adult zebrafish brain, however, ventricular ependymoglia responds to brain injuries with increased generation of new neurons, which are recruited to the injury site. A key mechanism regulating differentiation and proliferation of neuronal precursors in zebrafish is the aryl hydrocarbon receptor (AhR) pathway. In other organs like the hematopoietic system, AhR is well known to control essential biological functions including stress response and maintenance, proliferation and differentiation of stem cells.

As reactive astrocytes, one of the main actors in reactive gliosis, show features of neural stem cells, the aim of my thesis was to examine whether AhR signalling plays a role in reactive gliosis as well and to what capacity AhR activation affects the response to TBIs in the mammalian brain. To address this question, I looked at AhR expression in the intact and the injured mouse brain and analysed the effects of AhR activation in the injured cerebral cortex at cellular and molecular levels. For this, I used bromodeoxyuridine (BrdU) incorporation to examine proliferation of different glial cells in vivo, proteome analysis and the neurosphere assay, an in vitro tool to assesses the key features of neural stem cells: proliferation, self-renewal, and multipotency.

In the intact brain, AhR was only detectable in the dentate gyrus of the hippocampus, which is known for its high neurogenic activity. Following brain injuries, however, AhR was also expressed in reactive astrocytes around the injury site and AhR activation significantly altered proliferation of reactive astrocytes in vivo. Oral application of an AhR agonist additionally enhanced stem cell properties of reactive astrocytes in vitro. It increased sphere formation of cells isolated from the injured cerebral cortex without limiting their self-renewing capacity or neurogenic potential. In brain regions where AhR is not expressed, treatment with an AhR agonist did not increase sphere formation. Proteome analysis confirmed the effects observed in vivo and in vitro and gave

important hints about the mechanisms by which AhR signalling might induce changes in proliferation and in the potential of reactive astrocytes.

These findings suggest AhR signalling as modulating factor in reactive gliosis and as key player in the mediation of stem cell properties in reactive astrocytes. It provides an interesting target for the reactivation of neurogenesis after brain damage and should therefore be subject of further research in order to aid the development of novel therapeutic strategies for all neurological conditions associated with a loss of functional neurons.

Zusammenfassung

Zahlreiche neurologische Erkrankungen, beispielsweise Schädel-Hirn-Traumata und Schlaganfälle, gehen mit dem Verlust von Neuronen einher und bewirken eine umfassende Reaktion glialer Zellen. Diese „reaktive Gliose“ führt bei Säugetieren zur Ausbildung einer permanenten Glianarbe. Aus diesem Grund und da untergegangene Nervenzellen im adulten Gehirn nicht durch die auf wenige Stammzellnischen begrenzte Neurogenese ersetzt werden können, gehen diese Erkrankungen beim Menschen häufig mit einer dauerhaften Behinderung sowie weitreichenden sozioökonomischen Belastungen einher.

Beim Zebrafisch hingegen bewirkt eine Verletzung des Gehirns, anders als bei Säugetieren, die vermehrte Bildung neuer Neurone durch ventrikuläre Ependymzellen im Telencephalon, welche an den Ort der Verletzung rekrutiert werden. Ein Schlüsselmechanismus bei der Regulation von Differenzierung und Proliferation der neuronalen Vorläuferzellen im Zebrafisch ist der Aryl-Hydrocarbon-Rezeptor(AhR)-Signalweg. In anderen Organsystemen wie dem hämatopoetischen System kontrolliert der AhR-Signalweg ebenfalls essentielle biologische Funktionen einschließlich der Erhaltung, Proliferation und Differenzierung von Stammzellen.

Auch reaktive Astrozyten, wichtige Mediatoren der reaktiven Gliose, weisen einige Merkmale neuronaler Stammzellen auf. Diese Arbeit widmet sich daher der Frage, ob der AhR-Signalweg auch in der reaktiven Gliose eine Rolle spielt und inwiefern die Aktivierung des AhR im Mausmodell die Reaktion auf Verletzungen des zerebralen Kortex beeinflusst. Hierzu untersuchte ich zunächst immunhistochemisch das Expressionsmuster des AhR im intakten und im verletzten Gehirn der Maus und analysierte die Effekte der AhR-Aktivierung im verletzten Großhirnkortex auf zellulärer und molekularer Ebene. Die systemische Gabe von Bromodeoxyuridin (BrdU), welches sich in neu synthetisierte DNA einlagert, erlaubte dabei die Bestimmung der Proliferationsraten einzelner Gliazellen in vivo und mit dem Neurosphären-Assay konnten die wichtigsten Stammzelleigenschaften in vitro erhoben werden: Proliferation, Selbsterneuerung und Multipotenz. Ergänzend wurde eine Proteomanalyse durchgeführt.

Im intakten Gehirn konnte der AhR lediglich im Gyrus dentatus des Hippocampus, einer Region mit bekannt hoher neurogener Aktivität, nachgewiesen werden. Nach Verletzung des Kortex exprimieren jedoch auch benachbarte Astrozyten den AhR und die

Aktivierung des AhR änderte die Proliferationsrate reaktiver Astrozyten in vivo signifikant. Zudem förderte die orale Gabe eines AhR-Agonisten die Ausbildung von Stammzelleigenschaften reaktiver Astrozyten in vitro: Zellen, die aus der verletzten Kortexregion isoliert wurden, bildeten vermehrt Neurosphären ohne Einbußen ihres neurogenen Potentials und der Fähigkeit zur Selbsterneuerung. In Gehirnregionen ohne AhR-Expression änderte sich die Anzahl der Neurosphären nach Gabe eines AhR-Agonisten hingegen nicht. Proteomanalysen unterstützten die Beobachtungen in vivo und lieferten wichtige Hinweise zu den Mechanismen, mit denen der AhR-Signalweg Änderungen der Proliferation und des Stammzellpotentials reaktiver Astrozyten induziert.

Die im Rahmen dieser Arbeit erhobenen Daten legen den AhR-Signalweg als modulierenden Faktor der reaktiven Gliose und möglichen Schlüsselmechanismus in der Vermittlung von Stammzelleigenschaften reaktiver Astrozyten nahe. Dies macht den AhR zu einem vielversprechenden Ansatzpunkt bei der Suche nach neuen therapeutischen Strategien für alle neurologischen Erkrankungen, die mit einem Verlust von Neuronen assoziiert sind. Deshalb sollte der AhR auch zukünftig Gegenstand der Forschung auf diesem Gebiet sein.

1 Introduction

1.1 Relevance of traumatic brain injuries

According to the World Health Organization (WHO), traumatic brain injuries (TBI) are one of the major causes of death and permanent disability worldwide. TBI account for more years of disability than any other disease since children and young adults are especially exposed to risk factors for TBI, i.e. motor vehicle traffic, sports, construction and violence (Faul, Xu, Wald, & Coronado, 2010). For Europe, an annual incidence of 235 cases per 100,000 inhabitants is estimated (WorldHealthOrganization, 2006).

TBI do not only affect patients, but also society as a whole. In Europe alone, TBIs cause enormous socioeconomic costs of approximately 33 billion Euros per year. Direct and especially indirect health costs due to loss of productivity are a huge burden for every economy, above all in developing countries, where TBIs are much more frequent than in Europe.

The WHO and national governments countered the social and economic relevance of TBIs with prevention measures. By means of seat belts, child safety seats, speed limits and stricter occupational safety regulations, the incidence of TBIs declines in industrialized countries. Due to medical advances, the lethality of TBI also dropped for about three-quarters from the 1970s to the beginning of the 21st century. But at the same time, the number of people living with disabilities resulting from TBI increased concomitantly. Treatment of TBI is still restricted to maintenance of vital functions, avoidance of secondary brain damage and compensation of resulting disabilities. Current guidelines focus on measures to ensure sufficient oxygen supply to the brain and to avoid a critical increase in intracranial pressure (Firsching et al., 2015). These therapies merely limit consequential damage due to hypoxia or elevated intracranial pressure, but none of them are capable of reversing neuronal damage and the complications thereof.

In contrast to humans and other mammals, whose brains and spinal cords do not regenerate, other species like zebrafish have remarkable regenerative capacities. Neurogenesis in the ventricular zone of the zebrafish telencephalon increases in response to brain injuries and provides new neurons that are recruited to the parenchyma and replace the lost ones. Therefore, the adult zebrafish telencephalon might provide a useful model for understanding the mechanisms required for neuronal regeneration, which is the basis for the development of causal therapies for TBI and

other disease conditions that are associated with a loss of functional neurons like stroke and neurodegenerative diseases.

1.2 Response to traumatic brain injuries

Traumatic brain injuries (TBIs) always lead to a loss of functional brain parenchyma due to primary and/or secondary brain damage. Primary brain damage results from direct mechanical forces that take effect right at the moment of injury and is therefore inaccessible to medical therapies. Secondary brain damage, however, is the focus of acute medical care. It evolves gradually over the first hours to days after injury and results from an entire array of changes in the central nervous system (CNS) homeostasis. Complications such as ischemia, hypoxia, cerebral oedema, inflammation, leakage of the blood-brain barrier (BBB) and excitotoxicity of neurotransmitters further damage vital brain tissue and thereby determine the extent of secondary brain damage.

Apart from the initial trauma severity, the extent of the secondary brain damage also depends critically on how effective wound healing is able to restore CNS integrity and homeostasis. The process of wound healing can be divided into three distinct phases: Cell death and inflammation, cell replacement and tissue remodelling (Burda & Sofroniew, 2014) **(Figure 1.1).**

The first, acute phase is dominated by cell death and the initiation of an inflammatory response. Following cerebral trauma, the blood-brain-barrier (BBB) breaks down and plasma proteins, electrolytes, platelets and immune cells, which are normally excluded from the central nervous system, penetrate the brain parenchyma and disrupt the chemical and ionic environment (Obermeier, Daneman, & Ransohoff, 2013). At the same time, the release of danger associated molecular patterns (DAMPs) by damaged glial cells and neurons evokes an inflammatory reaction at the site of injury. This inflammation reinforces the invasion of immune cells by expressing leucocyte adhesion molecules (Icam1, Vcam1, E- and P-selectines) on endothelial cells (Daneman, 2012). It also initiates phagocytic clearance of cell debris by microglia and macrophages and reactivates glial cells (Zhang et al., 2010).

The reactivation of glial cells and other local cells like pericytes and endothelial progenitors introduces the phase of tissue replacement, which is crucial to restore the BBB and to limit the spread of damage. Microglia and NG2-glia respond early to brain insults, migrate towards the injury site and increase proliferation (Simon, Gotz, & Dimou, 2011; Stence, Waite, & Dailey, 2001). Astrocytes on the contrary do not migrate

and proliferation is delayed (Bardehle et al., 2013). The proliferation of glial cells, above all astrocytes, creates a boarder that protects surrounding functional neural tissue from inflammatory and cytotoxic factors in the immediate lesion core and the proliferation of endothelial progenitors, fibroblasts and pericytes helps to replace damaged blood vessels.

About 7 days after injury, in the phase of tissue remodelling, the formerly beneficial astrocytic boarder transforms into a persisting astrocytic scar, which is regarded to be the main inhibitor of axonal regeneration in the CNS. This transformation illustrates, that the beneficial effects of reactive gliosis in the fist days after injury impede functional recovery afterwards (Reviewed in (Pekny & Pekna, 2016). For this reason, finding ways to specifically block the detrimental effects of scar formation without diminishing the beneficial effects is one of the major challenges of current research in this field.

Figure 1.1

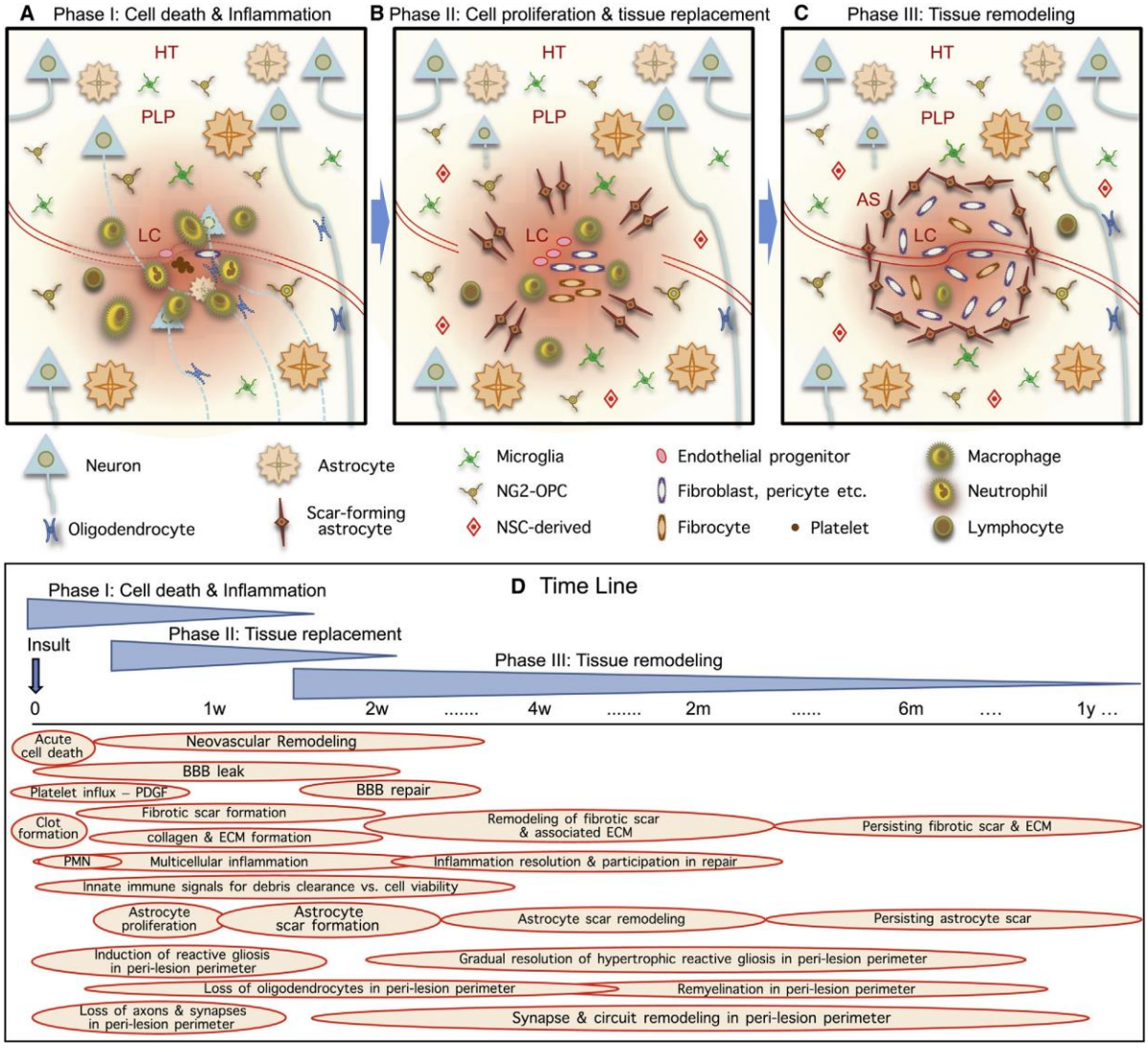

Figure 1.1 Phases and Time Course of Multicellular Responses to Acute Focal CNS Damage
During periods of cell death (A), cell replacement (B), and tissue remodelling (C), numerous overlapping events occur (D) that involve interactions among CNS intrinsic neural cells, CNS intrinsic non-neuronal cells, and cells infiltrating from the circulation. Based on Burda and Sofroniew (2014)

1.3 Glial cells and their role in reactive gliosis

1.3.1 NG2 glia

NG2 glia came into focus for neuroscientists, since they are the only CNS intrinsic cells that proliferate outside the neurogenic niches (Dimou, Simon, Kirchhoff, Takebayashi, & Gotz, 2008) and possess the remarkable ability to self renew throughout a lifetime (Hughes, Kang, Fukaya, & Bergles, 2013). NG2 glia gives rise to cells of the oligodendrocytic lineage, but also to a low number of astrocytes during development (Zhu, Bergles, & Nishiyama, 2008; Zhu et al., 2011) and researchers have even described an in-vitro fate switch into neurons (Kondo & Raff, 2000). Due to these hints of multipotency, the long cell cycle length and their self-renewal capacity, stem cell-like properties of NG2 glia have been discussed (Richardson, Young, Tripathi, & McKenzie, 2011).

In the healthy cortical gray matter of three months old mice, 80% of all NG2 glia proliferate with a long cell cycle length of approximately 37 days (Simon et al., 2011). After injury, however, their proliferation rate bursts, they become hypertrophic, upregulate NG2, polarize and migrate towards the lesion site (Simon et al., 2011; Tan, Zhang, & Levine, 2005). This behaviour strongly implies a role of NG2 glia in wound healing and scar formation after traumatic brain injuries, although their impact is not yet fully understood. In NG2-knockout mice, traumatic brain injuries lead to enhanced numbers and a fulminant reaction of activated Iba-1+/CD45+ microglia/macrophages and infiltrating CD45+ leukocytes as well as increased neurotoxicity and a worse neurological outcome (Huang et al., 2016). On the other hand, NG2 glia have also proven to be inhibitory for axonal regrowth after CNS damage (reviewed in Tan et al. (2005)).

1.3.2 Microglia

The function of microglia is intensively studied. Microglia account for approximately 10% of all cells in the adult brain (Lawson, Perry, Dri, & Gordon, 1990) and with functions similar to peripheral macrophages, they are the major operators of active immune defence in the central nervous system. They monitor their environment with highly ramified and motile processes and phagocyte accumulated metabolites and tissue

debris (Nimmerjahn, Kirchhoff, & Helmchen, 2005). Under physiological conditions, the immunosuppressive environment of the CNS keeps microglia in this surveying state. This downregulation of immune response is, among other factors, mediated by microgial surface receptors for CD200 (OX2), which are expressed on neurons, and CXCCL1 (Fractalkine), released by neurons and astrocytes (Kettenmann, Hanisch, Noda, & Verkhratsky, 2011). Loss of these factors and all kinds of homeostatic disturbances shift the activity state of microglia from a resting to a reactive state. Potent activators of microglia, including cytokines, chemokines, DAMPs that were released from damaged cells, plasma proteins and proteins that are present in critical concentrations or in abnormal structures, are listed in **Table 1.1**.

Within minutes after injury, microglia transform into hypertrophic, mobile phagocytes with amoeboid morphology (Nimmerjahn et al., 2005), commence proliferation, polarize and migrate towards the injury site (Davalos et al., 2005). Depending on their polarization, they display either pro-inflammatory (referred to as M1-like microglia in analogy with nomenclature of macrophages) or immunosuppressive phenotypes (M2-like microglia) (Chhor et al., 2013; Hu et al., 2012; Kigerl et al., 2009). In the first week after injury, alternative M2-like activated microglia express immunoregulatory, anti-inflammatory and neuroprotective factors like brain-derived growth factor (BDNF) and insulin-like growth factor 1 (IGF1), which support repair and regeneration after injury. In addition, they promote angiogenesis, matrix remodelling and suppress the release of pro-inflammatory cytokines, nitric oxide and other mediators of detrimental immune responses (Franco & Fernandez-Suarez, 2015). However, the neuroprotective M2 response is transient and within one week after injury, the polarization pattern shifts towards a predominantly M1-like phenotype (Hu et al., 2012; Kigerl et al., 2009). The M1-like phenotype is characterized by the release of oxidative metabolites, pro-inflammatory cytokines (IL-1, IL-6, and TNF-α) and increased phagocytic activity (Gao et al., 2013). This is essential for host defence but prolonged M1 activity after TBI provokes neuroinflammation and cell death, which in turn exacerbates progressive tissue damage and loss of functional brain areas (A. Kumar & Loane, 2012).

Table 1.1

Class of compound	Examples
Viral, bacterial or fungal surface structures, DNA/RNA	Agonists of members of the pattern recognition receptor families, (TLR1/2, TLR3, TLR4,TLR6/2 and TLR9), bacterial LPS or cell wall proteoglycans and lipoteichoic acid (LTA), gp41, gp120
Abnormal endogenous proteins	β-amyloid (aggregates), prion protein (PrP)
Complement	Complement factors C1q, C5a
Antibodies	Immunoglobulin (IgA, IgG, IgM), presented in immune complexes
Cytokines	Colony stimulating factors (M-CSF, GM-CSF), IL-1β, IL-2, IL-4, IL-6, IL-10, IL-12, IL-15, IL-18, IFN-γ, TGF-β, TNF-α
Chemokines	Ligands for chemokine receptors: CCR3, CCR5, CXCR2, CXCR, CXCR4, CX3CR1, IL-8R
Neurotrophic factors	Brain-derived neurotrophic factor (BDNF), glial-derived neurotrophic factor (GDNF), nerve growth factor (NGF), neurotrophin 3 (NT-3), NT-4
Plasma components	Albumin, fibronectin, fibrinogen, thrombin
Other proteins and peptides	Apolipoprotein E (ApoE), heat shock proteins hsp60 and hsp70, CD40L, melanocyte-stimulating hormone (MSH), endothelin, S100 proteins, vasoactive intestinal peptide (VIP)
Neurotransmission-related compounds	ATP (and related purines), β-adrenergic agonists, glutamate, kainate, NMDA
Ions	K^+, Mn^{2+}
Other compounds	Cannabinoids, ceramide, gangliosides, lysophosphatidic acid (LPA), melatonin, opioids (endomorphines), platelet-activating factor (PAF), prostaglandin E_2 (PGE_2), steroid hormones, vitamin D_3

Table 1.1 Examples of signals and modulators of microglial activation. (Hanisch & Kettenmann, 2007)

1.3.3 Astrocytes

Astrocytes, the most abundant cell type in the mammalian brain, are a heterogeneous population of cells. For a long time, it has been assumed, that astrocytes are limited to their supportive function. However, studies of the last few decades have found them to play a much more active role. Astrocytes perform a remarkably wide range of functions. They control extracellular ion homeostasis, contribute to the formation of the BBB, regulate the local CNS blood flow and promote myelination by mature oligodendrocytes. They also store glycogen to break it down to lactate, which can then be transferred to adjacent neurons or axons during times of hypoglycaemia or intense neuronal activity (Brown & Ransom, 2007; Gordon, Mulligan, & MacVicar, 2007; Olsen et al., 2015; Rose & Verkhratsky, 2016). Furthermore, they remove surplus neurotransmitters, modulate formation, maturation, maintenance, and stability of synapses, and influence synaptic

transmission by regulated release of synaptically active molecules (Perea, Navarrete, & Araque, 2009).

The reaction of astrocytes to injury and disease, referred to as reactive astrogliosis, is an important issue in basic and clinical neuroscience. Astrocytes are key players in the multicellular response to TBIs and several mechanisms are known to regulate their reactivation. The extent of their reaction is highly heterogeneous but correlates with the severity of tissue damage. Disruption of the BBB leads to an influx of cells and molecules, which are normally excluded from the CNS. Plasma proteins like thrombin (Nishino et al., 1993; Shirakawa et al., 2010) fibrinogen (Ryu, Davalos, & Akassoglou, 2009), endothelin (Gadea, Schinelli, & Gallo, 2008), SHH (Sirko et al., 2013) and many others have been shown to modulate the response of astrocytes. Mechanical stress upon tissue damage activates mechanosensitive ion channels, which leads to a rapid influx of Ca^{2+} and subsequently to a calcium-induced release of ATP via astrocyte connexin hemi-channels. The resulting ATP gradient recruits microglia and other cells of the innate immune system to the site of injury (Burda, Bernstein, & Sofroniew, 2015). Danger-associated molecular patterns (DAMPs) like K^{+}, heatshock proteins, HMGB1 and mitochondrial DNA, which are released by injured and dying cells, initiate NFkB-signalling in adjacent astrocytes and induce the release of pro-inflammatory cytokines like tumor necrosis factor α (TNFα), α-chemokines and the inflammatory mediators cyclooxygenase 2 (COX2) and matrix metalloproteinase 9 (MMP-9). This, too, helps astrocytes to recruit microglia and other cells involved in reactive gliosis (Burda et al., 2015; Mathew et al., 2012). HMGB1 for example stimulates endothelial cells and their progenitors to repair the BBB after brain injury. In an immediate response after TBI, astrocytes change their gene expression to increase phagocytosis of cellular debris and to restore the extracellular milieu. Morphological equivalents of the altered function are hypertrophy and the upregulation of intermediate filaments like the classical reactive astrocyte marker GFAP, Vimentin and Nestin (Zamanian et al., 2012).

These changes can be observed in the course of all homeostatic disturbances in the CNS. In the stab wound injury model, a model for acute, penetrating CNS injuries, this early and ubiquitous response is followed by polarization towards the injury and the upregulation of proliferation genes between 3 and 5 days post injury (dpi) (Zamanian et al., 2012). Thus, with a peak at 5 to 7 dpi (Bardehle et al., 2013; Buffo et al., 2008; Simon et al., 2011; Sirko et al., 2013), proliferation of astrocytes is delayed compared to proliferation of NG2 glia and microglia. Notably, the behaviour of individual astrocytes

upon TBI is quite heterogeneous, which supports the hypothesis of various astrocytic subtypes with distinct functions. In vivo imaging revealed that only about one half of all reactive astrocytes polarise. Even less, only about 15%, reenter the cell cycle in response to TBI and it has also been shown, that proliferation is limited to juxtavascular astrocytes (Bardehle et al., 2013). Unlike microglia and NG2 glia, astrocytes do not migrate towards the injury site. Therefore, solely newly generated astrocytes and protruding processes of polarized reactive astrocytes perform the most important function of astrocytes in acute brain injuries: The formation of a glia limitans to protect vital neuronal tissue from the neurotoxic inflammatory processes in the lesion core. The juxtavascular position of proliferating astrocytes strongly suggests a function in regulating and restoring the BBB.

Cells with an astrocytic identification also serve as neuronal stem cells during development and in the adult brain's neurogenic niches, i.e., the SEZ at the lateral wall of the lateral ventricle, which generates olfactory blub-neurons, and the subgranular zone of the hippocampus, which gives rise to new neurons for the granular cell layer of the dentate gyrus. Reactive parenchymal astrocytes and astrocytes that function as neuronal stem cells in these neurogenic niches share many common features **(Table 1.2).**

Table 1.2

Protein	Neuroepithelial cells	Radial glia early	Radial glia late	Adult neural stem cell	Mature astroglia	Reactive astroglia	Ependymal cell
GFAP	–	–/+	+/++	+++	–/++	+++	+
GLAST (Slc1a3)	–	++	++	++	+++	+++	++
GLT1 (Slc1a2)	–	–	+	++	+++	++	++
Glutamine synthetase	–	–	+	++	+++	+++	–
S100-β	–	–	+	+	++	+++	+++
Connexin 43 (Gja1)	–	–	++	+++	+++	+++	++
Aquaporin 4	Not defined	Not defined	Not defined	++	+++	+++	+
KIR 4.1/2.1	–	+	++	+++	+++	++	++
Aldlhl1	–	–	+	+	+++	+++	++
Nestin (RC1/RC2)	+++	+++	+++	+++	–	+++	++
Vimentin	–	+	++	+++	–	+++	+++
BLBP	++	+++	+++	+++	–	+++	–
TN-C	–	+++	+++	++	–	+++	–
Phosphacan/DSD-1	–	+++	+++	+++	–	++	–

Table 1.2 Similarities and Differences Between Glial Cell Types in Terms of Some Marker Gene Expressions. Adopted from Gotz, Sirko, Beckers, and Irmler (2015)

But despite these similarities, reactive astrocytes do not possess the ability of long-term self-renewal and in-vivo neuronal generation. If astrocytes divide after injury, they do it

only once and always stay within their lineage. In vitro, however, the formation of multipotent, self-renewing neurospheres demonstrated that parenchymal astrocytes indeed have the intrinsic capacity to produce neurons. But only one third of all neurospheres derived from reactive astrocytes generate neurons, whereas all neurospheres derived from SEZ-neuronal stem cells do so. Hence, the different potential in vivo can in part, but not exclusively, be explained by cell-intrinsic differences. Furthermore, adult neural precursor cells transplanted to the neocortex produce only glial cells (Herrera, Garcia-Verdugo, & Alvarez-Buylla, 1999; Seidenfaden, Desoeuvre, Bosio, Virard, & Cremer, 2006), whereas in their physiological localization, they continuously contribute new neurons to the olfactory bulb (Lois & Alvarez-Buylla, 1994; Luskin, 1993) or the granule cell layer of the dentate gyrus (Seri, Garcia-Verdugo, McEwen, & Alvarez-Buylla, 2001). This demonstrates that brain injuries can activate parts of the neurogenic capacity in a subset of astrocytes. But this potential cannot be used to replace lost neurons. For this reason, further research has to aim to identify signals that retain astrocytes within their lineage in vivo, in order to pave the way for innovative therapeutic approaches in the treatment of traumatic brain injuries and other conditions correlated with a loss of neurons.

1.4 Arylhydrocarbon receptor

AhR was first discovered in 1976 by Poland et al. as a specific binding site for the environmental toxin and carcinogen 2,3,7,8-Tetrachlorodibenzo-p-dioxine (TCDD) (Poland, Glover, & Kende, 1976). Since then, AhR had predominantly been studied as a mediator of toxic TCDD-effects and became a prototype for our current understanding of receptor-driven toxic responses. In the last few years, however, it became evident that AhR is far more than a mere mediator of toxic phenomena. The AhR gene is expressed in many different cell types and is highly conserved throughout species, which proves its fundamental role in biological systems (Hahn, Karchner, Shapiro, & Perera, 1997).

1.4.1 Protein structure

AhR structure is determined by two functional domains: The basic helix-loop-helix (bHLH) and the PER-ARNT-SIM (PAS) domain. The N-terminal bHLH domain, which is composed of two aliphatic α-helices and an adjacent region of basic amino acids, mediates DNA binding and protein dimerization, whereas the PAS domain serves as docking site for hetero- or homodimerization with other PAS proteins or the molecular chaperone heat-shock protein 90 (HSP90) (Fukunaga, Probst, Reisz-Porszasz, &

Hankinson, 1995). A glutamine-rich transactivation domain (TAD) at the C-terminal end of the AhR protein allows targeted gene activation by interacting with numerous transcriptional co-activators (M. B. Kumar & Perdew, 1999). Nuclear transport is regulated via an N-terminal nuclear localization signal (NLS) and a nuclear export signal (NES) within the PAS domain (Ikuta, Eguchi, Tachibana, Yoneda, & Kawajiri, 1998).

Figure 1.2

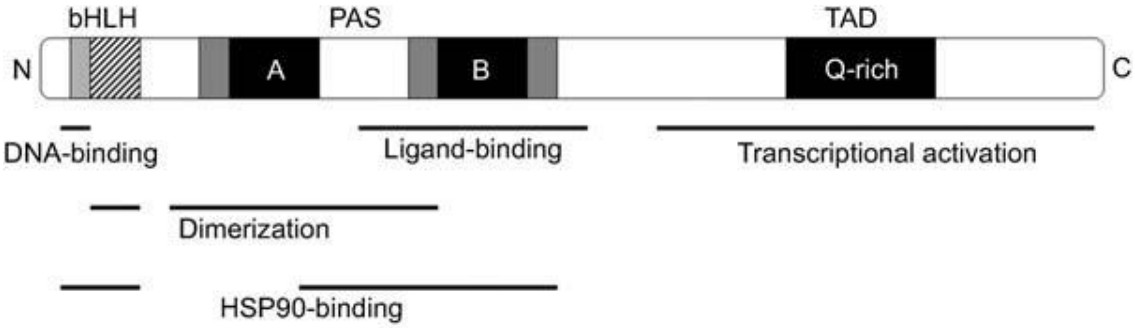

Figure 1.2 Protein structure of mouse AhR. From Abel and Haarmann-Stemmann, 2010 (Abel & Haarmann-Stemmann, 2010).

1.4.2 AhR ligands

AhR was initially discovered as a xenobiotic receptor and therefore, the search for ligands focussed mainly on polycyclic aromatic hydrocarbons (PAH) and planar halogenated aromatic hydrocarbons (HAH, most of all TCDD) with strong agonist activity. But since AhR-deficient mice showed developmental abnormalities and deficiencies in the immune system (Fernandez-Salguero et al., 1995; Mimura et al., 1997; Schmidt, Su, Reddy, Simon, & Bradfield, 1996), scientists started to look for natural AhR ligands. These natural ligands were found to be either exogenous ligands, introduced by nutrition (e.g. flavonoids and indoles), or endogenous ligands, mainly tryptophan metabolites (Murray, Patterson, & Perdew, 2014). These ligands show lower AhR affinity and elicit less toxic responses from the AhR pathway.

Lipids, cAMP or bilirubin can also activate AhR (Denison, Soshilov, He, DeGroot, & Zhao, 2011). Since structures of these natural agonists differ extremely from the classical HAH and PAH structures, the ligand-binding site of AhR must be highly promiscuous and might bind far more exogenous and endogenous molecules than we currently know. Different ligands have different binding affinities and metabolic degradation. PAHs and most natural ligands cause only a temporally limited AhR activation, whereas HAHs like

TCDD induce permanent AhR-dependent gene expression, which is responsible for AhR-dependent toxicity (Denison et al., 2011).

1.4.3 Regulation of AhR

1.4.3.1 Canonical pathway

AhR is a ligand-dependent transcription factor. In absence of a ligand, AhR is restrained in the cytoplasm by a chaperone complex, consisting of an Hsp90 dimer and the co-chaperones p23 and AIP (AhR-interacting protein) (Petrulis & Perdew, 2002). The binding of a ligand induces phosphorylation of two protein kinase C sites adjacent to the nuclear localization sequences (NLS), which enables importin β to recognize the NLS and to shuttle the AhR–Hsp90–AIP complex into the nucleus. Here, AhR has to dissociate from Hsp90 in order to heterodimerize with ARNT (AhR nuclear translocator), another member of the basic helix–loop–helix Per-ARNT-Sim (bHLH/PAS) protein superfamily (Heid, Pollenz, & Swanson, 2000). This AhR–ARNT heterodimer then binds to regulatory regions of its target genes, the so called xenobiotic responsive elements (XRE), and when bound to DNA, it recruits components of the general transcription machinery to loosen the chromatin structure and to initiate transcription by RNA polymerase II (Hankinson, 2005; Hestermann & Brown, 2003). AhR target genes mainly encode for enzymes involved in phase I and II drug metabolisation and for proteins that regulate cell growth and differentiation (Bock & Kohle, 2006).

Figure 1.3

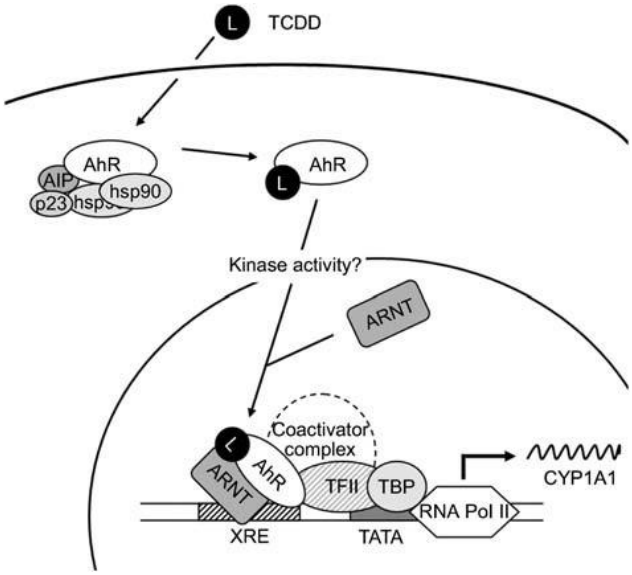

Figure 1.3 Canonical AhR pathway. From Abel and Haarmann-Stemmann, 2010 (Abel & Haarmann-Stemmann, 2010)

1.4.3.2 AhR crosstalks

Apart from the canonical pathway described above, several alternative effect mechanisms are described in literature. Ligand binding of AhR releases c-src, a tyrosine kinase and part of the cytosolic AhR complex. The active c-src subsequently translocates to the cell membrane, phosphorylates EGFR, and thereby initiates EGFR signalling via the MAPK pathway (Haarmann-Stemmann, Bothe, & Abel, 2009; Xie, Peng, & Raufman, 2012). Notably, the activation of EGFR in response to ligand binding works also in cell- and nucleousfree conditions (Enan & Matsumura, 1995). Thus, the crosstalk with the EGFR must be completely independent from the canonical nuclear pathway and from associated changes in gene transcription.

Figure 1.4

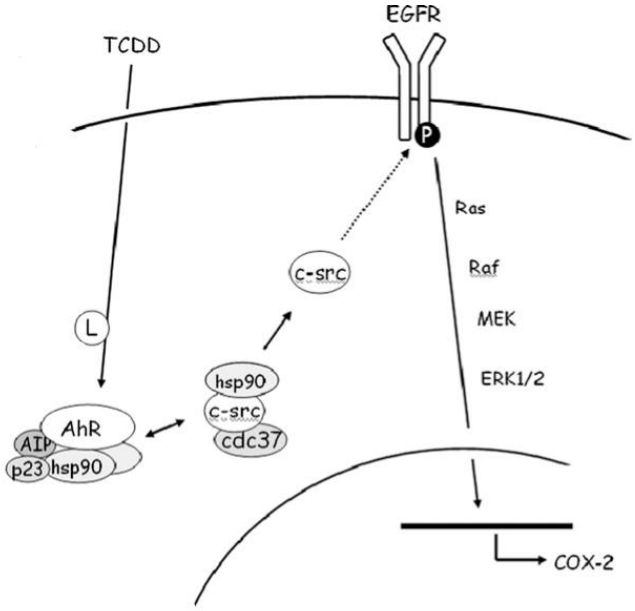

Figure 1.4 Cross-talk of AhR and EGFR signal transduction. From Haarmann-Stemmann et al. 2009 (Haarmann-Stemmann et al., 2009)

Furthermore, interactions with retinoblastoma protein (RB), Nuclear factor kappa-light-chain-enhancer of activated B cells (NFκB), estrogen or androgen receptors, tumor necrosis factor-α (TNF-α), and transforming growth factor-β (TGF-β) have been described (Haarmann-Stemmann et al., 2009; Ohtake, Fujii-Kuriyama, & Kato, 2009; Puga, Ma, & Marlowe, 2009; Tian, 2009).

1.4.4 Physiological functions of AhR

AhR in the immune system helps to control the extent of inflammatory reactions in barrier organs like skin, gut and lung. (Reviewed in: (Stockinger, Di Meglio, Gialitakis, & Duarte, 2014)). It is highly expressed in Th17 cells and to lower extents also in

regulatory T-cells (T_{reg}), but not in type 1 and type 2 T-helper cells (Veldhoen et al., 2008). The effects of AhR activation on T_{reg} and Th17 differ greatly among different experimental settings and seem to be ligand dependent (Quintana et al., 2008). B-cells also upregulate the expression of AhR upon activation, and AhR activation by TCDD inhibits B-cell differentiation into plasma cells (Sulentic & Kaminski, 2011). In macrophages, AhR activation supports M2 differentiation. M2 macrophages produce high levels of IL-10 and thereby restrict inflammatory responses and protect against persistent inflammation. Correspondingly, activation of macrophages in AhR deficient mice increases production of pro-inflammatory cytokines such as IL-6 (interleukin-6), IL-12 and TNF-α, which are typically secreted by M1 polarized macrophages (Biswas & Mantovani, 2010; Kimura et al., 2009).

During development, AhR is involved in the differentiation of many organ systems by regulating the expansion and differentiation of progenitor cells. At least in liver progenitors, altered differentiation and proliferation could be traced back to a downregulation of Wnt/β-catenin pathway target genes (Prochazkova et al., 2011).

Induction of AhR signalling arrests proliferation of intrathymic lymphocyte progenitor cells (Laiosa et al., 2003), whereas attenuating AhR signalling promotes the expansion of human hematopoietic stem cells (Boitano et al., 2010; Rentas et al., 2016).

Since loss of AhR in stem cells regularly results in a loss of quiescence and since prolonged or inappropriate stimulation of AhR attenuates stem cells proliferation, balancing stem cell quiescence, proliferation, migration, and differentiation is assumed to be the principal physiological task of AhR (Gasiewicz, Singh, & Bennett, 2014).

1.4.5 AhR in the CNS

The physiological function of AhR in the CNS is not very well understood. Similar to its effects in macrophages, ligand-dependent AhR activation restricts microglial activation (Lee et al., 2015; Rothhammer et al., 2018), and in a model of experimental autoimmune encephalomyelitis (EAE), interferon (IFN)-β-induced AhR signalling in astrocytes reduced CNS inflammation (Rothhammer et al., 2016). Thus, AhR activity seems to attenuate inflammatory processes in the CNS. Following cerebral ischemia however, AhR activation worsened the outcome, whereas treatment with AhR antagonists had neuroprotective effects (Cuartero et al., 2014). Taken together, the impact of AhR signalling in the injured or diseased CNS still remains uncertain and depends inter alia on the way of AhR activation or inactivation and the disease model used.

During embryonic development, neuronal precursor cells express high levels of AhR, and TCDD-induced AhR activation impairs their proliferation in a concentration dependent manner (Latchney et al., 2011). In the adult mouse brain, AhR activation impairs proliferation of neural progenitor cells in the dentate gyrus (Latchney et al., 2011) and deletion of AhR in cerebellar granule neuron precursors compromises neurogenesis (Dever et al., 2016).

In the injured adult zebrafish telencephalon, AhR pathway is specifically regulated in a subpopulation of ependymogia in the dorsal subventricular zone. Under physiological conditions, AhR signalling is downregulated within 2 dpi and returns to normal levels within 7 dpi. Maintaining AhR signalling at high levels by vetricular injections of an AhR agonist changes the fate of ependymoglia towards the production of new neurons at the expense of ependymocyte proliferation. Persisting inhibition of the AhR pathway accordingly increased ependymocyte proliferation. This demonstrates the critical role of the AhR pathway in maintaining the balance between neuronal differentiation and maintenance of the stem cell pool in the adult zebrafish brain.

1.5. Aims of the thesis

Given the important role of AhR signalling in differentiation of neuronal progenitors in the zebrafish telencephalon in response to traumatic brain injuries, the main purpose of my thesis was to elucidate, weather AhR signalling also plays a role in neurogenesis and reactive gliosis of the adult mouse brain. Therefore I addressed following questions:

1. Where is AhR expressed in the intact mouse brain?
2. Which cells express AhR in the injured mouse brain?
3. How does AhR activation affect reactive gliosis?

Thus, I first determined the expression pattern of AhR in the intact and injured mouse brain. Afterwards the effects of AhR activation on reactive gliosis were investigated in vivo. Since specifically reactive astrocytes were found to express AhR in the lesioned cerebral cortex, I also analysed the impact of AhR activation on reactive astrocytes´ stem cell properties in vitro. Finally, we performed a proteome analysis to get an idea by which mechanisms AhR signalling affects reactive gliosis and stem cell properties of reactive astrocytes.

2 Materials

2.1 Immunocytochemistry and Immunohistochemistry

2.1.1 Primary Antibodies

Table 2.1

Antigen	labelled cell type / structure	Host-animal	Working dilution IC= Immunocytochemistry IH =immunohistochemistry	Pretreatment	Supplier
AhR	cells expressing AhR	rabbit	1:5000 (tyramide kit) (0,5% Tx, 10% NGS)		Biomol, 031714-FITCH
BrdU	cells undergoing S-phase during BrdU administration	rat IgG2a	1:200 (0,5% Tx, 10% NGS)	1h 2N HCl, 2x15 min borate buffer (pH8.0)	Abcam, Ab-6326-250
DCX	immature neurons	guinea pig	1:1000 (IH) 1:2500 (IC) (0,5% Tx, 10% NGS)		Millipore, AB5320
GFAP	adult NSC, (reactive) astrocytes	mouse IgG1	1:500 (IC) 1:200 (IH) (0,5% Tx, 10% NGS)		Sigma, G3893
Iba1	microglia	rabbit	1:500 (0,5% Tx, 10% NGS)		WAKO 019-19741
Ki67	cells in the active phases of the cell cycle (G1, s, G2, M-phase)	rabbit	1:500 (0,5% Tx, 10% NGS)	30 min Antigen retriever	Novocastra NCL-Ki67p
Ki67		rat	1:300 (0,5% Tx, 10% NGS)	30 min Antigen retriever	DAKO M7249
Nestin		mouse IgG1	1:200 (0,5% Tx, 10% NGS)		Millipore MAB 5326
NeuN	mature neurons	mouse IgG1	1:80 (0,5% Tx, 10% NGS)	30 min Antigen retriever	Millipore MAB 377
NG2	oligodendrocyte precursor cells	rabbit	1:250 (0,5% Tx, 10% NGS)		Millipore AB 5320
O4	late oligodendrocyte progenitors	mouse IgM	1:200 (10% NGS)		Millipore MAB 345
Olig2	initially proliferating NG2+ progenitors	rabbit	1:200 (0,5% Tx, 10% NGS)		Millipore AB 9610

Table 2.1 Primary antibodies

2.1.2 Secondary antibodies

Immunocytochemistry and Immunohistochemistry were performed with the appropriate species- or subclass-specific secondary antibodies conjugated to either AlexaFluor 488, AlexaFluor 543 or AlexaFluor 633 (1:1000, Life technologies). For signal amplification with the tyramide kit, biotinylated secondary antibodies (goat anti-rabbit biotin; 1:1000; Vector: BA-1000) were used.

2.2 Buffers and solutions

Phosphate-buffered saline (PBS):

NaCl	137 mM
KCl	2.7 mM
$Na_2HPO_4 \cdot 7H_2O$	8.3 mM
KH_2PO_4	1.4 mM

Storing solution

Glycerol	30 ml
Ethyleneglycol	30 ml
H2O	30 ml
PO4-buffer 10x	10 ml

(13.8 g $Na_2HPO_4 \cdot 7H_2O$; 3 g NaOH, 40 ml H_2O)

Borate buffer 0.1 M pH 8.5

$Na_2B_4O_7$	20.1 g
H_2O	1,0 l
HCl	adjust pH to 8.5

PFA 4% pH 7.3

PFA	40 g
NaOH	3 pellets
PBS	900 ml
HCl	adjust pH to 7.3

NP40 buffer pH 7.4

Tris-HCl,	50 mM
NaCl	150 mM
NP40	1%

UA buffer: Urea (Sigma U5378) buffer,

Urea	8 M in

Tris/HCl; 0.1 M; pH 8.5

Solution 1: pH adjusted to 7.5

D/Glucose	stock: 300 mg/ml; 9 ml
HEPES	1 M; 7.5 ml
HBSS 1X	fill up to 500 ml

Solution 2: pH adjusted to 7.5

Sucrose	154 g
HBSS	fill up to 500 ml

Solution 3: pH adjusted to 7.5

HEPES	10 ml
BSA	20 g
EBSS	fill up to 500 ml

Neurosphere Medium:

DMEM/ F12 + Glutamax	48 ml
B27 supplement	1 ml
Pen/Strep	0.5 ml
Hepes buffer, 1 M	0.5 ml

Anesthesia solution

NaCl (0.9 mg/ml)	2.5 ml
Ketamin	1 ml
Rivapoun	0.25 ml

MMF (Sleep) mix

Fentanylcitrat	0.25 ml
Midazolam	0.5 ml
Medetomidin	0.25 ml
NaCl (0.9%)	4 ml

Awake mix

Naloxon	1.5 ml
Flumazenil	2.5 ml
Atipamezol	0.25 ml
NaCl (0.9%)	0.75 ml

2.3 Tissue culture reagents

Reagents used for tissue culture experiments.

Reagent	Company	Ordering Number
B-27 Serum-Free Supplement	Gibco (Life technologies)	17504044
Bovine serum albumin (BSA)	Sigma	A9418
D-Glucose (Stock 45%)	Sigma	G8769
DMEM:F12 (Dulbecco's Modified Eagel Medium:Nutrient Mixture F12) + GlutaMAX	Gibco (Life technologies)	31331
DMSO	Sigma	D2438
DNAse I	Roche	1284932
EBSS (Earle's Balanced Salt Solution)	Gibco (Life technologies)	14155063
EGF (Epidermal Growth Factor)	Roche	855573
FCS (Fetal Calf Serum)	Pan	2602-P290705
FGF2 (Fibroblast Growth Factor-2)	Roche	10555400
HBSS (Hank's balanced salt solution)	Gibco (Life technologies)	24020
HEPES (1M)	Gibco (Life technologies)	15630
Hyaluronidase	Sigma	H3884
Penicillin/Streptomycin (Pen/Strep)	Gibco (Life technologies)	15140
Poly-D-Lysine (PDL)	Sigma	P0899
Sucrose	Sigma	S0389
TCDD	Sigma	48599
Trypsin	Sigma	T4665
Trypsin (EDTA), 0.05%	Gibco (Life technologies)	25300

2.4 Reagents for proteomic

Reagents used for FASP

Product	Company	Ordering Number
2-Iodacetamid	Merck	8047440025
Acetonitrile	Merck	1000301000
Ammoniumbicarbonat	Sigma	A6141
Dithiothreitol	Sigma	D7701
Lys-C	Wako	125-05061
Trifluoroacetic acid	Sigma	T6508
Trypsin	Promega	V511A
Urea	Sigma	U5378

2.5 Animal treatment

Product	Company	Ordering Number
20G x 1,5" feeding needle 1,9mm Tip	Cadence science	9921

Corn oil	Sigma	C8267
V-Lance knife, 19g	Alcon	8065911901

Chemical	Company	Ordering Number
4,6-dasmindino-2-phenylindol (DAPI)	AppliChem	A1001
5'-bromo-2'-deoxyuridine (BrdU)	Sigma	16880
Agarose	Biozym	870055
Bovine serum albumin (BSA)	Sigma	A9418
EDTA	Merck	1084180250
Ethanol	Merck	107017
Glycerol	Sigma	3783
Glycerol	Sigma	3783
Glycine	AppliChem	A4554
HEPES	Roth	9105
Hydrochloric acid (32%)	Merck	109057
Hydrogen peroxide	Roth	8070
Isopropanol	Merck	1096342500
Normal goat serum (NGS)	Vector Laboratories	S-1000
Paraformaldehyde (PFA)	Roth	0335
Potassium chloride	Merck	104936
Potassium dihydrogen phosphate (KH2PO4)	Merck	104873
Sodium hydroxide	Roth	6771
Sodium phosphate (Na2HPO4•7H2O)	Merck	T876
Triton-X100	Roth	3051
Tris-HCl (1M)	Rockland	MB004
H_2O_2 (30%)	Sigma	31642

2.6 Kits

Kit	Company	Ordering number
Tyramide Signal Amplification kit Plus Fluorescein System	Perkin Elmer	NEL741
TSA™, Plus Tetramethylrhodamine (TMR) System	Perkin Elmer	NEL742
streptavidin-HRP conjugate	Perkin Elmer	NEL750
RNeasy Mini Kit	Qiagen	74106
Maxima First Strand cDNA Synthesis Kit for RT-qPCR	Invitrogen	K1642

2.7 PCR Primers

Kit	Sequence
mouseCyp1a1for	AGAGGTTGGCGACTTTGACCCTTA
mouseCyp1a1rev	ACCTCCCGAAACTGATTGCTGAGA
mouseRpl13for	TTCGGCTGAAGCCTACCAGAAAGT
mouseRpl13rev	GCATCTTGGCCTTTTCCTTCCGTT

3 Methods

3.1 Animals

3.1.1 Mouse strains

C57BL/6J mice at the age of 8 to 10 weeks were used for all experiments.

3.1.2 Stab wound injury

Animals anaesthetized by i.p. injection of 400 µl "Sleep" (20 ml/kg bodyweight), sustained a 0.6 mm deep and 1.0 mm long stab wound in the somatosensory cortex of the right hemisphere. Using the V-Lance knife under the control of a stereotactic device guaranteed a reproducible injury size and location (0.6 mm in depth, 1.5 mm lateral and from 1.0 mm to 2.0 mm caudally from the bregma) **(Figure 3.1)**. I.p. injection of 400 µl "Awake" reversed anaesthesia after the intervention.

Figure 3.1

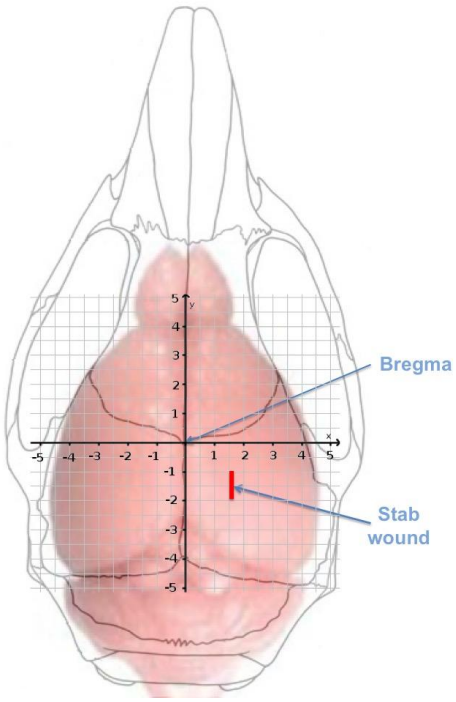

Figure 3.1 Localisation of the stab wound. Stab wound was located 1.5 mm lateral and from 1.0 mm to 2.0 mm caudally from the bregma and reached to 0.6 mm in depth. Scale units: mm

3.1.3 Oral TCDD administration

Every second day mice of the experimental group obtained TCDD, diluted in 150 µl corn oil to a final concentration of 0.346 µM by oral application. The first TCDD-

administration was 5 h prior to the performance of the stab wound. The second and the third gavage took place at 2 and 4 dpi. At the end of one experiment each animal was exposed to 0,156 nmol TCDD dissolved is 450 µl of corn oil **(Figure 3.2)**. Animals that were not exposed to TCDD underwent the same treatment but were gavaged with corn oil only.

Figure 3.2

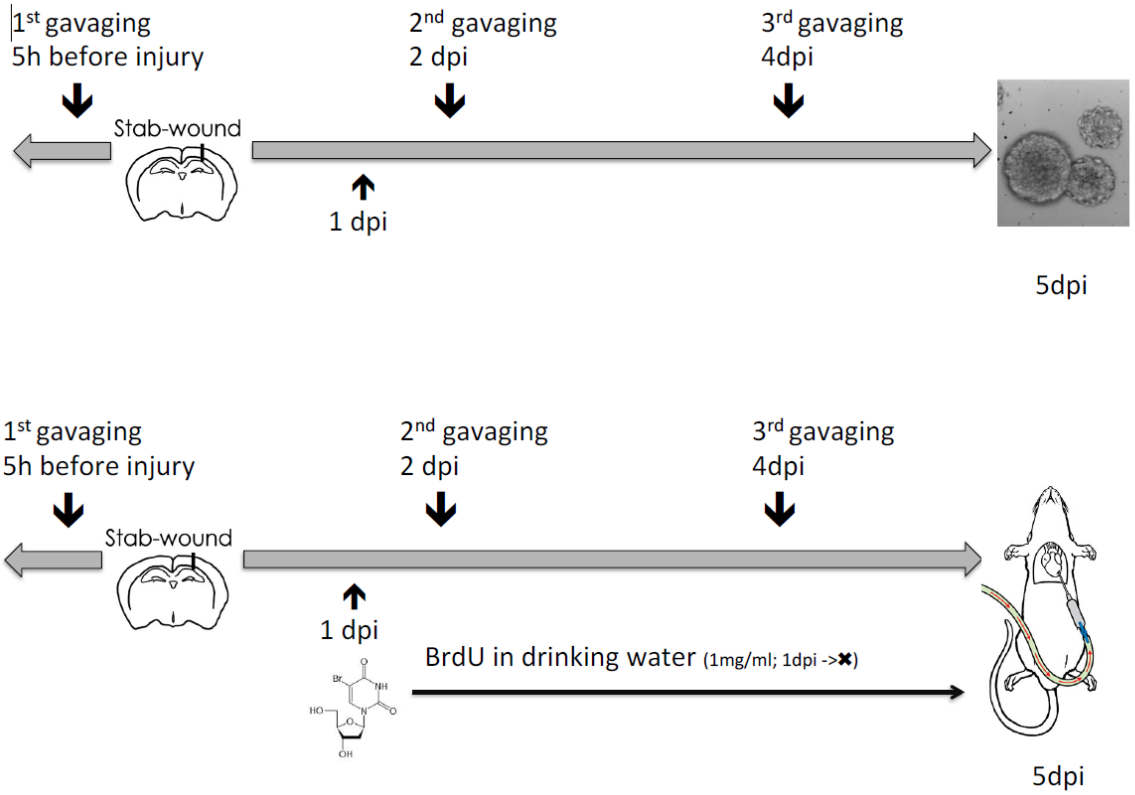

Figure 3.2 Schedule of systemic TCDD treatment. For systemic treatment, mice were gavaged 3 times (0 dpi, 2 dpi and 4 dpi) with TCDD diluted in corn oil or with the vehicle only.

3.1.4 Local TCDD administration

For local TCDD treatment, animals underwent a second surgery at day 3 post injury. (Anaesthesia: see stab wound injury). 0.2 pmol TCDD dissolved in 1 µl artificial CSF and 1.28 nl DMSO or respectively the same amount of DMSO and aCSF only were injected in the centre of the stab wound (coordinates from bregma: x= -1.0 mm; y= -1.5 mm; z= -0.6 - -0.2 mm) with an extended capillary and an infusion speed of 2 µl/sec **(Figure 3.3)**.

Figure 3.3

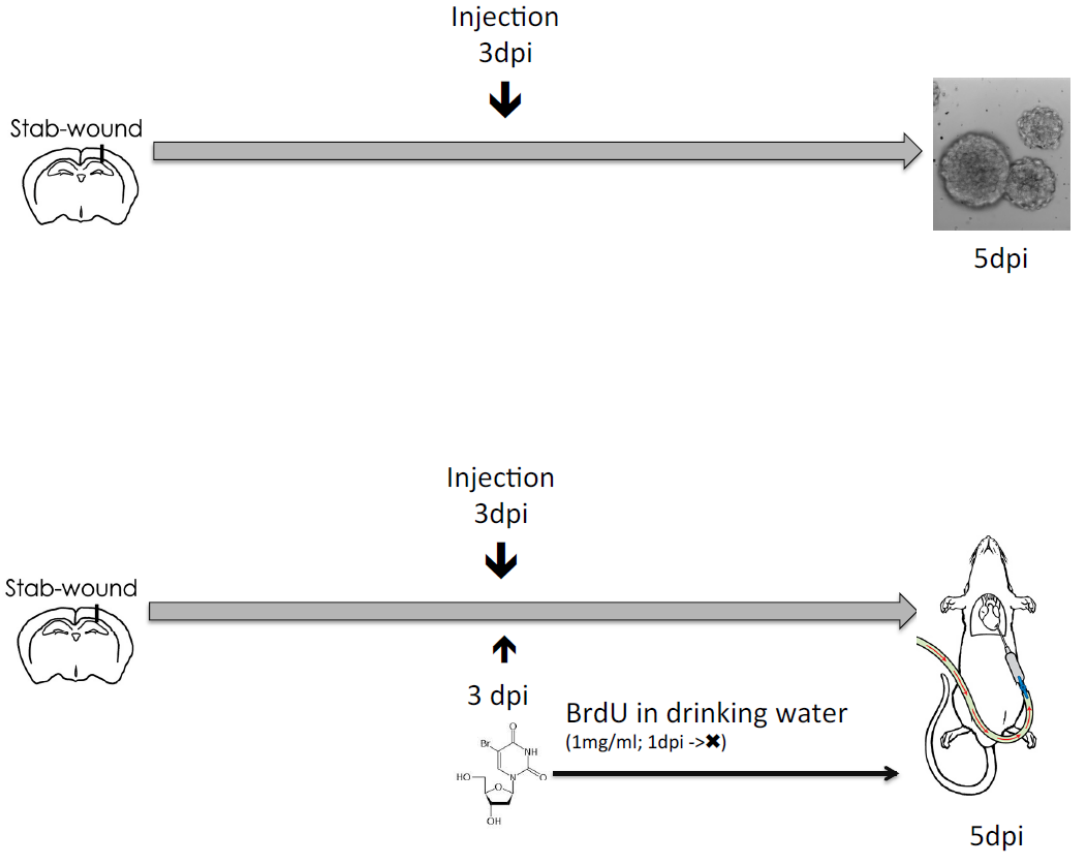

Figure 3.3 Schedule of local TCDD treatment. For local treatment, TCDD was injected directly into the stab wound at 3 dpi.

3.2 Histology

3.2.1 BrdU labelling

BrdU, a thymidine analogue incorporates into newly synthesized DNA and can be detected by specific antibodies. Therefore, a continuous administration of BrdU in the drinking water (1 g BrdU per 1 l water) from 1 dpi (for systemic TCDD treatment) or immediately after the second surgery (for local TCDD administration) until sacrifice at 5 dpi, allows visualization of all cells undergoing S-phase in this period.

3.2.2 Perfusion and preparation of free floating vibratome sections

Transcardial perfusion 5 days after injury fixed the brain tissue. Animals anesthetised by i.p. injection of Ketamin (Ketaminhydrochlorid; 100 mg per 1 kg of body weight) and Rompun (Xylazinhydrochlorid; 20 mg per kg body weight) were first perfused with PBS to wash blood out, followed by approximately 50 ml of PFA 4% in PBS.

Brains were removed, post fixed in 15 ml PFA 4% for 2 h at 4 °C, washed with PBS and embedded in 3% agarose in PBS to be finally cut with the vibratome into 60 µm thick slices.

Sections collected in PBS were kept at 4 °C for immediate use or transferred to storage solution for long time storage at -20 °C.

3.2.3 Immunohistochemistry

3.2.3.1 Standard protocol

Indirect antigen labelling requires two steps. First sections were incubated over night at 4 °C with primary antibodies, recognizing the antigens of interest, followed by 2 hours of incubation at room temperature with subclass specific secondary antibodies which are conjugated to fluorescent dyes (Alexa 488, Alexa 543, Alexa 647) or tagged with biotin to visualize the antigen bound primary antibody.

All antibodies were diluted in 0.1 M PBS containing 0.5% Triton-X-100 to permeabilize cell membranes and non-specific binding was reduced by addition of 10% NGS as well as three washing steps with PBS following each antibody incubation.

Finally sections were put on a microscope slide, topped with a drop of mounting medium and covered with a cover slide.

3.2.3.2 Antigen retrieval

Some antigens are inaccessible for antibodies (BrdU) or get masked during tissue fixation. Therefore, some epitopes demand special pretreatments (see **Table 2.1**)

3.2.3.3 DNA denaturation with HCl

BrdU can only be detected in single stranded DNA. Consequently it was necessary to denature DNA with 2 M HCl for 30 minutes at room temperature and neutralize the acid with 0.1 M sodium tetraborate buffer (pH 8.5) for 30 minutes afterwards.

3.2.3.4 Target retrieval solution

Target retrieval solution, diluted 1:10 in water, was heated to 100°C and put on sampels for 30 minutes to loose fixation induced, epitope masking protein crosslinks. After incubation, sections were washed three times with PBS and stained as described above.

3.2.3.5 Signal amplification

Tyramide Signal Amplification (TSA™) technology enabled the detection of AhR, what was impossible with the standard protocol. After incubation with the primary antibody, (see “Immunohistochemistry - general treatment) pre-treatment with saturating amounts of hydrogen peroxide (0.3% in PBS) for 30 minutes was necessary to inactivate

endogenous peroxidase activity and avoid unspecific deposition of fluorophore tyramides later on.

Incubation with a biotinylated secondary antibody (1h room temperature; dilution: 1:1000 in blocking solution) provides binding sides for streptavidin. During the incubation time of 1 hour horseradish-peroxidase coupled streptavidin (diluted 1:100 in PBS) binds to biotin and therefor immobilizes horseradish-peroxidase at that position where the antigen of interest was initially bound by the primary antibody.

The enzymatic activity of horderadish-peroxidase converts the fluorophore tyramides (Fluorescein or Tetramethylrhodamine diluted 1:100 in amplification diluent) into an extremely reactive intermediate that binds within 5 minutes to adjacent proteins.

Three washing steps with PBS followed every individual step of the protocol.

Figure 3.4

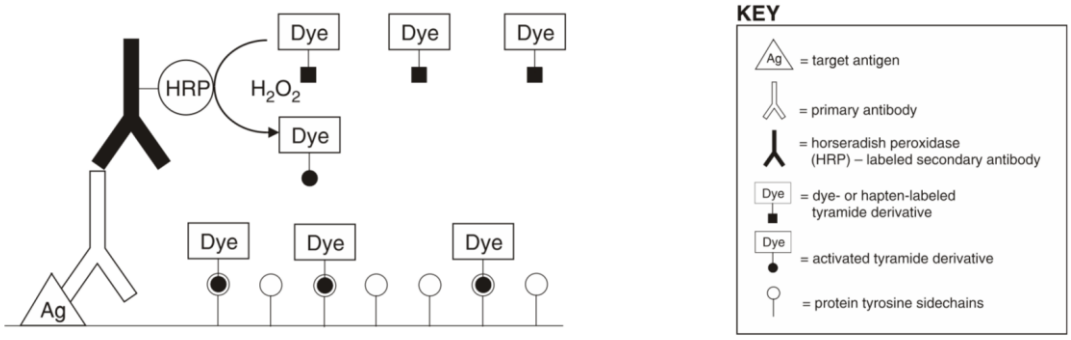

Figure 3.4 Schematic representation of TSA™ detection applied to immunolabeling of an antigen. Adopted from Thermo Fisher Scientific´s Manual for Tyramide Signal Amplification Kits[1]

3.3 Neurosphere assay

3.3.1 Dissection and dissociation of adult mouse SEZ and cortex for culture of primary neurospheres

After cervical dislocation and decapitation, brains were removed and stored in ice-cold HBSS containing 10 mM Hepes until their immediate dissection in the same medium.

Cortical grey matter was taken with a punch of 3.5 mm in diameter and to isolate the SEZ, brains were cut coronally at the level of the optic chiasm and separated into the two hemispheres. After removal of the hippocampus to expose the SEZ, it was then

[1] https://tools.thermofisher.com/content/sfs/manuals/mp20911.pdf; last visited: 01/09/2018

separated from underlying striatum by cutting out a thin layer of tissue. (Fischer et al., 2011)

Samples collected on ice in 2 ml dissociation medium were then split into single cells by a combination of mechanical and enzymatic dissociation. Two steps of incubation at 37 °C for 15 minutes digested the extracellular matrix and pipetting tissue pieces up and down with a 1 ml pipette tip before and following each incubation step supported the production of a single cell suspension.

Subsequent addition of 3 ml solution III stopped the activity of trypsin.

The cell suspension was then transferred though a 70 µm strainer into a new falcon tube and centrifuged for 5 min at 1200 rpm (200 g).

Next, the supernatant was removed, cells were resuspended in 10 ml solution II containing 30% of sucrose, and centrifuged for 10 min at 2000 rpm. Dead cells fail to precipitate under these conditions and can be removed with the supernatant.

Pelleted cells were resuspended in 2 ml ice cold solution III and added to another 10 ml solution III in a new 15 ml Falcon tube, centrifuged again for 7 min at 1500 rpm and seeded at a cell density of 15.000 to 25.000 cells/5 ml neurosphere medium in a cell culture flask (for SEZ neurospheres) or 6-well plates (for ipsi- and contralateral cortical spheres).

All centrifugation steps were performed in a Hettich Rotana 460R Centrifuge at 4 °C. Incubation lasted 1 (SEZ) or 2 weeks (cortex ipsi- and contralateral) at 37 °C with 95% air and 5% CO_2. Every third day, fresh EGF and FGF2 were added at a final concentration of 10 ng/ml (SEZ) or 20 ng/ml (cortex ipsi- and contralateral).

3.3.2 Passage of neurospheres

To reveal the neurospheres self-renewing capacity, spheres were split by enzymatic dissociation with 0.05% trypsin-EDTA and re-plated as single cells at a density of 5.000 cells per millilitre.

Cortical spheres were split separately. Therefor single spheres were picked with a 200 µl pipette tip, transferred into 1.5 ml tubes filled with 0.2 ml 0.05% trypsin-EDTA and incubated for 5 minutes at 37 °C. After addition of 0.3 ml solution III to stop trypsin activity, a single cell suspension was generated by pipetting neurospheres up and down with a 200 µl pipette tip.

Centrifugation at 200 g for 5 min (Eppendorf Centrifuge 5415D) pelleted the cells, which were then resuspended in 0.5 ml neurosphere medium containing 10 to 20 ng EGF and

FGF and plated in 48 well plates. At the end each well contained 0.5 ml medium together with all cells derived from one single sphere

SEZ spheres were split as a bulk. For this purpose all spheres were collected in a 15 ml falcon tube and centrifuged down for 5 min at 200 g. The supernatant, passed through a 20 µm filter, served as conditioned medium.

A single cell suspension was also generated by incubation for 5 minutes at 37 °C in 0.75 ml 0.05% trypsin-EDTA, whose activity was stopped afterwards with an equal amount of solution III, and mechanical dissociation with a 200 µl pipette tip. Centrifugation for 5 min at 1000 rpm at 4 °C in a Hettich Rotana 460R Centrifuge separated supernatant and cells which were subsequently resuspended in a mixture of fresh and conditioned neurosphere medium and plated at a density of 5 cell/µl in a cell culture flasks.

3.3.3 Differentiation of neurospheres and immunocytochemistry

This part of the neurosphere assay provides evidence of the spheres´ mulitpotency. SEZ neurospheres within neurosphere medium were directly transferred into 24-well plates containing PDL coated glass cover slips and the next day, neurosphere medium was replaced by differentiation medium.

Cortical spheres were picked separately with a 200 µl pipette, placed on a poly-ornithine (PORN) and laminin coated glass coverslip which was covered with 100 µl differentiation medium and after 2 h, when spheres attached to the substrate, wells were filled completely with differentiation medium.

After 7 days neurospheres were fixed for 15 minutes with 4 % PFA and stained as described in Histology -> Immunohistochemistry -> standard protocol.

3.4 Data analysis

3.4.1 Quantification of marker positive cells in brain sections

The number of marker positive cells was assessed at an Olympus FV1000 laser-scanning confocal microscope with optical sections of 1 µm in at least 3 vibratome sections per brain. Immunohistochemically labelled cells around the stab wound were quantified per volume in the region of 300 µm lateral and medial to the lesion core and up to a depth of 600 µm from the cortical surface. Proliferating cells in the SEZ were counted in coronal sections along the whole lateral length of the ventricle and normalized to the corresponding area.

3.4.2 Neurospheres

Differentiated and stained neurospheres were analysed with a Zeiss Axioplan2 light microscope and to measure the size of SEZ neurospheres, Zeiss AxioVision 4.8 microscope software was used.

3.4.3 Statistics

Shapiro–Wilk test designated whether data sets are in conformity with normal distribution and, accordingly, Mann-Whitney-U-test or two-sample t-test were used to test for statistical significance. Since it is impossible to test for normal distribution in samples smaller than five, t-test was performed in all these cases. T-test is relatively robust against violation of the assumption for standard distribution and in simulations with very small sample sizes, the type I error rate normally does not exceed the nominal value of 5%. Compared to alternative tests, t-test provides high power, an important feature in hypothesis generating testing (De Winter, 2013).

Data were considered significant with $p<0.05$ (*), very significant with $p<0.01$ (**) and highly significant with $p<0.001$ (***). All error bars present standard errors of the mean (± S.E.M).

3.5 Proteomic

3.5.1 Filter aided sample preparation (FASP)

LC-MSMS-based comparative Proteomics detected quantitative changes in protein expression. Therefore the cortical gray matter round the stab wound or an identical area of unlesioned cortex was isolated at 5 dpi with a punch of 2.5 mm in diameter, collected in 125 µl NP40-buffer and stored at -80 °C.

To set up samples for filter-aided sample preparation, they were defrosted and lysed in NP40-buffer by repetitive cycles of sonification for 10 sec, vortexing and cooling down on ice.

Following a Bradford protein assay to determine the lysates protein concentrations, 20 µg proteins of each sample in 400 µl UA buffer were denatured by adding 4 µl 1M DTT for 30 minutes at 60 °C and alkylated with 40 µl 300 mM IAA in another 400 µl of UA buffer for 30 min at room temperature in the dark.

The obtained protein solutions were transferred to a filter unit (Microcon YM-30) and centrifuged for 15 min at 14,000 g before washing the filter membrane three times with 200 µl UA buffer and twice with 100 µl 50 mM ABC buffer.

Afterwards exposure to 1 µg Lys-C in 40 µl 50 mM ABC buffer for 2 h at RT started protein digestion on the membrane and resulting peptides could be centrifuged (14.000 g; 15 min) through the filter and collected in a new LoBind Eppendorf cup (2 ml).
The remaining material on the filter underwent an additional digestion step at 37 °C over night with 2 µg Trypsin in 10 µl ABC buffer. Peptides were also centrifuged through the filter and collected in another LoBind Eppendorf cup (2 ml).
Both eluates were acidified with Trifluoroacetic acid (TFA) to a pH of 2 and finally subjected to LC-MS/MS. (Hauck et al., 2010)

3.5.2 Validation of AhR activation

RNA was isolated from liver tissue of animals used for proteome analysis using the Rneasy Mini kit (Qiagen) according to the manufacturer's recommendation including the digestion of remaining genomic DNA. Upregulation of CYP1A1, a biomarker for AhR activation, upon systemic TCDD treatment has been confirmed by qPCR.

3.5.2.1 cDNA Synthesis

2.5 µg RNA of each liver sample served as a template for cDNA synthesis using the Maxima First Strand cDNA Synthesis Kit for RT-qPCR (Invitrogen) according to manufacturer's protocol.

Raction temperature:	15 min	25 °C
	30 min	50 °C
	5 min	85 °C

3.5.2.2. Real Time PCR (RT-PCR)

Expression levels of Cyp1A1 were determined by quantitative Real Time PCR on a DNA Engine OpticonTM machine (Biorad) using SYBR Green mastermix (Biorad) to stain and quantify double-stranded DNA.
Cyp1A1 levels were expressed relative to the concentration of the housekeeping gene RLP13 as $2^{-(\Delta Ct)}$, while ΔCt is the difference in the number of cycles that is necessary to achieve a certain amount of DNA represented by threshold levels of fluorescence.
Conditions for the RT-PCR:

Initialising	95 °C	5 min	
Denaturation	95 °C	30 sec	40 cycles
Annealing	60 °C	30 sec	
Elongation	72 °C	30 sec	
Final elongation	72 °C	10 min	

4 Results

4.1 AhR expression in the adult mouse brain

Until few years ago, our knowledge about AhR signalling had been limited to the induction of xenobiotic metabolizing enzymes in response to environmental pollutants and, even though, more and more studies focus on the physiological roles of AhR, only very little is known about its expression and function in the central nervous system (Cuartero et al., 2014; Latchney, Hein, O'Banion, DiCicco-Bloom, & Opanashuk, 2013; Latchney et al., 2011; Petersen et al., 2000). Hence, my first aim was to evaluate the existence of AhR in the adult mouse brain using immunohistochemistry. This technique makes it possible to visualize the exact anatomical distribution of AhR as well as its localization within single cells. Thus, immunohistochemical stainings reflect the situation in vivo, when they are performed in tissue sections.

Figure 4.1

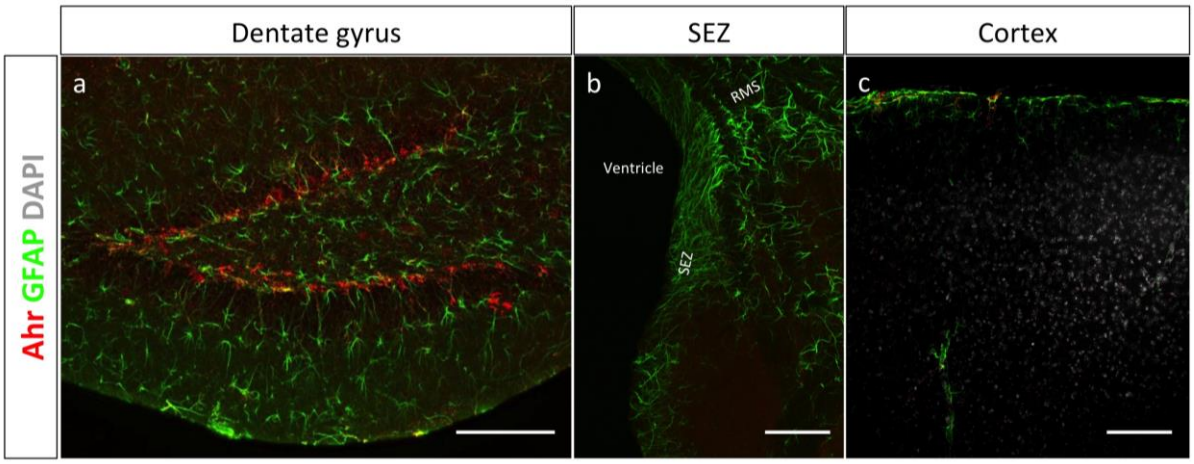

Figure 4.1 AhR expression pattern in the intact adult mouse brain. Coronal brain sections stained against AhR and GFAP. In the intact brain AhR is only detectable in the dentate gyrus of the hippocampus **(a).** AhR was not detectable in the SEZ **(b)**, the intact cortex **(c)**, the cerebellum or the mid brain (not shown).
Scale bars: 100 µm; RMS = rostral migratory stream; SEZ = subependymal zone

The expression of AhR-mRNA in neural progenitor cells of the dentate gyrus – the part of the hippocampus, where adult neurogenesis occurs – has previously been reported (Latchney et al., 2013) and immunohistochemical stainings accordingly confirmed these results **(Figure 4.1 a)**. Strikingly, the second main neurogenic niche in the adult mammal brain, the subependymal zone, did not exhibit detectable levels of AhR **(Figure 4.1 b)** and AhR was also abscent in the cerebellum and the mid brain.

AhR expression in the intact cerebral cortex was below the detection range, too **(Figure 4.1 c)**. But this changed after brain injuries. AhR levels were not detectable until 24 hours post injury **(Figure 4.2 a)**, peaked at 3 dpi **(Figure 4.2 b)** and persisted at least until 5 dpi **(Figure 4.2 c)**. Here it is remarkable that AhR appeared simultaneously with the upregulation of GFAP in astrocytes, the classical indicator for reactive gliosis in the central nervous system. Immunoreactivity for AhR was highest right beside the site of injury and regressed gradually over 300 to 400 µm. In the intact contralateral cortex, AhR had at no time been detectable.

Figure 4.2

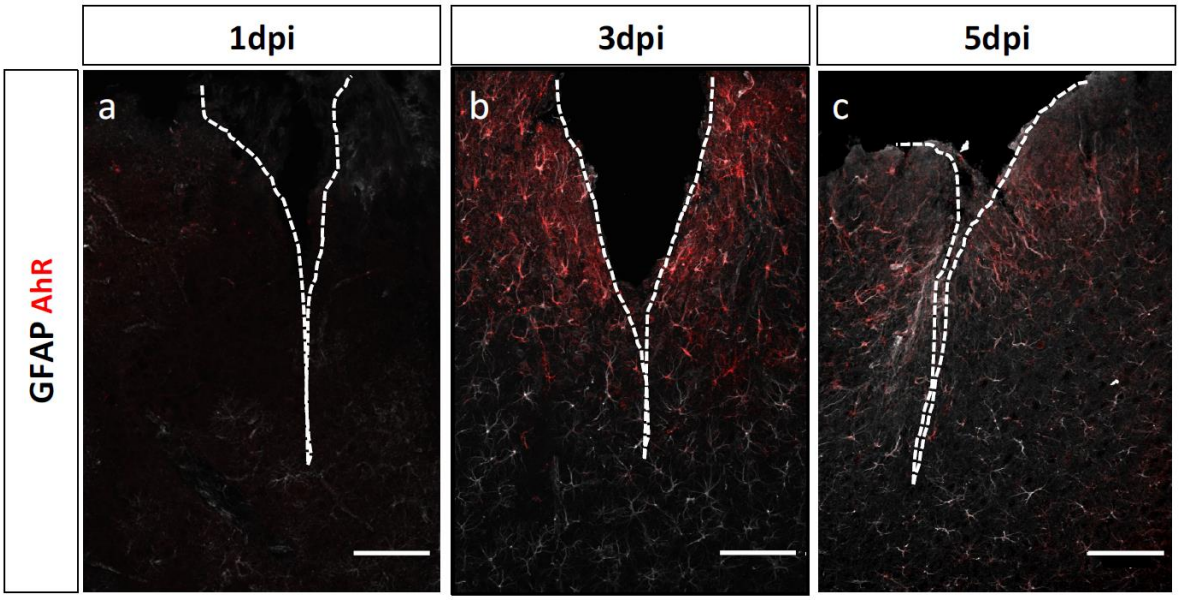

Figure 4.2 AhR immunostaining in response to stab wound injury. Coronal brain sections stained against AhR and GFAP. Stab wound injury of the cortex induced distinct expression of AhR simultaneously with the upregulation of GFAP in reactive astrocytes. Confocal images show AhR expression in the lesioned cortex at different time points after stab wound injury: 1 dpi **(a)**, 3 dpi **(b)** and 5 dpi **(c)**. Dashed lines indicate the site of injury. Scale bars: 100 µm

Reactive gliosis, the universal response to brain injuries, involves the reaction of various cells from different lineages, whereby astrocytes, oligodendrocytes and microglia play a key role. Since different cell types have diverse functions in that process of wound closure and tissue repair, it is essential to know which cell types express AhR in order to investigate its potential role in reactive gliosis. For this reason I stained tissue sections from the injured brain for specific glial cell markers (astrocytic GFAP, microglial Iba1 or Olig2 plus NG2 for cells of the oligodrendrocytic lineage) and examined them for colocalization with AhR.

Figure 4.3

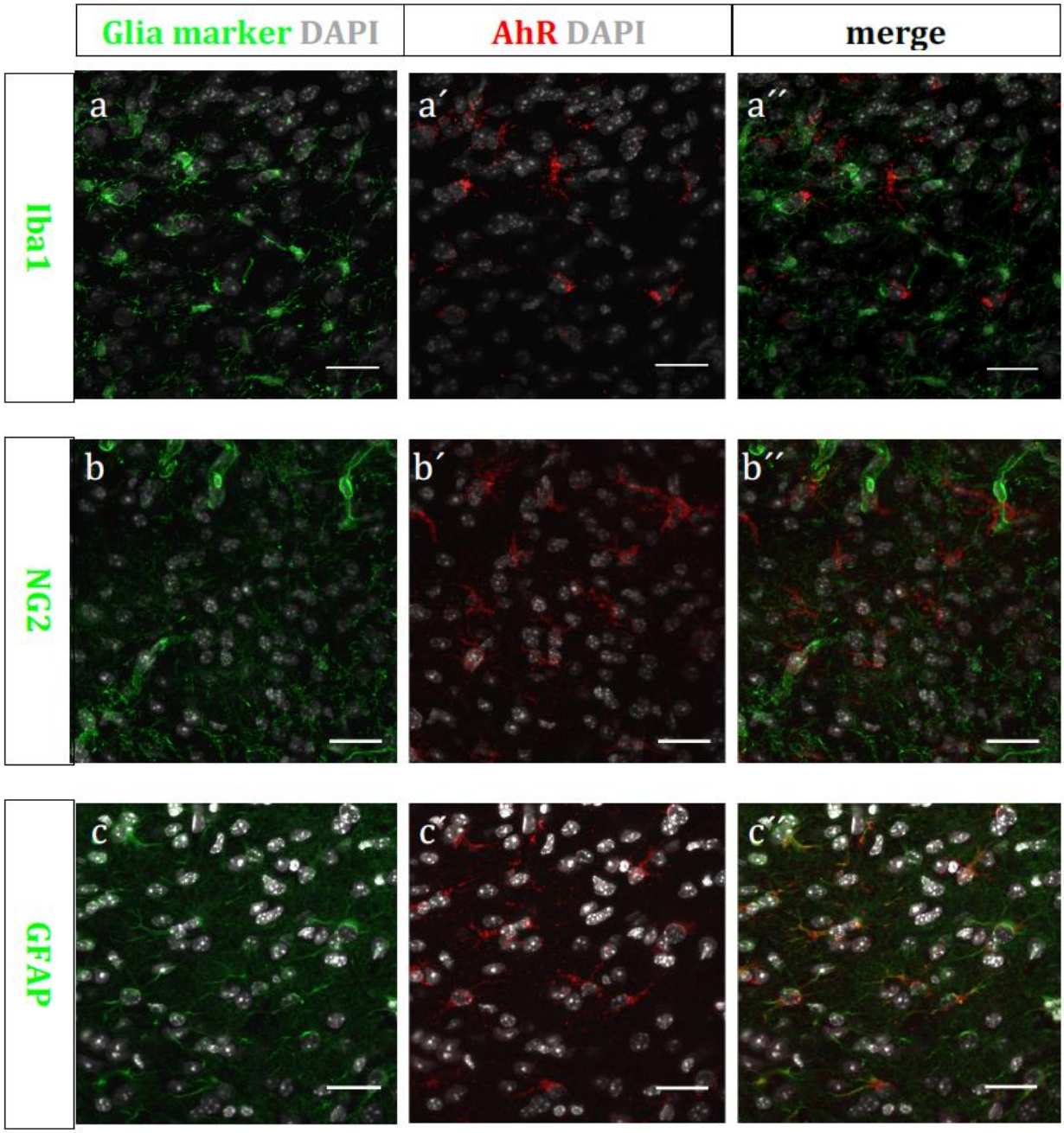

Figure 4.3 AhR immunostaining of different glial cell types. Immunostaining against AhR and markers for different glial cells in sections of the injured cortex at 5 dpi. There was no colocalization of NG2 (oligodendrocyte progenitor cells) **(a-a´´)** or Iba1 (microglia) **(b-b´´)** while all AhR+ cells proved to be GFAP+ reactive astrocytes **(c-c´´)**. Scale bars: 25 µm

Microglia, the immune cells in the central nervous system, are the first cells that get activated after brain injury. They proliferate, migrate towards the site of lesion, phagocytose debris and activate the other glial cells, including NG2+ oligodendrocyte progenitor cells and astrocytes. Several studies imply that AhR plays a role in the

activation of microglia at least in vitro (Lee et al., 2015; Xu et al., 2014). However, I could not observe any cell expressing Iba1 and AhR at the same time **(Figure 4.3 a-a´´)**, indicating that microglia do not contain detectable levels of AhR protein in vivo.

NG2+ oligodendrocyte progenitors also respond to brain injuries with morphological changes, increased proliferation and migration towards the injury (Simon et al., 2011), but also these cells were not AhR immunopositive **(Figure 4.3 b-b´´)**.

In double staining with GFAP, however, virtually all AhR+ cells proved to be reactive astrocytes **(Figure 4.3 c-c´´)**. The response of astrocytes to brain injuries is well studied. We know that they become hypertrophic, upregulate GFAP and can reenter the cell cycle to form a compact astrocyte scar. A not yet characterized subset of astrocytes even acquires stem cell potential including multipotency and long-term self-renewal under neurosphere conditions in vitro.

4.2 AhR activation with TCDD

The evidence of AhR in reactive astrocytes naturally leads to the crucial question of my thesis: How does AhR signalling contribute to reactive gliosis, and to astrogliosis in particular?

To address this question, I activated AhR with TCDD, a very potent and intensively studied AhR-agonist (Latchney et al., 2013; Poland et al., 1976), which was administered either systemically by gavage in three single doses throughout the duration of the experiment **(Figure 4.4 a)** or locally via direct injection into the stab wound at 3 dpi **(Figure 4.4 b).** The exact experimental procedure is described in chapter **3.1.3 / 3.1.4.**

Figure 4.4

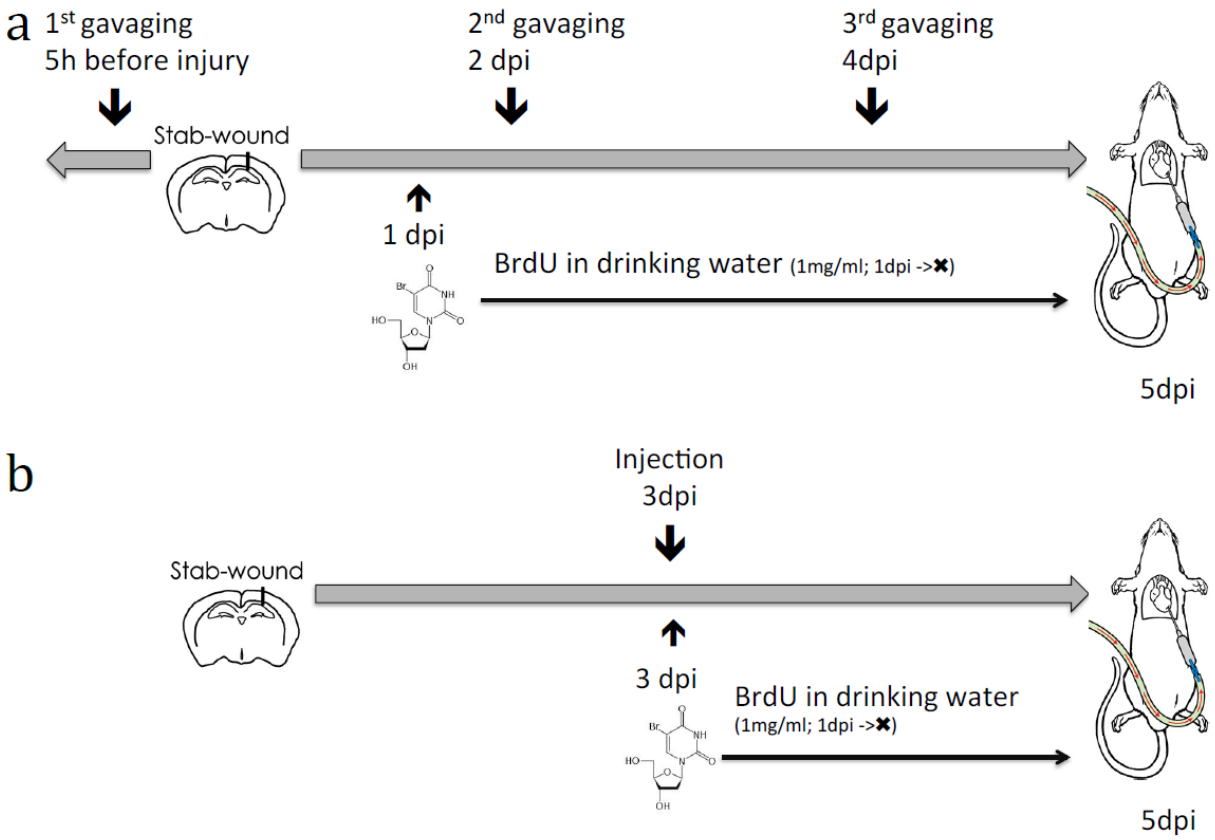

Figure 4.4 Schedule of systemic (a) and local (b) TCDD treatment. For systemic treatment, mice were gavaged 3 times (0 dpi, 2 dpi and 4 dpi) with TCDD diluted in corn oil or with the vehicle only. BrdU in the drinking water labelled proliferating cells from 1 dpi until perfusion at 5 dpi **(a)**. Local treatment includes direct injection of TCDD into the stab wound at 3 dpi and subsequent BrdU administration in the drinking water. Here animals were also perfused at 5 dpi **(b).**

4.2.1 Efficiency confirmation of TCDD treatment in AhR activation

I first validated the effectiveness of AhR activation. In an inactive state a complex of proteins, including HSP90, restrains the receptor in the cytoplasm. After binding a ligand, AhR dissociates from the HSP90-complex and subsequently translocates into the nucleus where it heterodimerizes with AhR nuclear translocator (ARNT) to act as a transcription factor **(see introduction; Figure 4.5)**. Therefore the localization of AhR in reactive astrocytes at 5 dpi can be used to monitor its activity. The nuclear localization displays the biologically active state, while a cytoplasmic localization represents the inactive state.

Figure 4.5

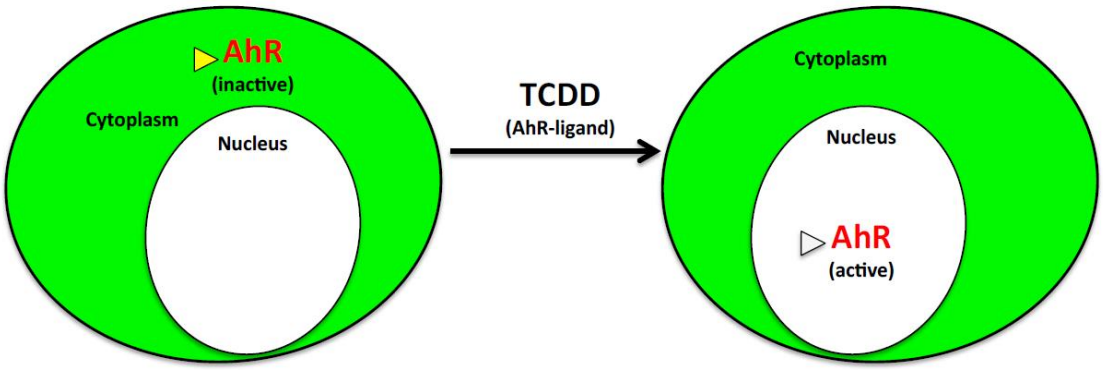

Figure 4.5 Simplified scheme of AhR activation. Note, that the inactive receptor is restrained in the cytoplasm and only binding of a ligand can release AhR to translocate into the nucleus.

Following systemic or local TCDD-treatment, I could indeed observe numerous reactive astrocytes with nuclear AhR **(Figure 4.6 b-b´´)** whereas in absence of TCDD AhR was merely present in the cytoplasm and, thus, inactive in terms of the canonical AhR signalling pathway **(Figure 4.6 a-a´´).**

Orthogonal projections of confocal images depict precisely the intracellular distribution of AhR immunoreactivity in absence **(Figure 4.6 c)** and presence of TCDD **(Figure 4.6 d)**. Under control conditions AhR was scattered all over the cytoplasm, but triggered by TCDD, AhR accumulated in the perinuclear region and translocated into the nucleus.

Due to the above-mentioned properties of AhR as a ligand dependent transcription factor, these findings provide evidence for the effectiveness of local and systemic TCDD treatment.

Figure 4.6

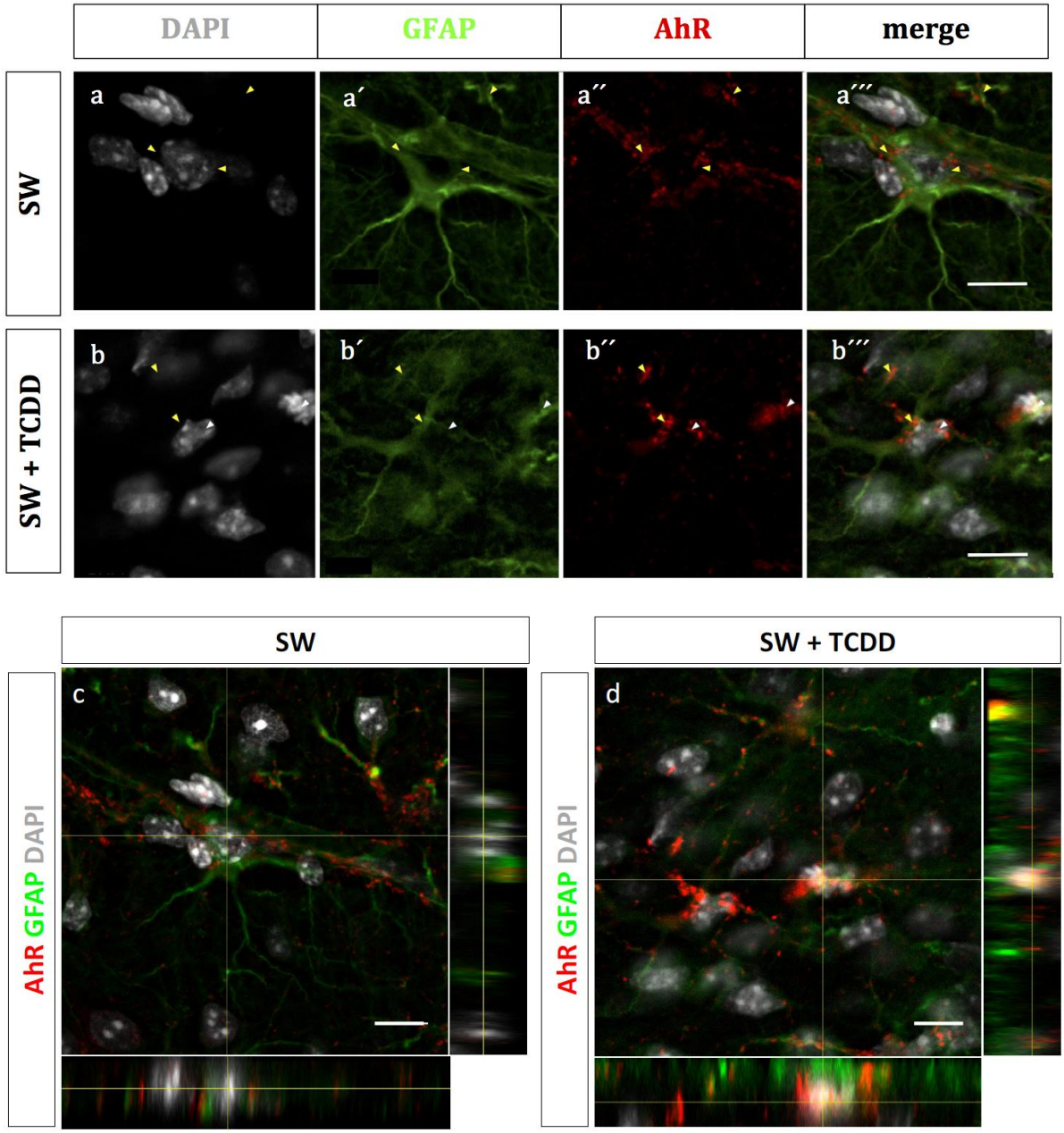

Figure 4.6 AhR activation by systemic TCDD administration. At 5 dpi, single plane confocal images of reactive astrocytes stained against GFAP and AhR show exclusively cytoplasmic AhR (yellow arrows) in absence of a ligand **(a-a´´´)** while in presence of TCDD, AhR (consistent with the biologically active state) could also be traced in the nucleus (white arrows) **(b-b´´´)**. Orthogonal projections of confocal images additionally demonstrate the cytoplasmic localization of AhR in absence of a ligand **(c)** and its undisputable nuclear localization as a result of TCDD treatment **(d)**. Similar effects were observed 5 dpi after local TCDD administration (not shown).
Sale bars: 10 µm

Systemic TCDD treatment affects all organs including liver, where AhR is well-known to regulate xenobiotic-metabolizing cytochrome P450 enzymes. Expression levels of CYP1A1, a target gene of AhR and member of the P450 enzyme family (Conney, 1982;

Ko, Okino, Ma, & Whitlock, 1996), were quantified by the use of realtime PCR to verify the transcriptional activity of AhR. The protocol I used for systemic TCDD treatment increased the number of CYP1A1-RNA transcripts in liver tissue by the factor 10,293 (relative expression levels: 1.00 ± 0.45 vs. 10,292.63 ± 2,134.51) **(Figure 4.7),** confirming the efficiency of TCDD as an AhR activator.

Figure 4.7

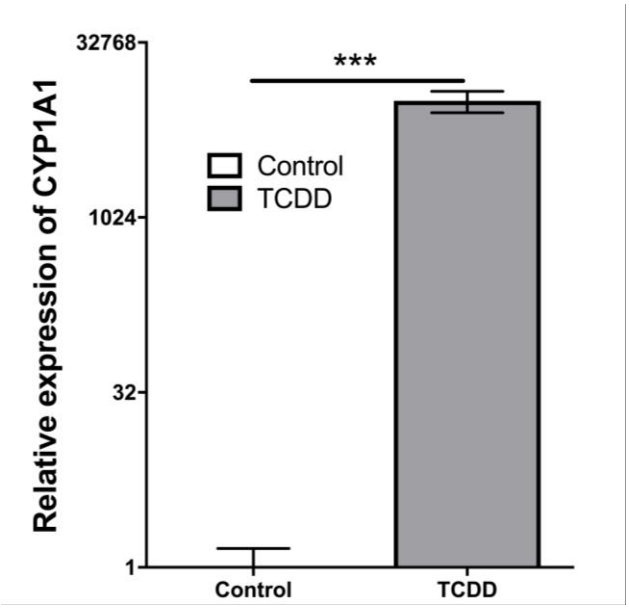

Figure 4.7 Expression level of CYP1A1 in liver evaluated by qPCR. The histogram depicts CYP1A1 mRNA-levels (relative to RLP13 mRNA-levels) in liver tissue, which were more than 10,000 fold higher in mice treated with TCDD than in mice treated with the vehicle only (1.00 ± 0.45 vs. 10,292.63 ± 2,134.51).
Bars in the histogram represent mean ± S.E.M. Asterisks depict the significance levels (***= $p \leq 0.001$) obtained by t-test; n = 3.

4.2.2 Effects of AhR activation on reactive gliosis in vivo

After efficiency of TCDD treatment was confirmed, I investigated the effects of AhR activation on reactive gliosis in vivo with special focus on proliferation of different glial cell types in an area of 600 x 600 µm around the stab wound.

4.2.2.1 Effects of systemic TCDD administration on reactive gliosis in vivo

For these experiments animals were treated according to the schedule for systemic TCDD treatment **(Figure 4.4 a),** hence, all quantifications describe the injury state 5 dpi at the height of astrocyte proliferation (Bardehle et al., 2013).

Increased proliferation of glial cells is distinctive of reactive gliosis and addition of BrdU (an thymidine analogue that incorporates into newly synthesized DNA) to the drinking

water labelled precisely those cells that underwent S-phase during the time of application, while immunostaining against Ki67, a nuclear protein associated with cellular proliferation, detected cells that were still in the cell cycle at the time of perfusion.

Analysis of 5 animals per experimental group indicated a reduction by more than one third in the total number of BrdU+ cells in mice treated with TCDD compared to mice treated with the vehicle only (0.123 ± 0.0041 vs. 0.0817 ± 0.0082 cells per μm^3; n= 5, p =0.0032, t-test; **Figure 4.8**), while the number of Ki67+ cells did not differ significantly (0.0275 ± 0.0025 vs. 0.0227 ± 0.0013 cells per μm^3; n=5, t-test; **Figure 4.8**).

Figure 4.8

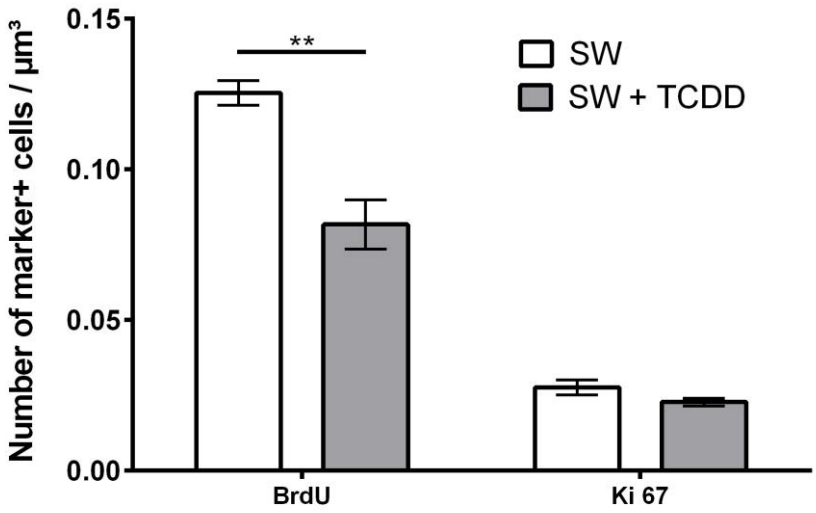

Figure 4.8 Proliferating cells in the injured brain. Systemic TCDD treatment significantly reduced the number of BrdU+ cells, but not the number of Ki67+ cells in response to stab wound injury at 5 dpi.
Bars in the histogram represent mean ± S.E.M. Asterisks depict the significance levels (**= p ≤ 0.01) obtained by t-test. Analysis was done 5 dpi; n = 5.

This change in the amount of BrdU+ cells is mainly due to impaired proliferation of microglia and astrocytes. In vehicle controls I counted 0.0239 ± 0.0025 reactive astrocytes per μm^3 that incorporated BrdU. TCDD reduced this number significantly to 0.0140 ± 0.0010 cells (n=5, p = 0.0136, t-test). The same applies for reactive astrocytes that were still in the cell cycle at the point of perfusion. Ki67+ astrocytes dropped from 0.0106 ± 0.0004 cells per μm^3 to 0.0062 ± 0.0005 cells per μm^3 (n=5, p = 0.0002, t-test) **(Figure 4.9 c).**

Figure 4.9

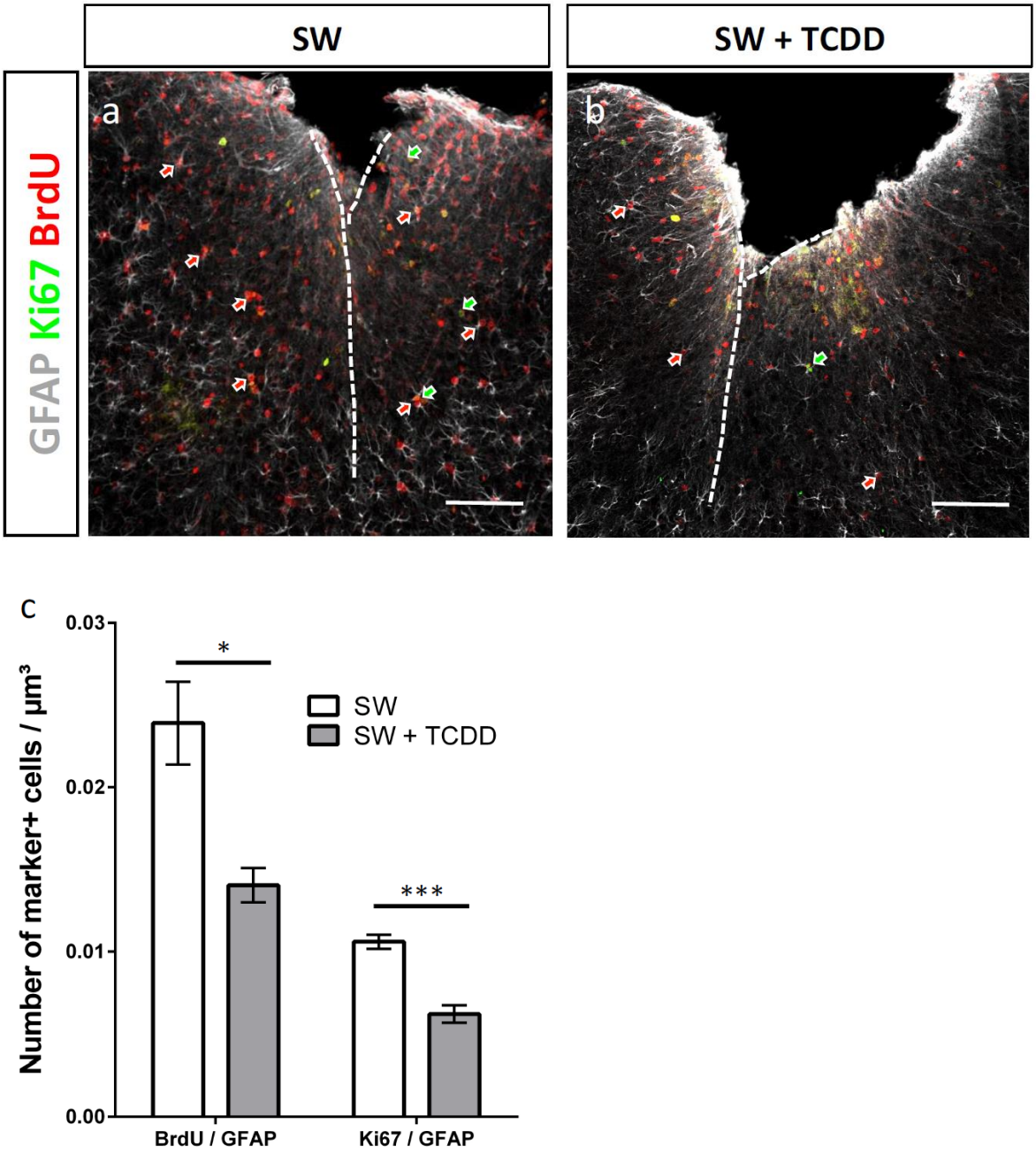

Figure 4.9 Effects of systemic TCDD administration on astrocyte proliferation. Confocal images of the lesioned cortex depict cells immunoreactivity for GFAP, Ki67 and BrdU. TCDD **(b)** reduced the numbers of proliferating astrocytes by more than one third compared to vehicle controls at 5 dpi **(a)**. Red arrows: BrdU+ astrocytes, green arrows: Ki67+ astrocytes.
Bars in the histogram **(c)** represent mean ± S.E.M. Asterisks depict the significance levels (*= $p \leq 0.05$; ***= $p \leq 0.001$) obtained by t-test. Scale bars: 100 µm; Analysis was done 5 dpi; n = 5; Dashed lines indicate the site of injury.

When exposed to TCDD, microglia, which accounted for the biggest proportion of BrdU+ cells, were also hindered from its full proliferative capacity **(Figure 4.10 c)** and the number of BrdU+ microglia consequently dropped more than 25 % from 0.0594 ±

0.0017 cells per µm³ in control conditions to 0.0429 ± 0.0025 cells per µm³ (n=3, p = 0.0073, t-test) in TCDD treated animals.

Figure 4.10

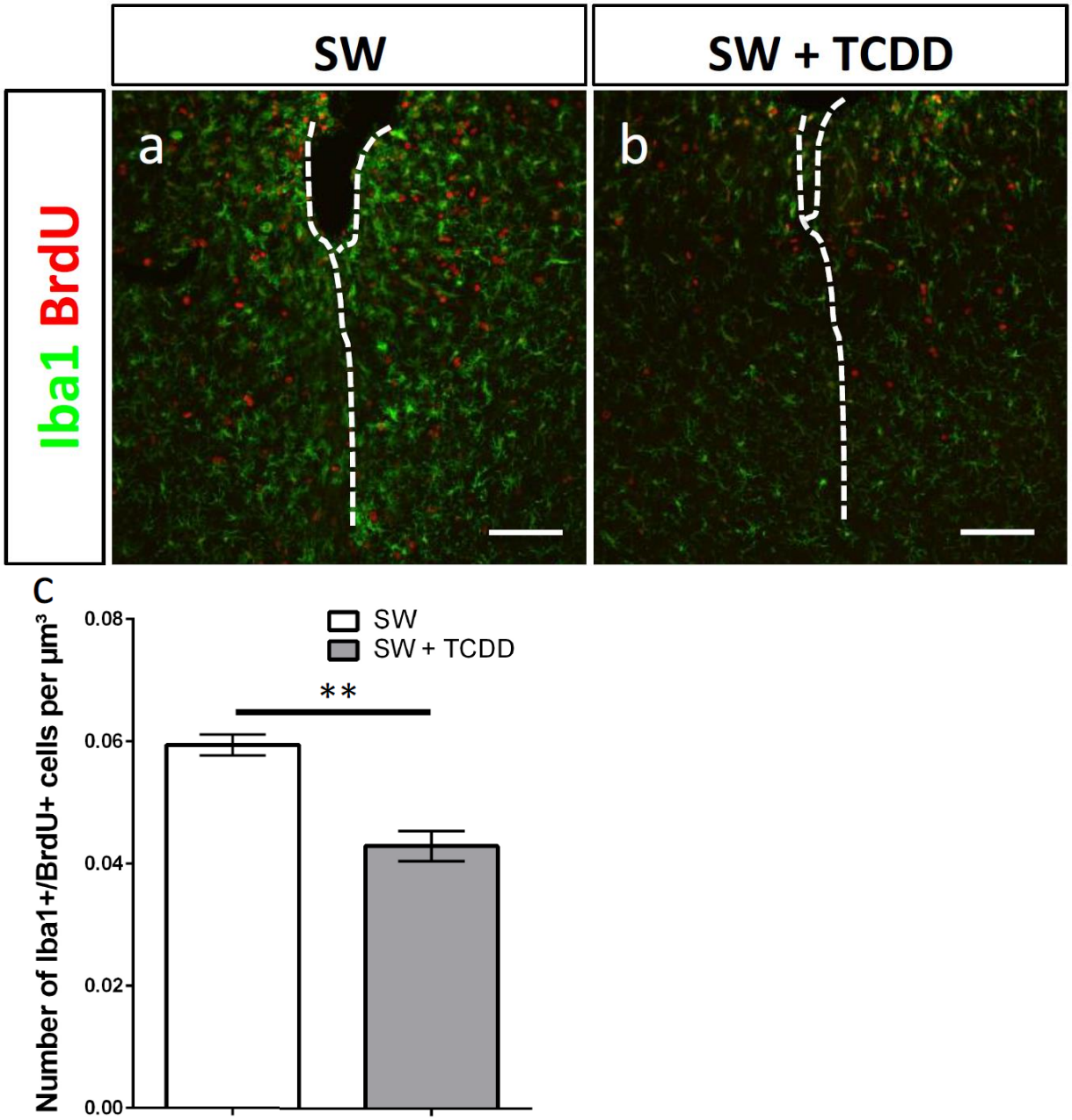

Figure 4.10 Effects of systemic TCDD administration on microglia proliferation.
Confocal images of the lesioned cortex stained against Iba1 and BrdU. In vehicle controls **(a)** microglia appear more numerous and hypertrophic and display a higher proliferative rate than in TCDD-treated animals at 5 dpi **(b).**
Bars in the histogram **(c)** represent mean ± S.E.M. Asterisks depict the significance levels (**= p ≤ 0.01) obtained by t-test. Scale bars: 100 µm; Analysis was done 5 dpi; n = 3; Dashed lines indicate the site of injury.

The only glial cells whose proliferation remained unaffected were cells of the oligodendrocytic lineage. Systemic TCDD treatment lowered the number of BrdU+

oligodendrocyte progenitor cells with 0.0271 ± 0.0067 cells per µm³ instead of 0.0316 ± 0.0016 cells per µm³ only slightly and not significantly **(Figure 4.11).**

Figure 4.11

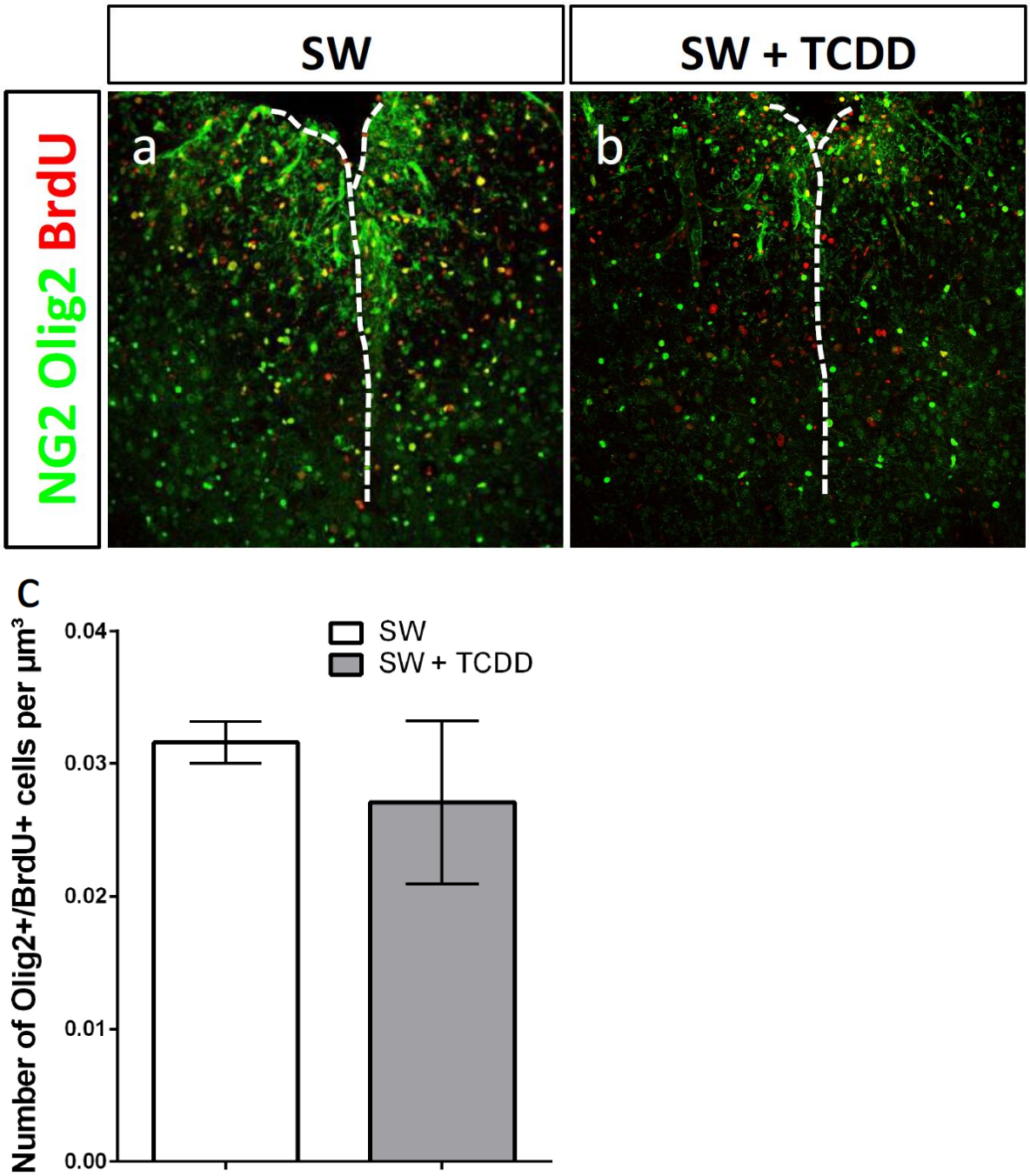

Figure 4.11 Effects of systemic TCDD administration on proliferation of oligodendrocyte progenitor cells.
Confocal images of the lesioned cortex stained against Olig2, NG2 and BrdU. TCDD treatment did not restrict proliferation of oligodendrocyte progenitors.
Bars in the histogram **(c)** represent mean ± S.E.M. Scale bars: 100 µm; Analysis was done 5 dpi; n = 3; Dashed lines indicate the site of injury.

Regarding the absolute numbers of marker+ cells, there was no obvious change in the quantities of GFAP+ reactive astrocytes and Olig2+ oligodendrocytes. Only microglial cells decreased significantly in number (n=3, p = 0.0297, t-test) **(Figure 4.12).**

Figure 4.12

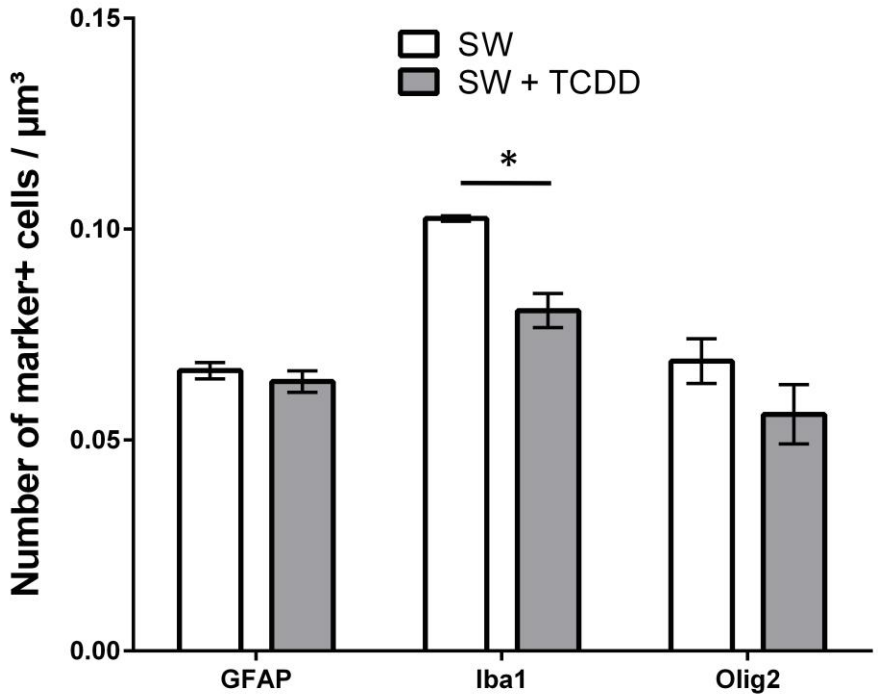

Figure 4.12 Numbers of different glial cells at the site of injury. The absolute numbers of astrocytes (GFAP) and oligodendrocyte progenitor cells (Olig2) did not change, while the number of microglia (Iba1) dropped significantly in response to systemic TCDD effects.
Bars in the histogram represent mean ± S.E.M. Asterisks depict the significance levels (*= $p \leq 0.05$) obtained by t-test. Analysis was done 5 dpi; n =5 for GFAP and n =3 for Iba1 and Olig2.

But AhR is only expressed in reactive astrocytes and not in microglia. Thus, similar effects of TCDD in both cell types surprise and raise the question if TCDD mediates the observed effects directly through AhR activation at the site of injury or rather through systemic changes that subsequently interfere with reactive glial cells.
Interestingly the number of proliferating cells in the SVZ (labelled by addition of BrdU to the drinking water for 4 days), where AhR is not expressed, was also significantly reduced upon systemic TCDD treatment (0.0314 ± 0.0020 vs. 0.0461 ± 0.0030 cells per μm^2; n=5, p = 0.0045, t-test) **(Figure 4.13)**. This rather suggests, that proliferation is affected due to indirect effects of systemic TCDD application **(Table 4.1).**

Figure 4.13

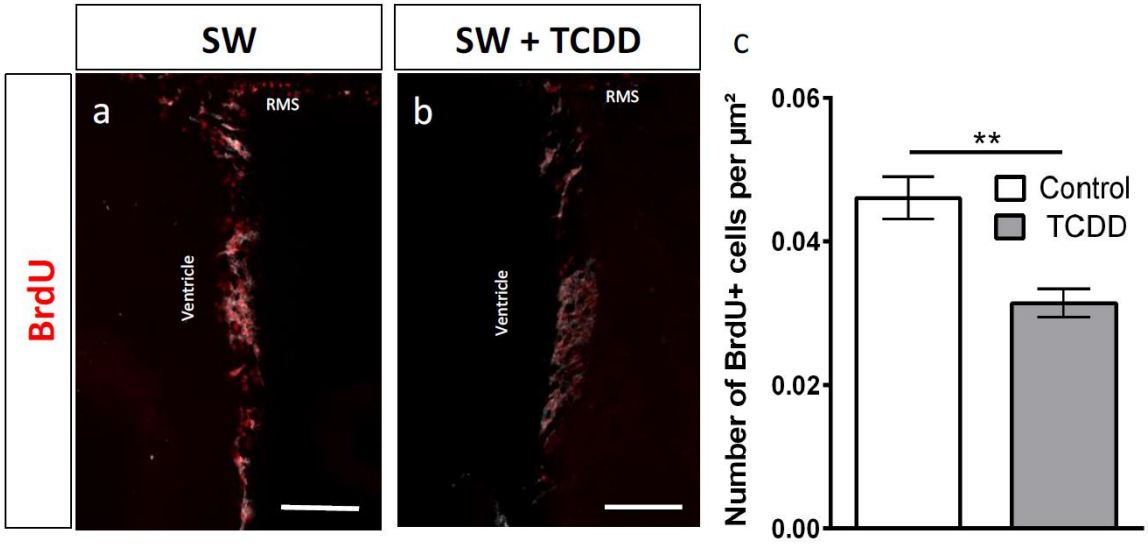

Figure 4.13 Effects of systemic TCDD administration on proliferation in the SEZ.
Confocal images of the lesioned cortex stained against BrdU. TCDD had an anti-proliferative effect on progenitor cells in the SEZ.
Bars in the histogram **(c)** represent mean ± S.E.M. Asterisks depict the significance levels (**= $p \leq 0.01$) obtained by t-test. Scale bars: 100 µm; Analysis was done after 4 days of BrdU infusion; n = 5. RMS = rostral migratory stream.

Table 4.1

Cell type	Changed proliferation upon systemic TCDD application	AhR expression
Astrocytes	Yes ✓	Yes ✓
Microglia	Yes ✓	No ✗
Oligodendrocyte progenitor cells	No ✗	No ✗
SEZ progenitors	Yes ✓	No ✗

Table 4.1 AhR expression and TCDD-induced changes in proliferation of different glial cell types.

Since newly proliferating astrocytes shield vital neuronal tissue against inflammatory and cytotoxic effects in the lesion core (Bush et al., 1999), we should make sure that neurons do not suffer any damage by TCDD-induced inhibition of proliferation. Concerning this issue, I counted the number of NeuN expressing neurons in the isocortex immediately adjacent to the stab wound, but I did not detect a significant change in the number of NeuN+ cells (0.0585 ± 0.0160 cells per µm³ in control conditions vs. 0.0480 ± 0.0039 cells per µm³ in TCDD treated animals) **(Figure 4.15)**

Figure 4.14

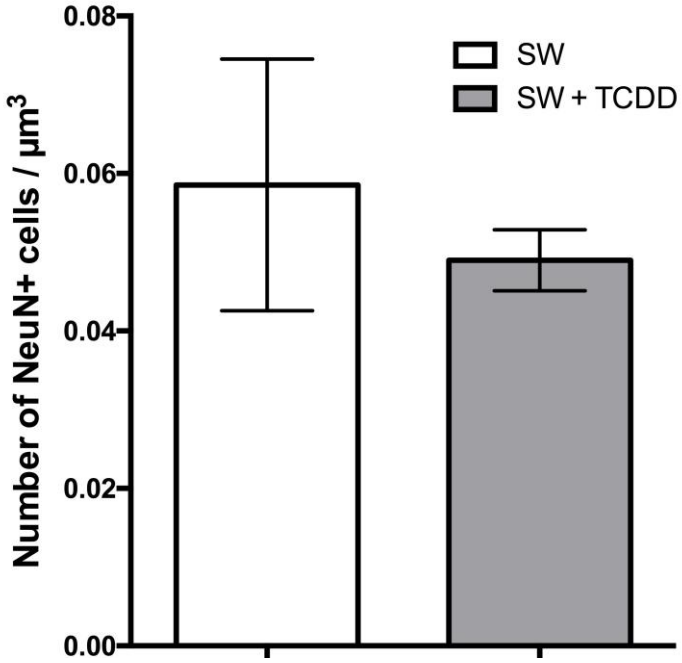

Figure 4.14 Numbers of NeuN+ cells at the site of Injury. Absolute numbers of NeuN+ cells (neurons) at the site of injury did not change upon systemic TCDD treatment. Bars in the histogram represent mean ± S.E.M; Analysis was done 5 dpi; n = 3.

4.2.2.2 Effects of local TCDD administration on reactive gliosis in vivo

To avoid systemic side effects of TCDD and to investigate the immediate function of AhR in reactive astrocytes, I changed the experimanetal approach towards local TCDD application **(Figure 4.4 b)**, by directly injecting TCDD into the stab wound 3 dpi and BrdU-labelling of proliferating cells from the point of injection until perfusion 5 dpi. In contrast to oral treatment, cortical TCDD injection did not interfere with proliferation in the SEZ **(Figure 4.15)**, supporting the assumption of a locally restricted TCDD effect.

Figure 4.15

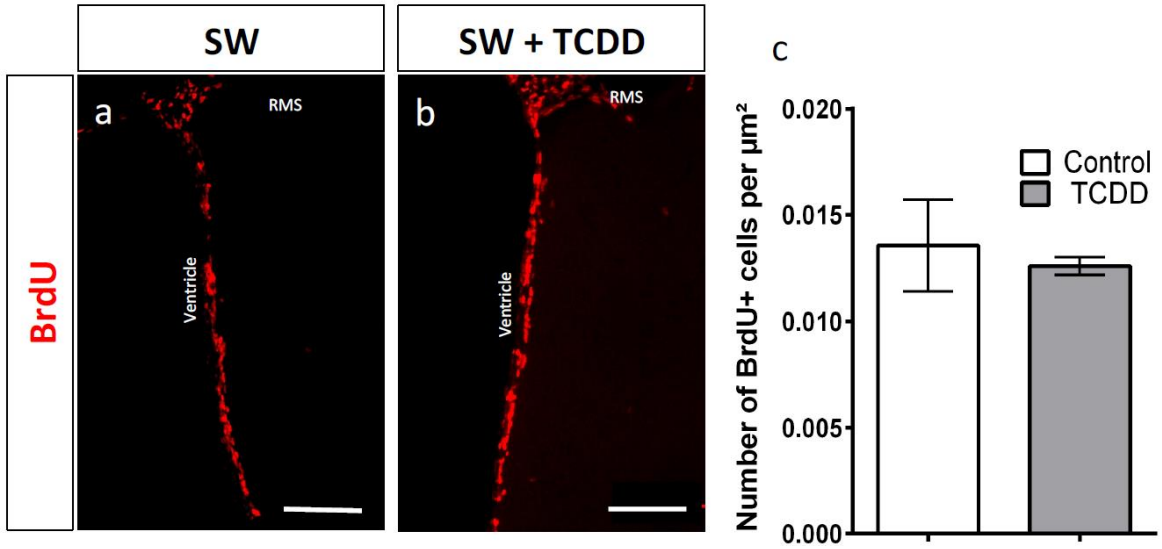

Figure 4.15 Effects of local TCDD administration on proliferation in the SEZ. Confocal images of the lesioned cortex stained against BrdU. Cortical TCDD injection did not interfere with proliferation of progenitor cells in the SEZ.
Bars in the histogram **(c)** represent mean ± S.E.M. Scale bars: 100 µm; Analysis was done after 2 days of BrdU infusion; n = 3. RMS = rostral migratory stream.

When administered locally, TCDD did not change the total numbers of BrdU+ cells and Ki67+ cells in the lesioned cortex. Quantification of proliferating cells gave 0.0091 ± 0.0016 Ki67+ cells and 0.0185 ± 0.0036 BrdU+ cells per μm^3 in vehicle controls and 0.0102 ± 0.0013 Ki67+ cells and 0.0254 ± 0.0028 BrdU+ cells per μm^3 in their TCDD-treated siblings **(Figure 4.16).**

Figure 4.16

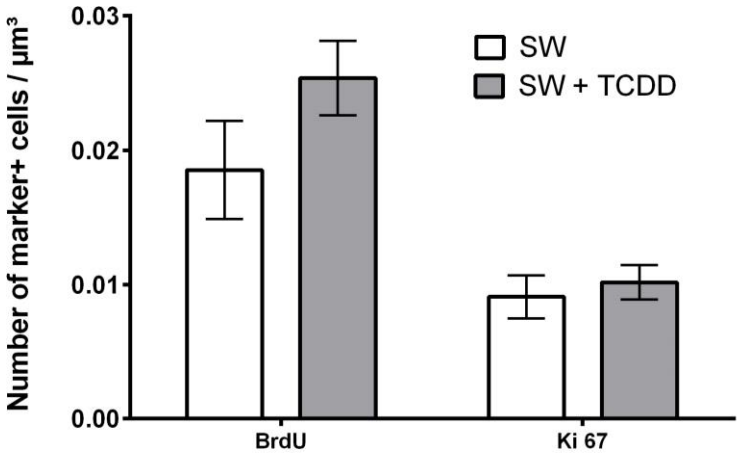

Figure 4.16 Proliferating cells in the injured cortex. Local TCDD treatment neither changed the number of BrdU+ cells, nor the number of Ki67+ cells at the site of injury significantly.
Bars in the histogram represent mean ± S.E.M. Analysis was done 5 dpi; n = 5.

Bearing in mind that systemic TCDD deprived proliferation of reactive astrocytes, I was surprised to see that local TCDD evoked the exact opposite effect. Injection of TCDD at the site of injury doubled the number of BrdU+/GFAP+ cells from 0.0040 ± 0.0005 cells per μm^3 to 0.0081 ± 0.0002 cells per μm^3 (n=5, p = 0.0003, t-test). The number of Ki67+/GFAP+ cells rose equally from 0.0023 ± 0.0001 cells per μm^3 to 0.0036 ± 0.0003 cells per μm^3 (n=5, p = 0.0106, t-test) **(Figure 4.17).**

Figure 4.17

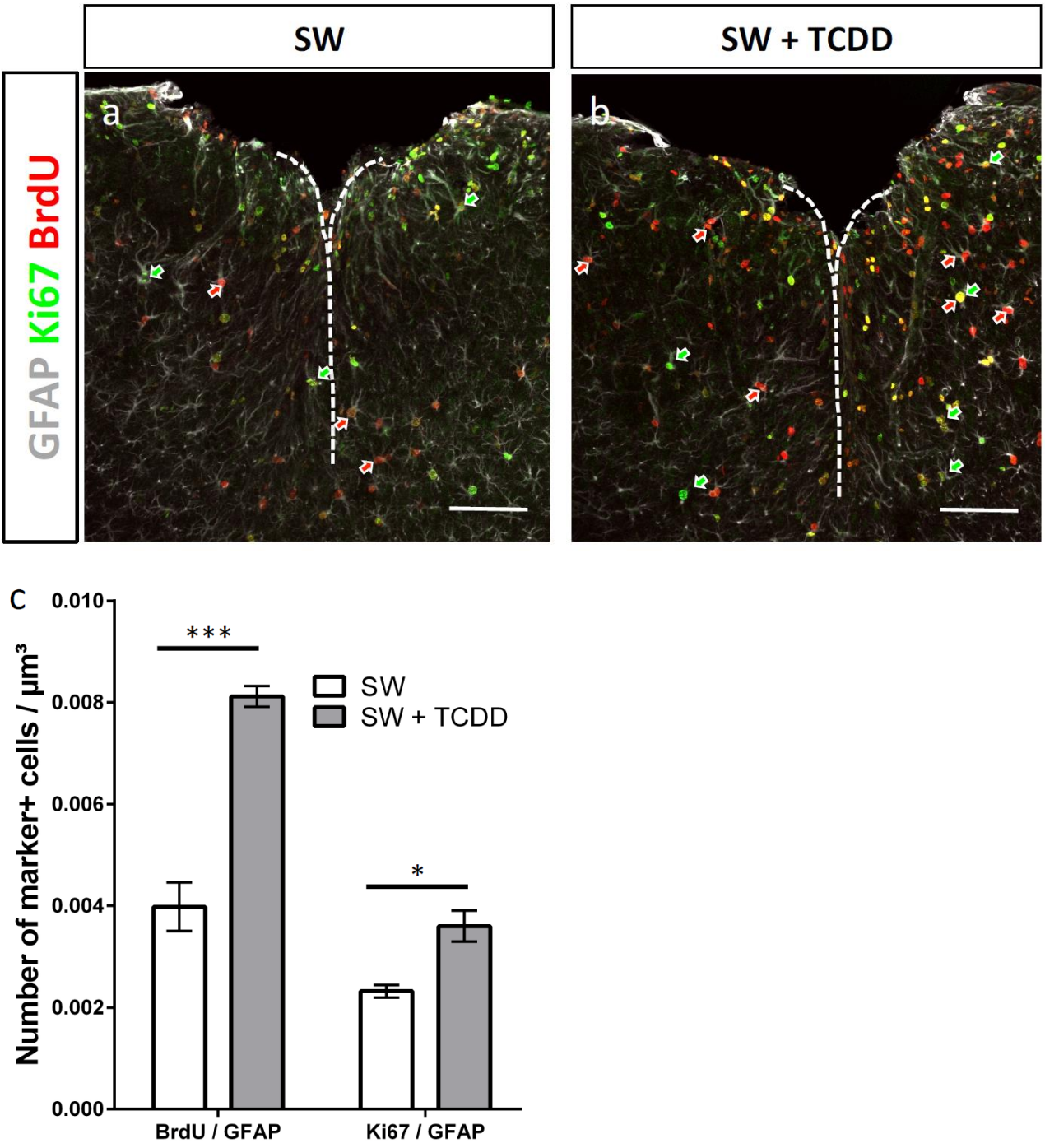

Figure 4.17 Effects of local TCDD administration on proliferation of astrocytes.
Confocal images of the lesioned cortex stained against GFAP, Ki67 and BrdU. TCDD **(b)** doubled the numbers of BrdU+ astrocytes compared to vehicle controls **(a)** and also increased the numbers of Ki67+ astrocytes. Red arrows: BrdU+ astrocytes, green arrows: Ki67+ astrocytes.
Bars in the histogram **(c)** represent mean ± S.E.M. Asterisks depict the significance levels (*= p ≤ 0.05; ***= p ≤ 0.001) obtained by t-test. Scale bars: 100 µm; Analysis was done 5 dpi; n = 5; Dashed lines indicate the site of injury.

Reactive gliosis is a complex process, which requires interaction of different cell types. Especially astrocytes and microglia are reported to interact by reciprocal activation and exchange of cytokines (Gao et al., 2013). Therefore it is worth examining the impact of AhR-induced changes in astrocytes on other glial cells, although local injection of TCDD avoided systemic side effects and although microglia and oligodendrocyte progenitor cells did not express AhR.

At 5 dpi I counted 0.0089 ± 0.0018 Iba1+/BrdU+ cells per µm³ under control conditions and 0.0094 ± 0.0024 Iba1+/BrdU+ cells per µm³ under TCDD treatment, what does not describe a significant difference between both groups **(Figure 4.18 a-a´´).** The same findings apply for the proliferation of cells from the oligodendrocytic lineage. 0.0064 ± 0.0009 Olig2+/BrdU+ cells per µm³ in vehicle controls compare with 0.0063 ± 0.0008 Olig2+/BrdU+ cells per µm³ in TCDD-treated animals **(Figure 4.18 b-b´´).**

Figure 4.18

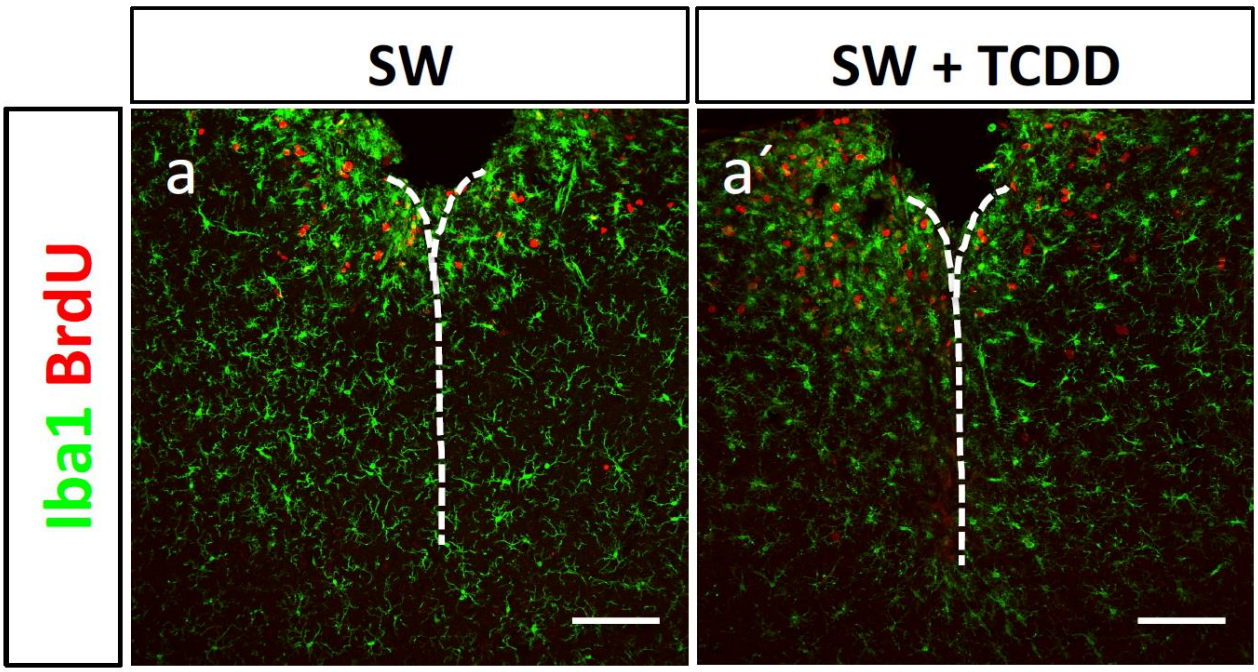

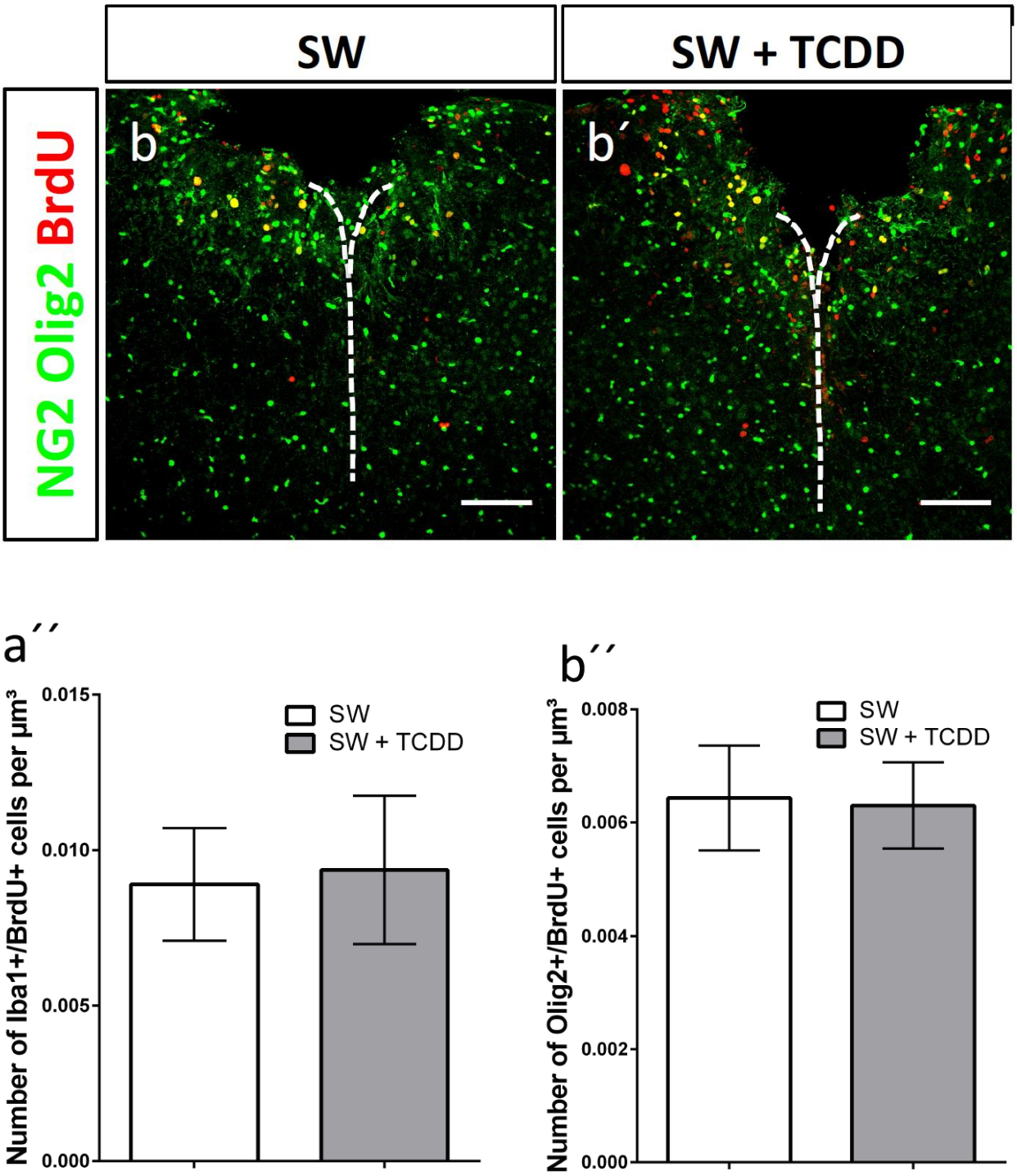

Figure 4.18 No effects of local TCDD administration on proliferation of microglia and oligodendrocyte progenitors.
Confocal images of the lesioned cortex stained against Iba1 and BrdU **(a, a´)** or Olig2, NG2 and BrdU **(b, b´)** Morphology and amount of Iba1+/BrdU+ cells appears similar in vehicle controls **(a)** and in TCDD-treated animals **(a´)**. Proliferation of oligodendrocyte progenitors also did not change under the influence of locally injected TCDD **(b´)**.
Bars in the histogram **(a´´, b´´)** represent mean ± S.E.M. Scale bars: 100 µm; Analysis was done 5 dpi; n = 3; Dashed lines indicate the site of injury.

In conclusion we can say, that local TCDD treatment acted specifically on astrocytes and allowed to study the pure effects of AhR activation in reactive astrocytes without interference of systemic side effects that would alter neurogenesis in the subependymal zone or proliferation of microglia and oligodendrocytes, as systemic TCDD-treatment did **(Table 4.2)**.

Table 4.2

Cell type	Changed proliferation upon local TCDD application	AhR expression
Astrocytes	Yes ✓	Yes ✓
Microglia	No ✗	No ✗
Oligodendrocyte progenitor cells	No ✗	No ✗
SEZ progenitors	No ✗	No ✗

Table 4.2 AhR expression and TCDD-induced changes in proliferation of different glial cell types.

Especially when TCDD is directly injected into the brain, it is essential to notice that the absolute numbers of glial cells remained stable **(Figure 4.19)**. With 0.0799 ± 0.0082 cells per µm³ in control conditions vs. 0.0728 ± 0.0036 cells per µm³ in TCDD treated animals, the numbers of NeuN+ neurons were also unaffected **(Figure 4.20)**.

Figure 4.19

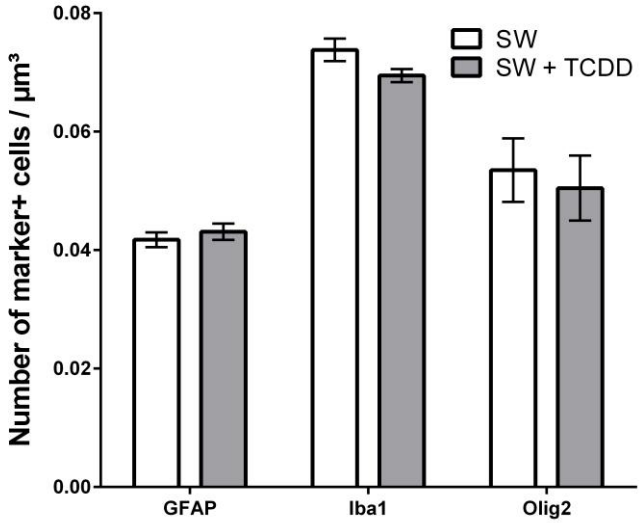

Figure 4.19 Numbers of different glial cells at the site of injury. Despite adjacent TCDD injection, the absolute numbers of astrocytes (GFAP), microglia (Iba1) and oligodendrocytes (Olig2) remained completely stable.
Bars in the histogram represent mean ± S.E.M. Analysis was done 5 dpi; n = 5 for GFAP and n = 3 for Iba1 and Olig2.

Figure 4.20

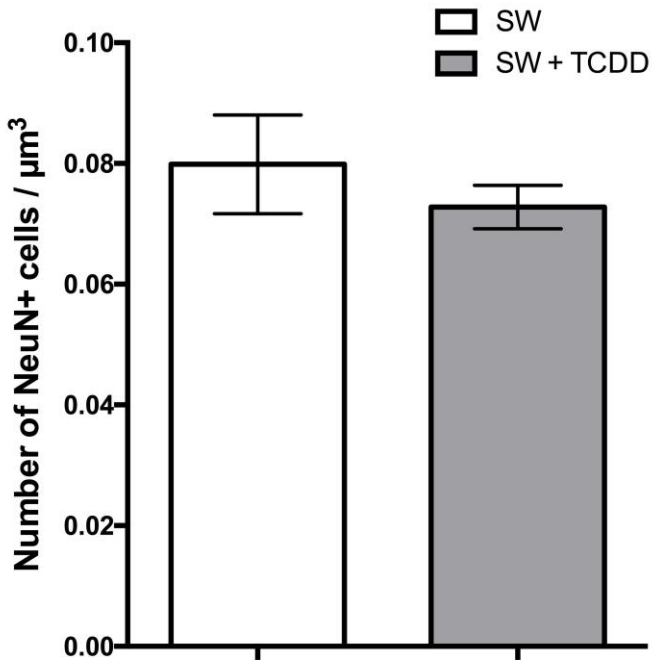

Figure 4.20 Numbers of NeuN+ cells at the site of injury. The absolute numbers of NeuN+ cells (neurons) at the site of injury did not change upon local TCDD treatment.
Bars in the histogram represent mean ± S.E.M; Analysis was done 5 dpi; n = 3.

4.2.3 Effects of AhR activation on Stem Cell Properties In Vitro

Immunohistochemistry showed that locally injected TCDD and subsequent AhR activation stimulates proliferation of reactive astrocytes. Reentering the cell cycle in order to proliferate requires mature astrocytes to dedifferentiate, what means that reactive astrocytes regain some features of glia in earlier developmental stages. Dedifferentiation confers reactive astrocytes with stem cell properties in vitro and causes expression of nestin, vimentin and tenascin-C in vivo.

These markers of immature glia are upregulated simultaneously with AhR; AhR plays a role in stem cells outside the brain, e.g. in the haematopoietic system (Boitano et al., 2010); and regulates embryonic stem cell differentiation (Gohlke, Stockton, Sieber, Foley, & Portier, 2009; Wang et al., 2013). This necessitates that we investigate whether AhR activation also supports the transition of mature astrocytes to immature progenitors with stem cell properties.

The neurosphere assay provides a tool to identify and quantify cells that form self-renewing and multipotent neurospheres in vitro and, hence, feature both hallmarks of stem cells: the ability to self-renew and the ability to differentiate into multiple cell types **(Chapter 3.3)**.

Figure 4.21

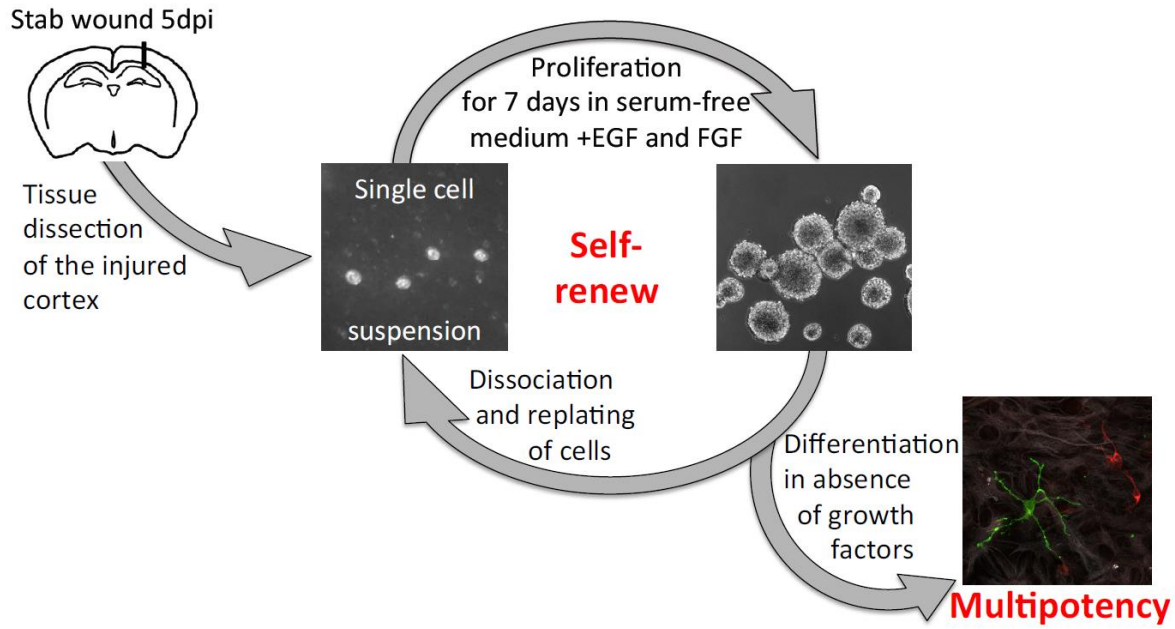

Figure 4.21 Scheme of the neurosphere assay. To address TCDD-induced changes in stem cell properties of reactive astrocytes, cells of the injured brain tissue were isolated at 5 dpi and plated in EGF-/FGF-containing neurosphere medium. Some of these cells formed neurospheres that were afterwards either differentiated to verify their multipotency or dissociated and replated to prove their self-renewing capacity.

4.2.3.1 Effects of local TCDD administration

For the following experiments I injected TCDD or the vehicle 3 dpi into the lesion site and isolated cells from the injured cortex 2 days later **(Figure 4.22 a)**. After 14 days of proliferation under neurosphere conditions, I could not detect any differences in the ability to from spheres. Cells obtained either from control animals **(Figure 4.22 b)** or TCDD-injected animals **(Figure 4.22 b´)** gave rise to a comparable number of spheres: i.e. 5.00 ± 0.58 spheres per 10,000 plated cells in controls and 6.33 ± 0.83 spheres per 10,000 plated cells upon TCDD **(Figure 4.22 c)**.

Figure 4.22

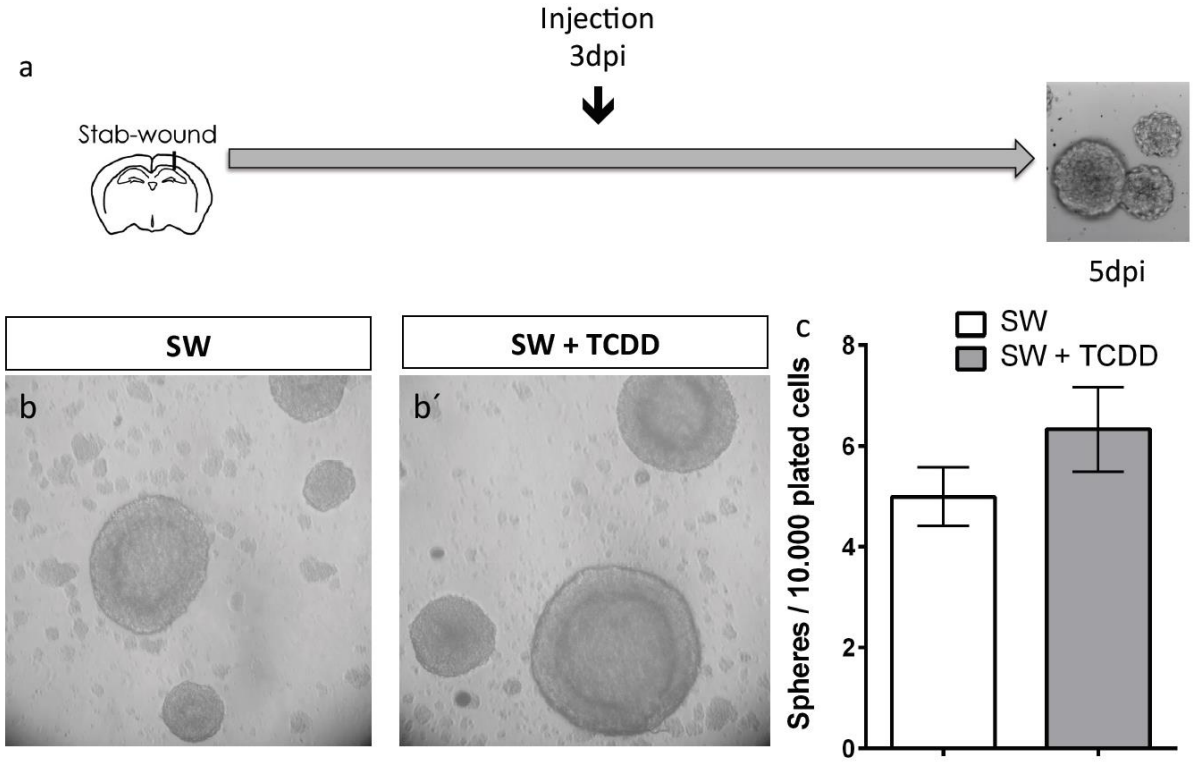

Figure 4.22 Effects of local AhR activation on injury-induced sphere formation in vitro. Scheme of local TCDD treatment **(a).** AhR activation by direct injection of TCDD 3 dpi was not sufficient to support sphere formation. After proliferation for 14 days in neurosphere medium neither number nor size of spheres appeared different. Brightfield images of primary neurospheres depict these observations **(b, b´).**
Bars in the histogram **(c)** represent mean ± S.E.M.**;** n = 3.

4.2.3.2 Effects of systemic TCDD administration

Local AhR activation did not affect sphere formation. Systemic AhR activation **(Figure 4.23 a)**, however, had a clear and unexpected effect. Although systemic TCDD treatment depleted the number of proliferating astrocytes in the injured cortex, it more than doubled the number of cells that kept proliferating under neurosphere conditions. Instead of 7.53 ± 0.052 cells per 10,000 plated cells, 16.47 ± 1.03 cells per 10,000 plated cells were able to form a primary neurosphere (n=3, p = 0.0001, t-test) within 14 days in culture **(Figure 4.23 c).**

Figure 4.23

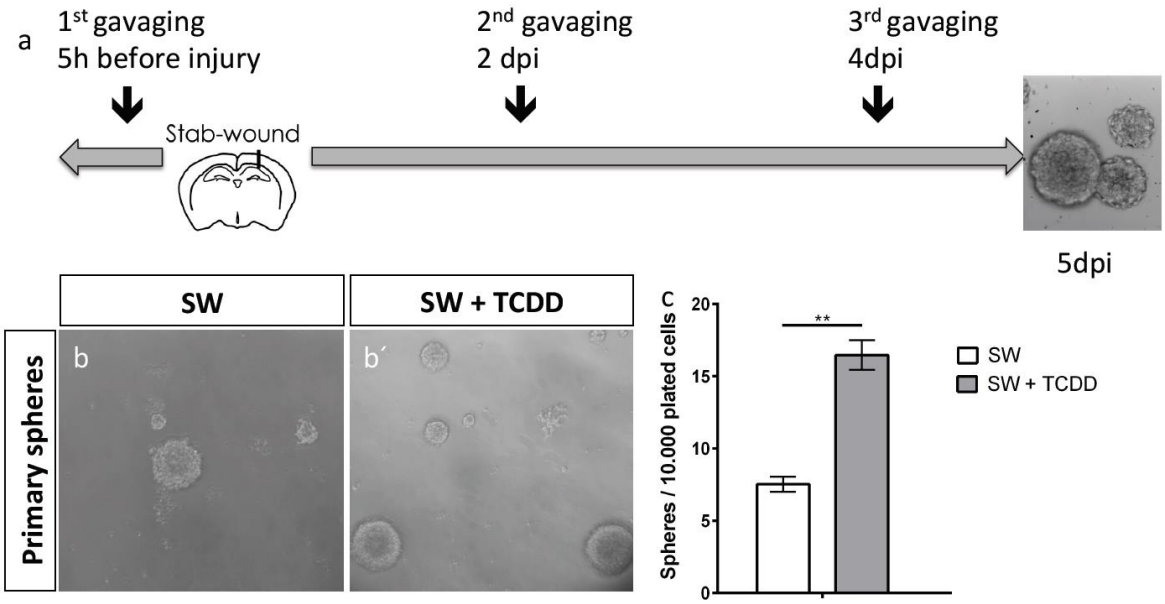

Figure 4.23 Effects of systemic AhR activation on injury-induced sphere formation in vitro. Scheme of systemic TCDD treatment **(a).** AhR activation by systemic TCDD application doubled the number of primary spheres **(c).** Brightfield images show representative primary neurospheres **(b, b´).**
Bars in the histogram **(c)** represent mean ± S.E.M.**;** n = 3.

But not only stem cells give rise to spheres in the neurosphere assay. Also transient amplifying cells might do so. Thus, stem cell properties of these spheres needed to be tested.

Differentiation on adhesive substrate in absence of mitogens reveals the potential of the cell that gave rise to a primary neurosphere. In order to be called multipotent, a cell must be able to generate cells from different lineages. In the case of neuronal stem cells these are neurons, oligodendrocytes and astrocytes. Immunohistochemic stainings after 7 days of differentiation **(Figure 4.24 a, a´)** showed that about one third of all spheres, no matter if derived from TCDD or vehicle treated animals, fulfilled this criterion **(Figure 4.24 b).**

Figure 4.24

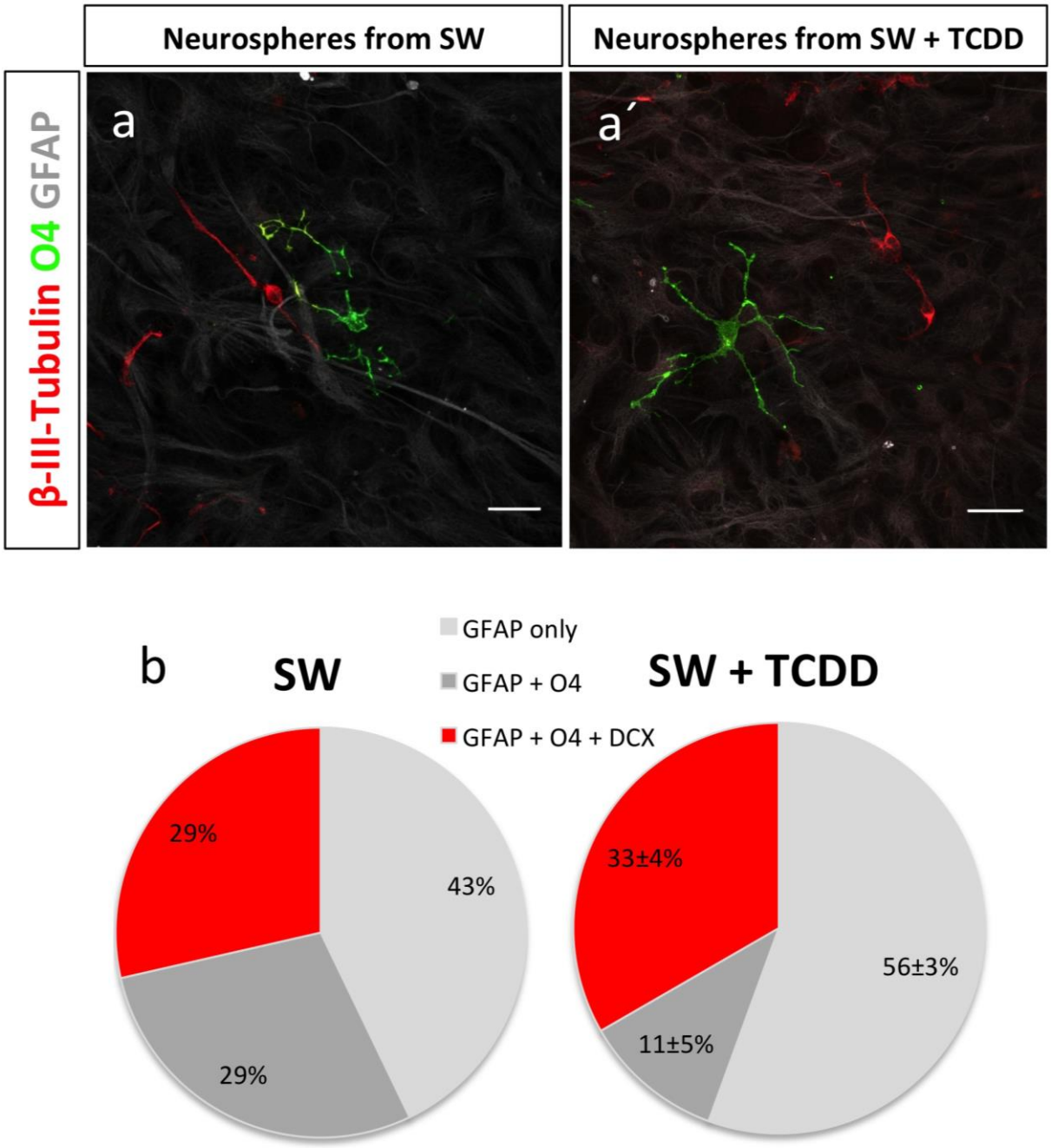

Figure 4.24 Multipotency of primary cortical neurospheres. Increased formation of primary neurospheres in response to systemic TCDD treatment did not affect their potential. In both conditions about one third of the spheres gave rise to neurons, astrocytes and oligodendrocytes **(b),** a feature that requires multipotency. Representatives of these multipotent spheres are pictured in confocal images **(a, a´).** Bars in the histogram **(c)** represent mean ± S.E.M.**;** n =3 for SW + TCDD, n=2 for SW only; Scale bars: 20 µm.

The second hallmark of stem cells is their ability to self-renew. If neurospheres that originate from stem cells are dissociated, re-plated as a single cell suspension and

afterwards cultured under neurosphere conditions for seven days, they will always give rise to new spheres **(Figure 4.21).**

Cells from systemic TCDD-treated animals initially produced twice as many primary neurospheres as did cells from vehicle-treated animals. But the following generations of spheres even produced many times more. After each passage, cells that originate from animals treated with TCDD gave rise to at least 7.69 times more neurospheres than did control cells **(Tab 7.3),** and it was not only the number of neurospheres, but also their size that was impressive **(Figure 4.25).** This increase in proliferation and self-renewing capacity lasted for at least three passages – and this means for at least 5 weeks – although the only thing that separated the two cultures was the previous TCDD administration in vivo.

Figure 4.25

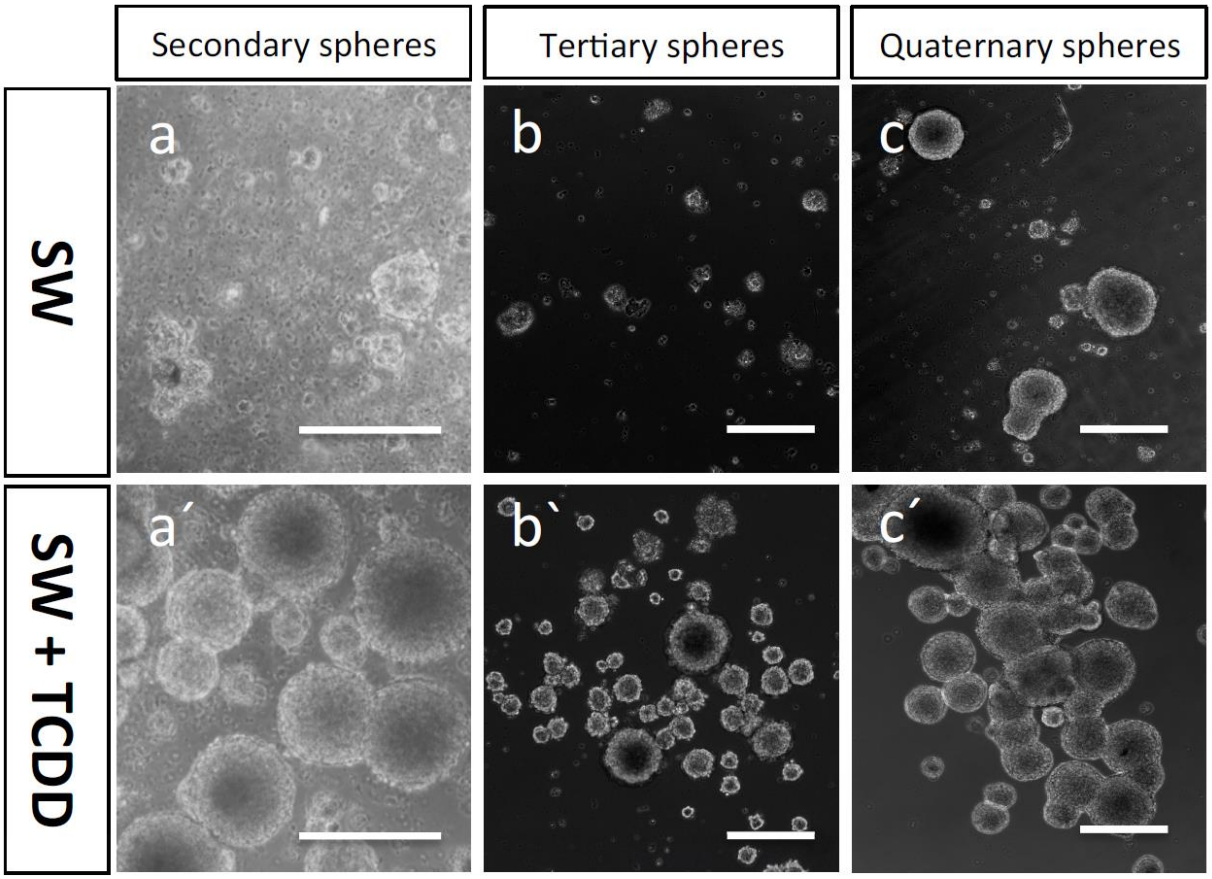

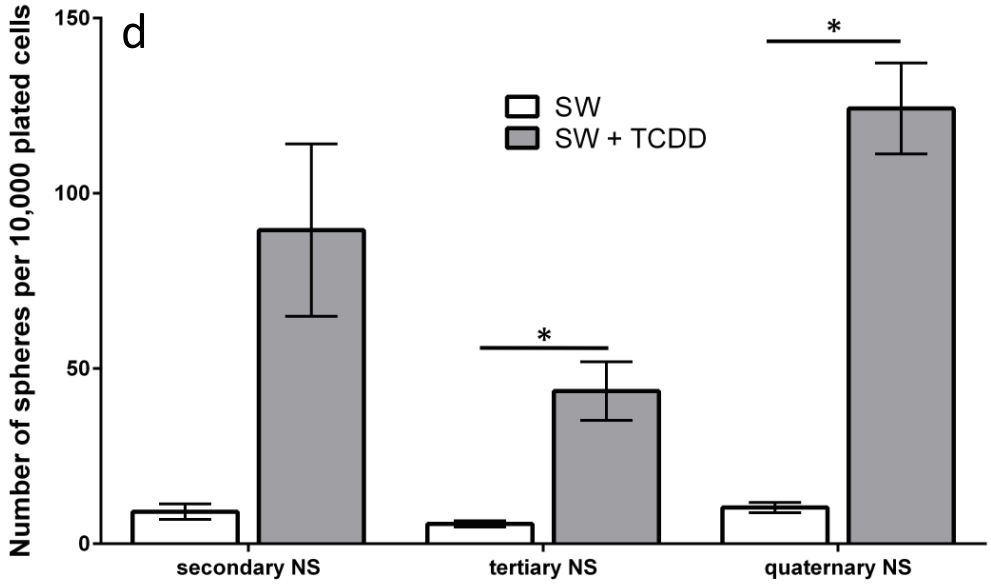

Figure 4.25 Self-renewing capacity of primary cortical neurospheres.
Systemic TCDD treatment increased proliferation and self-renewing capacity permanently. Spheres derived from TCDD treated animals were superior in size **(a, a´ - c, c´)** and number **(d).**
Bars in the histogram **(d)** represent mean ± S.E.M.**;** n = 3; p-value was obtained by t-test.
Scale bars: 200 µm.

Table 4.3

	Number of spheres per 10,000 plated cells		p-value	Fold change
	Vehicle	**TCDD**		
Primary spheres	7.53 ± 0.52	16.47 ± 1.02	0.0001	2.19
Secondary spheres	9.17 ± 2.19	89.50 ± 24.62	0.0813	9.76
Tertiary spheres	5.67 ± 0.88	43.56 ± 8.37	0.0441	7.69
Quaternary spheres	10.33 ± 1.45	124.22 ± 12.95	0.0119	12.02

Table 4.3 Sphere formation and self-renewing capacity of cells isolated from the injured cerebral cortex after systemic TCDD treatment.
Data is shown as mean ± S.E.M.; p-value was obtained by t-test.

When the neurosphere assay was performed with cells from the intact cortex or the SEZ, no significant changes in numbers or morphology of formed spheres were detectable. Cells isolated from the intact cortex contralateral to the SW gave rise to hardly any neurospheres. In vehicle controls these were 0.25 ± 0.25 spheres per 10,000 plated cells and 1.5 ± 0.50 spheres per 10,000 plated cells after systemic TCDD treatment. In both

conditions I was not able to passage these spheres, which questions, of course, their status as neurospheres.

Figure 4.26

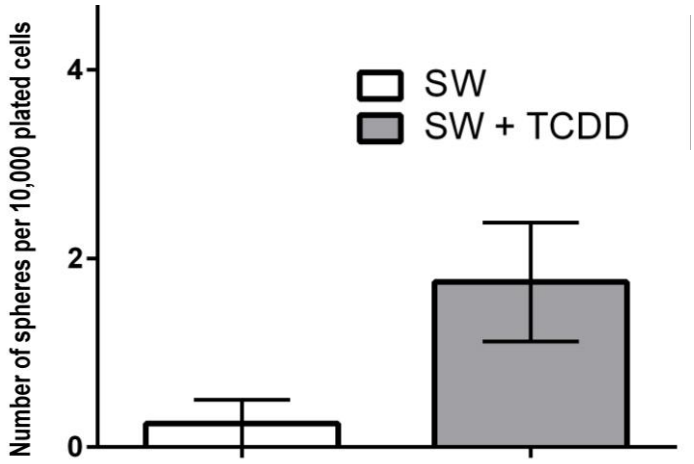

Figure 4.26 Effects of systemic AhR activation on sphere formation of the intact cortex. Without previous injury, systemic AhR activation did not change sphere formation.
Bars in the histogram **(a, b)** represent mean ± S.E.M.; n = 4

As expected from a neuronal stem cell niche, the SEZ generated a large number of neurospheres, but with 173.14 ± 59.40 spheres per 10,000 plated cells in controls and 187.89 ± 58.45 spheres per 10,000 plated cells upon TCDD treatment, the numbers of neurospheres did not change **(Figure7.27 a)**. Sphere size was also not significantly different **(Figure7.27 b)**.

Figure 4.27

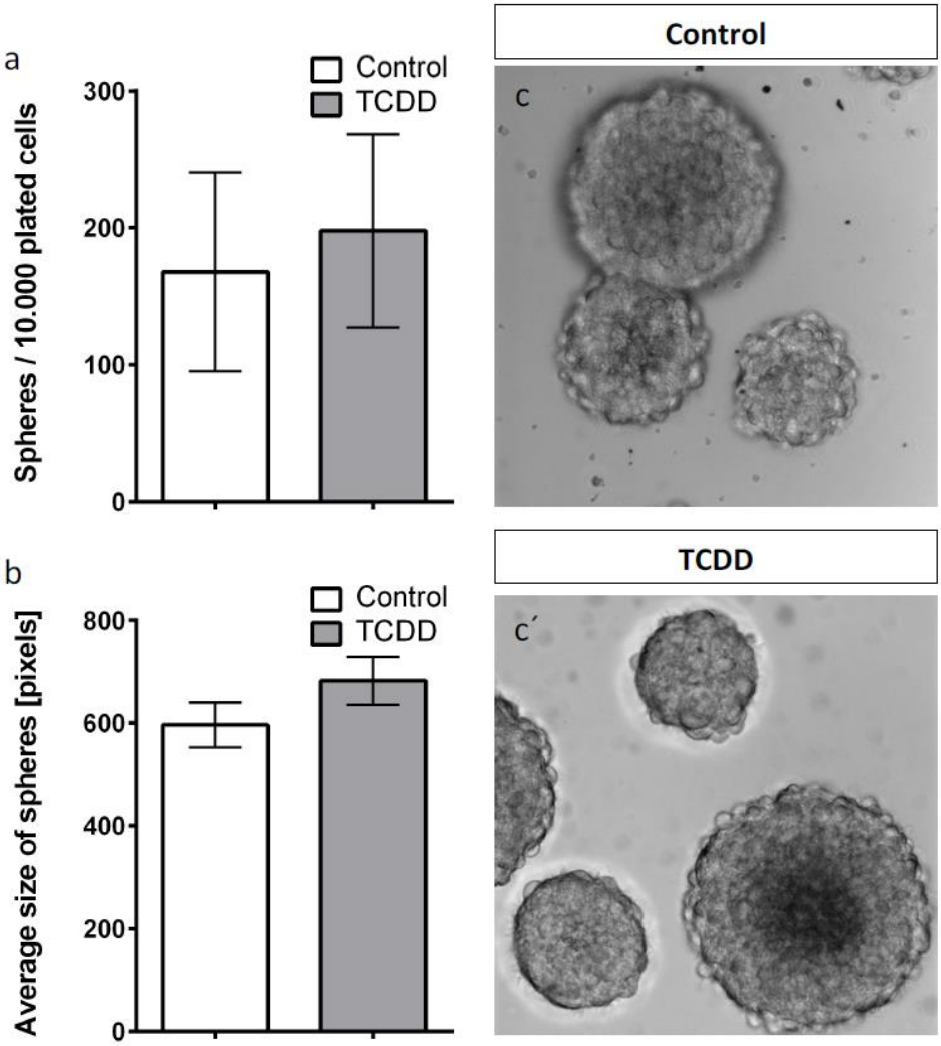

Figure 4.27 Sphere formation of the SEZ in response to systemic TCDD treatment. Systemic AhR activation did not affect neurosphere formation in the subependymal zone. Numbers **(a)** and size **(b)** of spheres remained unaltered. Representative brightfield images show primary SEZ neurospheres from controls or TCDD treated animals after 7 days in culture **(c, c´)**.
Bars in the histogram **(a, b)** represent mean ± S.E.M.; n = 6.

Table 4.4

Brain region	**Increased stem cell properties**		**AhR expression**
	TCDD local	**TCDD Systemic**	
Cortex intact	-	No ✗	No ✗
Cortex injured	No ✗	Yes ✓	Yes ✓
SEZ	-	No ✗	No ✗

Table 4.4 AhR expression and TCDD-induced changes in the stem cells content of different brain regions.

4.3 Proteomics

My previous experiments basically put forth three findings: **(Table 4.4)**

1.) Oral TCDD treatment was only able to increase sphere formation if the donor tissue expressed AhR.
2.) Systemic TCDD treatment, but not local TCDD treatment, was sufficient to increase sphere formation after stab wound injury.
3.) The major difference between these two methods of AhR activation in vivo was the extent of glial cell proliferation at the site of injury.

To further address the factors that enrich stem cells properties of reactive astrocytes upon systemic TCDD treatment, I submitted samples of the intact and injured cortex (5 dpi) with and without previous oral TCDD treatment to proteome analysis.[2] Analysis was performed on whole tissue samples to cover possible changes in reactive astrocytes as well as in their environment. Comparison of TCDD effects in the intact and the injured cortex was intended to distinguish between injury-related effects of TCDD and systemic effects that are independent from injury and cortical AhR expression.

Systemic side effects of TCDD treatment, which are not linked to AhR activation in the analysed cortical tissue and do not promote dedifferentiation of reactive astrocytes, might be present in both conditions: In the intact cortex and in the lesioned cortex. But TCDD-induced changes in protein expression that support the formation of neurospheres should only be present in the injured cortex but not in the intact cortex.

Label-free-LC-MSMS-based proteomic identified 2704 proteins. The normalized protein intensities were tested for differential expression in TCDD and vehicle treated mice and the resulting p-values were plotted against the ratios (TCDD / vehicle) in vulcano plots **(Figure 4.28).**

[2] Collaboration with Dr. Stefanie Hauck, Research Unit Protein Science, Helmholtz Zentrum München

Figure 4.28

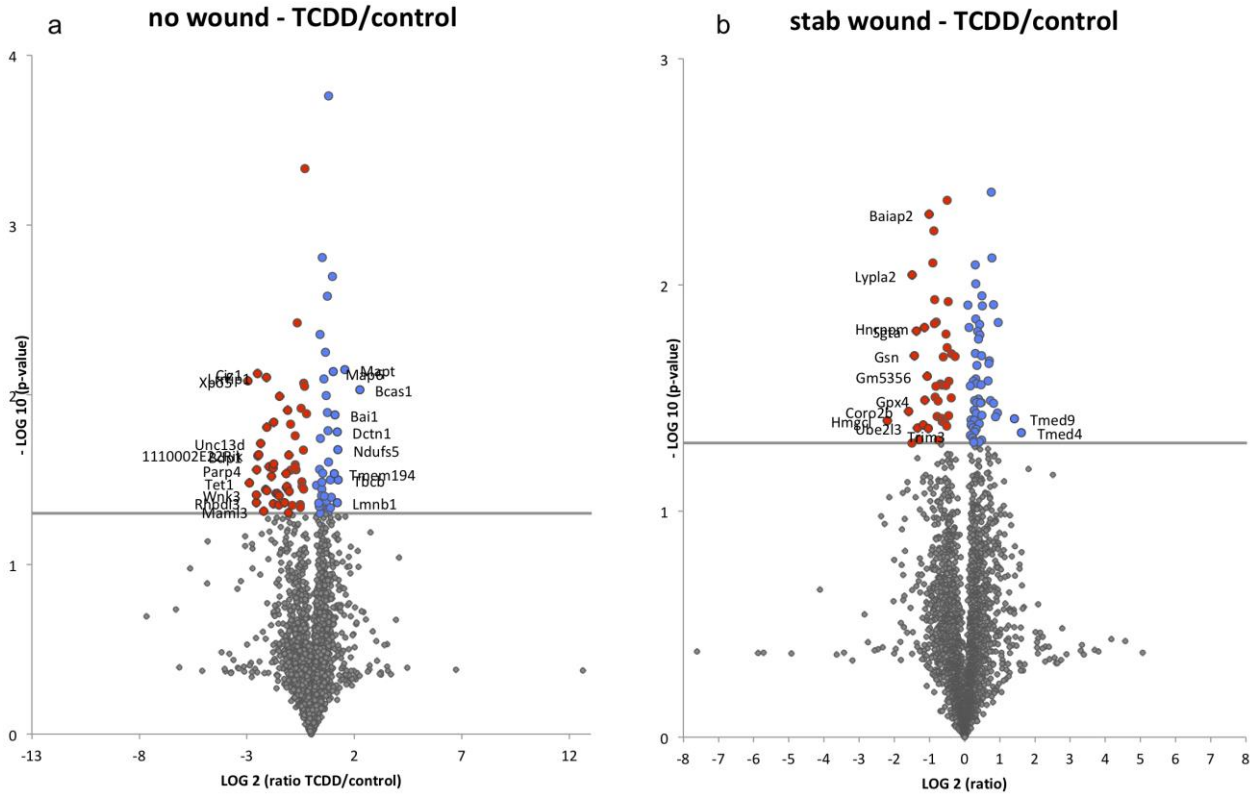

Figure 4.28 Volcano plots showing p- values (-log10) **and protein ratio** (log2) **of TCDD-treated vs. Vehicle-treated animals**. Dots above the horizontal line represent significantly enriched/depleted fractions in the intact cortex **(a)** and in the injured cortex **(b)** ($p < 0.05$). Dots on right sides represent proteins that are upregulated upon TCDD treatment and dots on left sides represent downregulated proteins. Significantly upregulated proteins are depicted in blue, significantly downregulated proteins are depicted in red.

In the injured cortex **(Figure 4.28 b)** we identified 95 proteins whose expression levels were significantly changed upon TCDD treatment. 54 were upregulated and another 41 were downregulated **(Table 4.5)**. TCDD treatment without injury resulted with 39 upregulated proteins and 53 downregulated proteins in altogether 92 differentially expressed proteins **(Figure 4.28 a)**. Remarkably, only 2 proteins changed concordantly in the injured and the intact cortex **(Table 4.5)** what points again to different effects of TCDD in both conditions.

Table 4.5

		Intact cortex			
	TCDD induced changes	Up	Down	No change	Sum
Injured cortex 5 dpi	Up	-	1	53	54
	Down	2	2	37	41
	No change	37	50	2522	2609
	Sum	39	53	2612	**2704**

Table 4.5 TCDD-induced changes in protein expression of the intact and injured cortex.

If we have a look at the significantly differently regulated proteins in the injured cortex, we can detect quite some interesting candidates, which are affected by AhR signalling or play a role in reactive gliosis. Slc7a2 for example is supposed to play a role in the classical or alternative activation of macrophages via its role in arginine transport (Yeramian et al., 2006). Otub1, whose expression rate was significantly lower upon TCDD, destabilizes the active ubiquitin E3 ligase GRAIL, which is crucial in the induction of CD4+ T-cell anergy (Soares et al., 2004). Akt/mTOR signalling controls stem cell pluripotency and differentiation (Yu & Cui, 2016). Since Akt is modulated by AhR signalling (Wu, Zhang, Hoagland, & Swanson, 2007; Xu et al., 2014) and since mTOR expression was significantly higher in samples of TCDD treated animals, this is one mechanism how AhR signalling might affect proliferation and fate of reactive astrocytes.
With the assistance of „The **D**atabase for **A**nnotation, **V**isualization and **I**ntegrated **D**iscovery (**DAVID**) v6.7" (Huang da, Sherman, & Lempicki, 2009), I tested all proteins that were upregulated upon TCDD treatment and all proteins that were downregulated upon TCDD treatment for enriched Gene Ontology (GO) terms, whereby the list of all identified proteins served as background. All significantly enriched GO terms (modified Fischer Exact Test: p-value $\leq$ 0.05) with at least 3 query genes are listed in **Table 4.6** and

Table 4.7.

Table 4.6

GO term	p-value	Fold enrich-ment	Proteins
Biological processes			
Cellular component assembly	0.0069	3.8	CORO1C, HIST1H2BC, GSN, BAIAP2, PAFAH1B1, PAK1, TUBB1
Cellular component biogenesis	0.0084	3.7	CORO1C, HIST1H2BC, GSN, BAIAP2, PAFAH1B1, PAK1, TUBB1
Cellular components			
Non-membrane-bounded organelle	6.64E-04	2.6	TCP1, HIST1H2BC, TWF2, SRCIN1, KIF5B, WASF1, GM9396, RPS5, CORO1C, CORO2B, GSN, PAFAH1B1, TUBB1, UBXN6
Intracellular non-membrane-bounded organelle	6.64E-04	2.6	TCP1, HIST1H2BC, TWF2, SRCIN1, KIF5B, WASF1, GM9396, RPS5, CORO1C, CORO2B, GSN, PAFAH1B1, TUBB1, UBXN6
Cytoskeleton	0.0012	3.1	CORO1C, CORO2B, TCP1, TWF2, KIF5B, SRCIN1, GSN, WASF1, PAFAH1B1, UBXN6, TUBB1
Cell leading edge	0.0237	6.1	GSN, WASF1, BAIAP2, PAFAH1B1
Microtubule cytoskeleton	0.0278	4.1	TCP1, KIF5B, PAFAH1B1, UBXN6, TUBB1
Centrosome	0.0369	9.4	TCP1, PAFAH1B1, UBXN6
Microtubule organizing centre	0.0433	8.6	TCP1, PAFAH1B1, UBXN6
Molecular function			
Cytoskeletal protein binding	0.0022	4.1	CORO1C, CORO2B, TWF2, KIF5B, GSN, WASF1, BAIAP2, PAFAH1B1
Actin binding	0.04114	3.7	CORO1C, CORO2B, TWF2, GSN, WASF1

Table 4.6 Go terms enriched in proteins that were significantly downregulated upon TCDD treatment in the injured cortex. P-value of enriched GO terms was obtained by Modified Fisher's Exact Test.

Table 4.7

GO term	p-value	Fold enrich-ment	Proteins
Biological processes			
Transport	0.0101	1.6	SYT1, COPA, SLC8A1, SYT2, SYT12, ATP1A3, SLC7A10, SFXN1, ARF6, ABCG3, TMED9, STXBP5L, RTN3, SLC32A1, TMED4, SLC25A25, SLC7A2, SLC30A1, SLC25A23, SEC22B, NDUFS2, RAB21
Establishment of localization	0.0106	1.6	SYT1, COPA, SLC8A1, SYT2, SYT12, ATP1A3, SLC7A10, SFXN1, ARF6, ABCG3, TMED9, STXBP5L, RTN3, SLC32A1, TMED4, SLC25A25, SLC7A2, SLC30A1, SLC25A23, SEC22B, NDUFS2, RAB21
Localization	0.0235	1.5	SYT1, COPA, SLC8A1, SYT2, SYT12, ATP1A3, SLC7A10, SFXN1, ARF6, ABCG3, TMED9, STXBP5L, RTN3, SLC32A1, TMED4, SLC25A25, SLC7A2, SLC30A1, SLC25A23, SEC22B, NDUFS2, RAB21
Cellular components			
Integral to membrane	1.60E-10	2.5	SYT1, COPA, SLC8A1, SYT2, SYT12, ATP1A3, SLC7A10, SFXN1, ARF6, ABCG3, TMED9, STXBP5L, RTN3, SLC32A1, TMED4, SLC25A25, SLC7A2, SLC30A1, SLC25A23, SEC22B, NDUFS2, RAB21
Intrinsic to membrane	3.30E-10	2.4	SYT1, COPA, SLC8A1, SYT2, SYT12, ATP1A3, SLC7A10, SFXN1, ARF6, ABCG3, TMED9, STXBP5L, RTN3, SLC32A1, TMED4, SLC25A25, SLC7A2, SLC30A1, SLC25A23, SEC22B, NDUFS2, RAB21
Membrane part	5.20E-07	1.7	SYT1, COPA, SLC8A1, SYT2, SYT12, ATP1A3, SLC7A10, SFXN1, ARF6, ABCG3, TMED9, STXBP5L, RTN3, SLC32A1, TMED4, SLC25A25, SLC7A2, SLC30A1, SLC25A23, SEC22B, NDUFS2, RAB21
Membrane	4.20E-06	1.6	SYT1, COPA, SLC8A1, SYT2, SYT12, ATP1A3, SLC7A10, SFXN1, ARF6, ABCG3, TMED9, STXBP5L, RTN3, SLC32A1, TMED4, SLC25A25, SLC7A2, SLC30A1, SLC25A23, SEC22B, NDUFS2, RAB21
Endoplasmic reticulum	0.0051	2.7	SYT1, COPA, SLC8A1, SYT2, SYT12, ATP1A3, SLC7A10, SFXN1, ARF6, ABCG3, TMED9, STXBP5L, RTN3, SLC32A1, TMED4, SLC25A25, SLC7A2, SLC30A1, SLC25A23, SEC22B, NDUFS2, RAB21
Plasma membrane	0.0112	1.7	SYT1, COPA, SLC8A1, SYT2, SYT12, ATP1A3, SLC7A10, SFXN1, ARF6, ABCG3, TMED9, STXBP5L, RTN3, SLC32A1, TMED4, SLC25A25, SLC7A2, SLC30A1, SLC25A23, SEC22B, NDUFS2, RAB21
Molecular function			
Transporter activity	0.0177	2.2	SLC32A1, SYT1, SLC8A1, SLC30A1, SLC7A2, SYT2, SLC25A23, SYT12, ATP1A3, SLC7A10, SFXN1
Transmembrane receptor activity	0.02082	4.5	EPHA4, GPR162, GABBR2, MOG, GPR37L1

Table 4.7 Go terms enriched in proteins that were significantly upregulated upon TCDD treatment in the injured cortex. P-value of enriched GO terms was obtained by Modified Fisher's Exact Test.

GO term analysis yielded several significantly ($p \leq 0.05$, Modified Fisher's Exact Test) downregulated terms **(Table 4.6)**. Among them are Cellular component biogenesis and

assembly, Cytoskeleton, Cell leading edge, Microtubule cytoskeleton, Centrosome and Microtubule organizing centre, reflecting the TCDD-induced impairment of proliferation after stab wound injury. The significantly overrepresented GO terms are mostly related to membrane proteins including proteins with transporter or receptor activity **(Table 4.7)**, reflecting differences in intracellular signalling pathways.

5 Discussion

The absence of AhR in the intact cortex and the massive upregulation in response to TBI demonstrates that TBI triggers AhR expression and that AhR signalling is involved in the subsequent process of wound healing.

Immunohistochemical stainings identified astrocytes as the only cell type expressing AhR and showed that AhR is expressed by all reactive astrocytes in a diameter up to 500 µm around the injury site. The expression of AhR in reactive astrocytes occurred simultaneously to the upregulation of GFAP, the classical marker for reactive astrogliosis, and peaked at 3 dpi, right at the time when astrocytes start proliferating and expressing markers of immature astrocytes like Nestin, Vimentin and tenascin-C (Robel, Berninger, & Gotz, 2011). This implies that AhR is either mediator or part of these reactive changes in astrocytes. Reactive astrocytes regain features of glia present at earlier developmental stages and stem cell properties, at least in vitro. AhR regulates differentiation and self-renewal of numerous stem cell populations, such as in the hematopoietic (Boitano et al., 2010; Smith et al., 2013) and the lymphoid system (Li et al., 2011), in the CNS (Dever et al., 2016; Latchney et al., 2011) and in liver (Walisser, Glover, Pande, Liss, & Bradfield, 2005). Therefore, the expression of AhR in reactive astrocytes also suggests that AhR has a role in the process of astrocyte reactivation, dedifferentiation and proliferation.

Consistent with previously published data (Latchney et al., 2013; Petersen et al., 2000), I found AhR expressing cells in the subgranular zone of the hippocampus, one of the two major brain regions where adult neurogenesis occurs. This emphasizes the role of AhR in the regulation of stem cell populations and confirms the reliability of my immunohistochemic stainings. But AhR was not detectable in the second neurogenic niche, the subependymal zone (SEZ) of the lateral ventricle. Thus, AhR seems to be involved in the proliferation and differentiation of various types of stem cells, including adult neuronal stem cells, but is not obligatory to this process.

Without potentiation of AhR signalling by TCDD, I located AhR exclusively in the cytoplasm of astrocytes. This corresponds to the inactive state of AhR and it is curious, why AhR in reactive astrocytes is highly expressed but inactive. Either I missed the time of physiological AhR activity, or the concentration of nuclear AhR was below the detection rate of my immunohistochemic staining. It is also possible that AhR does not act via the canonical AhR signalling pathway, but crosstalks with other signalling

pathways like the EGFR, which does not demand a nuclear transport of AhR (Enan & Matsumura, 1995).

The expression levels of AhR varied quite significantly among individual astrocytes. Some astrocytes express very high levels of AhR, comparable to cells in the subgranular zone of the hippocampus, whereas others show only slight AhR-stainings. As shown in co-stainings with BrdU and Ki67, this variability does not correlate with the proliferative stage of astrocytes. Although little is known about local differences of astrocytes, it is generally assumed that astrocytes are a heterogeneous group of cells (Anderson, Ao, & Sofroniew, 2014). The assumption of local heterogeneity among neighbouring astrocytes is supported by studies that report variable expression levels of different chemokines or cytokines (Hamby et al., 2012), the transcription activator Stat3 (Herrmann et al., 2008) and transcription factors that are necessary for sonic hedgehog signalling (Garcia, Petrova, Eng, & Joyner, 2010). Stab wound lesions of the cerebral cortex evoked elective proliferation of juxtavascular astrocytes, which points towards a functional specialization among reactive astrocytes (Bardehle et al., 2013). Similarly, AhR signalling might also acts on particular subpopulations and functions of reactive astrocytes.

5.1 Effects of AhR activation on reactive gliosis

In order to study the role of the AhR pathway in reactive gliosis, I potentiated AhR signalling by either local or oral administration of the potent and intensively studied AhR agonist TCDD. Both, oral and local TCDD administration, changed proliferation rate of reactive astrocytes significantly and, most strikingly, oral TCDD treatment more than doubled sphere formation in the neurosphere assay. Differentiation of spheres showed comparable neurogenic potential of spheres from TCDD-treated and untreated animals. However, they differed clearly in terms of self-renewal and proliferation. While primary spheres form TCDD-treated animals appeared marginally smaller than spheres from vehicle treated controls, subsequent generations of spheres from TCDD-treated animals were much bigger and much more numerous than control spheres. These changes lasted for several generations of spheres although culture conditions were exactly the same. This indicates robust, TCDD-induced changes within the sphere forming cells that also affect following generations of sphere forming cells.

The increase in neurosphere formation is a remarkable finding, especially since proliferation of reactive astrocytes in vivo was clearly impaired upon systemic TCDD

treatment. Until now, proliferation of astrocytes in vivo and sphere formation in vitro have always been regarded as two indicators of the same process: The differentiation of reactive astrocytes in response to brain injuries (Buffo et al., 2008; Sirko et al., 2013). Here on the contrary, decreased numbers of proliferating astrocytes were accompanied by increased generation of neurospheres. To my knowledge, this is the first time it is shown that proliferation and dedifferentiation do not necessarily go hand in hand and might depend on different mechanisms that are only effective in a distinct subtype of astrocytes. The inconsistent expression levels of AhR in neighbouring astrocytes support this hypothesis, although the correlation of AhR-expression with stem-cell properies still needs to be evaluated.

Importantly, neuronal survival was not impaired by increased stem cell properties and reduced proliferation of astrocytes and other glial cells. The number of NeuN+ cells round the injury did not change upon TCDD treatment and systemic treatment with TCDD increased stem cell properties without boosting reactive gliosis, which is regarded to be causative for the failure of neuronal regeneration after injury. Therefore, AhR is a promising target in the search for regenerative therapies for all kind of diseases that are associated with a loss of functional neurons.

Oral TCDD treatment generally reduced the number of proliferating cells in the stab-wounded cortex and in the SEZ. Hence, it was not clear, weather the observed changes in reactive gliosis are due to a direct effect of AhR activation in reactive astrocytes of if they are rather due to systemic effects of TCDD. TCDD did not act specifically on AhR expressing astrocytes but reduced proliferation of all glial cells and of progenitor cells in the SEZ, which rather suggests a systemic effect of TCDD. But it is also known that different glial cells interact in response to brain injuries. Therefore, reduced proliferation of reactive astrocytes as a direct effect of AhR activation might also alter the proliferation rate of neighbouring glial cells. In the contralateral intact cortex, where AhR is not expressed, TCDD treatment did not increase sphere formation and in the SEZ, proliferation but not sphere formation was affected by systemic TCDD treatment. These findings rather suggest that the increase of sphere formation in the injured cortex is due to a direct effect of AhR at the site of injury whereas the reduced proliferation of all glial cell lines reflects systemic TCDD effects.

AhR suppresses inflammatory responses (Huai et al., 2014; Rothhammer et al., 2018), induces a switch in T-cells from a stimulatory into a regulatory phenotype, the T_{reg}-cells, and suppresses T cell-dependent immune reactions (Mascanfroni et al., 2015; Mohinta

et al., 2015; Quintana et al., 2008). The activation of AhR in liver cells induces the release of TGF-β, a cytokine that limits inflammation after brain injuries and attenuates microglial activation (Cekanaviciute, Dietrich, et al., 2014; Cekanaviciute, Fathali, et al., 2014; Norden, Fenn, Dugan, & Godbout, 2014). Furthermore, astrocytic or microglial AhR activation by tryptophan metabolites limit CNS inflammation (Rothhammer et al., 2018). But inflammation triggers tissue repair and wound healing (Martin & Leibovich, 2005) and invasion of immune cells is necessary to evoke proliferation of astrocytes (Berger, Hiestand, Kindler-Baumann, Rudin, & Rausch, 2006). Thus, the reduced level of reactive gliosis might also mirror a suppressed immune response.

In order to look into direct effects of AhR activation at the site of injury, I injected TCDD 3 dpi directly into the stab-wounded cortex. Although the nuclear localization of AhR in the immunostainings proved the efficiency of both ways of AhR activation, the local and oral TCDD-administration, local treatment failed to increase sphere formation. But it specifically promoted proliferation of reactive astrocytes, the only AhR expressing cells in the injured cerebral cortex. Proliferation of other glial cell types at the site of injury and proliferation of progenitor cells in the SEZ was not affected, which argues for a direct effect of AhR activation in reactive astrocytes.

5.2 Discrepancy between effects of local and oral TCDD treatment

Following systemic TCDD treatment, I observed an increase in sphere formation specifically in the cortex, what rather suggests a direct effect of TCDD, but local TCDD administration failed to increase sphere formation. This can be attributed to a wrong time of administration or an ineffective dose of TCDD. In zebrafish, AhR was inactivated within 2 dpi. Permanent activation increased neuronal differentiation but depleted the number of proliferating progenitors. If we transfer these findings to mouse, we can hypothesize that the initial AhR signalling fosters dedifferentiation of reactive astrocytes and allows them, at least in vitro, to give raise to neurons. Afterwards, AhR signalling is reduced to promote proliferation of dedifferentiated astrocytes. This might also explain why we cannot detect AhR in the nucleus at 5 dpi. Injection of TCDD at 3 dpi might not be sufficient to keep AhR signalling at a high level until 5 dpi in order to increase sphere formation in the neurosphere assay or, if astrocytes are already primed towards their gliogenic fate, an injection at 3 dpi is too late to induce a more neurogenic fate by the potentiation of AhR signalling.

We should also consider, that systemic TCDD treatment did not only alter proliferation of astrocytes, but also the proliferation of each glial cell line. Reactive gliosis at the site of injury has got beneficial and detrimental effects. It helps to restore the BBB after TBI and protects still viable cells from further harm. But it also creates a gliogenic environment, which hinders neuronal regeneration and axonal regrowth. Thus, AhR activation alone might not be sufficient to increase stem cell properties of reactive astrocytes. Only if AhR activation occurs in a more permissive milieu with a lower degree of gliosis and less inflammation, it can increase stem cell properties of reactive astrocytes. The gliogenic environment of the cerebral cortex might not only hinder dedifferentiation of reactive astrocytes. It also keeps reactive, proliferating astrocytes within their lineage in vivo, whereas in vitro they are able to generate astrocytes, oligodendrocytes and neurons. Thus, it might be the combination of AhR activation, reduced inflammation and a lower degree of reactive gliosis at the site of injury that promotes stem cell properties.

5.3 Proteomic

We performed a proteome analysis to get a better understanding of the mechanisms by which systemic TCDD treatment favours neurosphere formation and stem cell properties at the site of injury. Subsequent GO term analysis of all downregulated proteins showed a significant increase of GO terms related to cell proliferation, which confirms the effects observed by immunostainings. Significantly upregulated upon TCDD treatment were mainly membrane proteins such as transmembrane receptors and transporters, which reflect differences in cell signalling and metabolism.

In order to get an idea of whether the increase in neurosphere formation is due to systemic or local effects of the oral TCDD treatment, I examined the proteome data for proteins that are annotated to the GO-terms “immune system process”, “transforming growth factor beta receptor signalling pathway” and “tumour necrosis factor-mediated signalling pathway”, since these domains are known to be affected by systemic TCDD treatment and interfere with reactive gliosis and neuroinflammation (Berger et al., 2006; Cekanaviciute, Dietrich, et al., 2014; Cekanaviciute, Fathali, et al., 2014; Cheon et al., 2007; Huai et al., 2014; Mohinta et al., 2015; Norden et al., 2014; Rier et al., 2001). Transforming growth factor beta and tumour necrosis factor alpha do not seem to cause the increase in stem cell properties, since none of the 18 identified proteins related to “transforming growth factor beta receptor signalling pathway” and none of the 25

identified proteins related to “tumor necrosis factor” or “tumor necrosis factor-mediated signalling pathway” differed significantly between TCDD treated animals and vehicle treated controls. I also found 236 proteins that are involved in “immune system processes” and 12 of them differed significantly between TCDD treated animals and vehicle treated controls. This resembles the general proportion of significantly different proteins (= 95/2704) and GO term analysis also did not show enrichment in terms related to the immune system. Most of these 12 proteins are not unique for the immune system, but play a general role in cellular metabolism, growth or microtubule-dependent processes.

Some of the differentially regulated proteins are quite interesting in context of reactive gliosis. Slc7a2 plays a role in the in classical or alternative activation of macrophages (Yeramian et al., 2006), Otub1 is crucial in the induction of CD4+ T-cell anergy (Soares et al., 2004) and Akt/mTOR signalling controls stem cell pluripotency and differentiation (Yu & Cui, 2016). Since Akt is modulated by AhR signalling (Wu et al., 2007; Xu et al., 2014) and since Mtor expression was significantly higher in samples of TCDD treated animals, this is one possible mechanism how AhR signalling affects proliferation and fate of reactive astrocytes. But we should be careful not to overestimate the functional relevance of these proteins. We see only single proteins without their involvement in certain functions and pathways and in order to get a reliable readout, the differential expression of these proteins still has to be validated by western blot or real-time PCR.

5.4 Outlook

My work demonstrates that AhR signalling affects reactive astrogliosis. However, the exact mode of action remains to be investigated. Oral TCDD treatment increased sphere formation in the neurosphere assay and it will be important to find out, which TCDD-induced changes really promote stem cell properties of reactive astrocytes. It should be verified, whether AhR activation in combination with a lower degree of gliosis can help to regenerate neurons from reactive astrocytes after TBI, similar to ependymoglia in the injured zebrafish telencephalon. At 5 dpi I could not observe any DCX (marker for immature neurons) positive cell at the site of injury, but this time period might be too short and should be extended to draw a definitive conclusion.

It is known that reactive astrocytes divide only once in response to TBIs before they reenter the post-mitotic state. In brain section of TCDD treated animals, however, several astrocytes were clustered in groups of at least 3. Clonal analysis techniques will

help to see, weather AhR activation is sufficient to keep astrocytes in their proliferative state, so that they divide more than once.

The most important task will be to examine the physiological function of AhR in reactive gliosis. Since the receptor affinity differs between TCDD and endogenous ligands and since ligand-dependent effects have been reported in other organs, activation studies are not appropriate for this aim. Furthermore, immunohistochemical stainings showed only cytoplasmic AhR in absence of the external ligand TCDD, which means that AhR might act via non-canonical pathways such as crosstalk with the EGFR. These restrictions ask for experimental settings in which AhR can be selectively blocked in reactive astrocytes. Conditional knockout mice with a floxed AhR-gene, which express CreER(T2) recombinase under the promoter of the astrocyte-specific glutamate transporter (GLAST) or GFAP, are a promising approach to investigate the physiological functions of AhR in reactive gliosis and to separate indirect, systemic effects of AhR activation from effects of AhR activation directly in reactive astrocytes.

6 References

Abel, J., & Haarmann-Stemmann, T. (2010). An introduction to the molecular basics of aryl hydrocarbon receptor biology. *Biol Chem, 391*(11), 1235-1248. doi:10.1515/BC.2010.128

Anderson, M. A., Ao, Y., & Sofroniew, M. V. (2014). Heterogeneity of reactive astrocytes. *Neurosci Lett, 565*, 23-29. doi:10.1016/j.neulet.2013.12.030

Bardehle, S., Kruger, M., Buggenthin, F., Schwausch, J., Ninkovic, J., Clevers, H., . . . Gotz, M. (2013). Live imaging of astrocyte responses to acute injury reveals selective juxtavascular proliferation. *Nat Neurosci, 16*(5), 580-586. doi:10.1038/nn.3371

Berger, C., Hiestand, P., Kindler-Baumann, D., Rudin, M., & Rausch, M. (2006). Analysis of lesion development during acute inflammation and remission in a rat model of experimental autoimmune encephalomyelitis by visualization of macrophage infiltration, demyelination and blood-brain barrier damage. *NMR Biomed, 19*(1), 101-107. doi:10.1002/nbm.1007

Biswas, S. K., & Mantovani, A. (2010). Macrophage plasticity and interaction with lymphocyte subsets: cancer as a paradigm. *Nat Immunol, 11*(10), 889-896. doi:10.1038/ni.1937

Bock, K. W., & Kohle, C. (2006). Ah receptor: dioxin-mediated toxic responses as hints to deregulated physiologic functions. *Biochem Pharmacol, 72*(4), 393-404. doi:10.1016/j.bcp.2006.01.017

Boitano, A. E., Wang, J., Romeo, R., Bouchez, L. C., Parker, A. E., Sutton, S. E., . . . Cooke, M. P. (2010). Aryl hydrocarbon receptor antagonists promote the expansion of human hematopoietic stem cells. *Science, 329*(5997), 1345-1348. doi:10.1126/science.1191536

Brown, A. M., & Ransom, B. R. (2007). Astrocyte glycogen and brain energy metabolism. *Glia, 55*(12), 1263-1271. doi:10.1002/glia.20557

Buffo, A., Rite, I., Tripathi, P., Lepier, A., Colak, D., Horn, A. P., . . . Gotz, M. (2008). Origin and progeny of reactive gliosis: A source of multipotent cells in the injured brain. *Proc Natl Acad Sci U S A, 105*(9), 3581-3586. doi:10.1073/pnas.0709002105

Burda, J. E., Bernstein, A. M., & Sofroniew, M. V. (2015). Astrocyte roles in traumatic brain injury. *Exp Neurol*. doi:10.1016/j.expneurol.2015.03.020

Burda, J. E., & Sofroniew, M. V. (2014). Reactive gliosis and the multicellular response to CNS damage and disease. *Neuron, 81*(2), 229-248. doi:10.1016/j.neuron.2013.12.034

Bush, T. G., Puvanachandra, N., Horner, C. H., Polito, A., Ostenfeld, T., Svendsen, C. N., . . . Sofroniew, M. V. (1999). Leukocyte infiltration, neuronal degeneration, and neurite outgrowth after ablation of scar-forming, reactive astrocytes in adult transgenic mice. *Neuron, 23*(2), 297-308.

Cekanaviciute, E., Dietrich, H. K., Axtell, R. C., Williams, A. M., Egusquiza, R., Wai, K. M., . . . Buckwalter, M. S. (2014). Astrocytic TGF-beta signaling limits inflammation and reduces neuronal damage during central nervous system Toxoplasma infection. *J Immunol, 193*(1), 139-149. doi:10.4049/jimmunol.1303284

Cekanaviciute, E., Fathali, N., Doyle, K. P., Williams, A. M., Han, J., & Buckwalter, M. S. (2014). Astrocytic transforming growth factor-beta signaling reduces subacute neuroinflammation after stroke in mice. *Glia, 62*(8), 1227-1240. doi:10.1002/glia.22675

Cheon, H., Woo, Y. S., Lee, J. Y., Kim, H. S., Kim, H. J., Cho, S., . . . Sohn, J. (2007). Signaling pathway for 2,3,7,8-tetrachlorodibenzo-p-dioxin-induced TNF-alpha production

in differentiated THP-1 human macrophages. *Exp Mol Med, 39*(4), 524-534. doi:10.1038/emm.2007.58

Chhor, V., Le Charpentier, T., Lebon, S., Ore, M. V., Celador, I. L., Josserand, J., . . . Fleiss, B. (2013). Characterization of phenotype markers and neuronotoxic potential of polarised primary microglia in vitro. *Brain Behav Immun, 32*, 70-85. doi:10.1016/j.bbi.2013.02.005

Conney, A. H. (1982). Induction of microsomal enzymes by foreign chemicals and carcinogenesis by polycyclic aromatic hydrocarbons: G. H. A. Clowes Memorial Lecture. *Cancer Res, 42*(12), 4875-4917.

Cuartero, M. I., Ballesteros, I., de la Parra, J., Harkin, A. L., Abautret-Daly, A., Sherwin, E., . . . Moro, M. A. (2014). L-kynurenine/aryl hydrocarbon receptor pathway mediates brain damage after experimental stroke. *Circulation, 130*(23), 2040-2051. doi:10.1161/CIRCULATIONAHA.114.011394

Daneman, R. (2012). The blood-brain barrier in health and disease. *Ann Neurol, 72*(5), 648-672. doi:10.1002/ana.23648

Davalos, D., Grutzendler, J., Yang, G., Kim, J. V., Zuo, Y., Jung, S., . . . Gan, W. B. (2005). ATP mediates rapid microglial response to local brain injury in vivo. *Nat Neurosci, 8*(6), 752-758. doi:10.1038/nn1472

De Winter, J. C. F. (2013). Using the Student's t-test with extremely small sample sizes. *Practical Assessment, Research & Evaluation, Vol18*(10), 1.

Denison, M. S., Soshilov, A. A., He, G., DeGroot, D. E., & Zhao, B. (2011). Exactly the same but different: promiscuity and diversity in the molecular mechanisms of action of the aryl hydrocarbon (dioxin) receptor. *Toxicol Sci, 124*(1), 1-22. doi:10.1093/toxsci/kfr218

Dever, D. P., Adham, Z. O., Thompson, B., Genestine, M., Cherry, J., Olschowka, J. A., . . . Opanashuk, L. A. (2016). Aryl hydrocarbon receptor deletion in cerebellar granule neuron precursors impairs neurogenesis. *Dev Neurobiol, 76*(5), 533-550. doi:10.1002/dneu.22330

Dimou, L., Simon, C., Kirchhoff, F., Takebayashi, H., & Gotz, M. (2008). Progeny of Olig2-expressing progenitors in the gray and white matter of the adult mouse cerebral cortex. *J Neurosci, 28*(41), 10434-10442. doi:10.1523/JNEUROSCI.2831-08.2008

Enan, E., & Matsumura, F. (1995). Evidence for a second pathway in the action mechanism of 2,3,7,8-tetrachlorodibenzo-p-dioxin (TCDD). Significance of Ah-receptor mediated activation of protein kinase under cell-free conditions. *Biochem Pharmacol, 49*(2), 249-261.

Faul, M., Xu, L., Wald, M. M., & Coronado, V. G. (2010). Traumatic Brain Injury in the United States: Emergency Department Visits, Hospitalizations and Deaths 2002–2006. *Atlanta (GA): Centers for Disease Control and Prevention, National Center for Injury Prevention and Control*.

Fernandez-Salguero, P., Pineau, T., Hilbert, D. M., McPhail, T., Lee, S. S., Kimura, S., . . . Gonzalez, F. J. (1995). Immune system impairment and hepatic fibrosis in mice lacking the dioxin-binding Ah receptor. *Science, 268*(5211), 722-726.

Firsching, R., Rickels, E., Mauer, U. M., Sakowitz, O. W., Messing-Jünger, M., Engelhard, K., . . . Schwerdtfeger, K. (2015). LEITLINIE SCHÄDEL-HIRN-TRAUMA IM ERWACHSENENALTER Update. *AWMF online*.

Fischer, J., Beckervordersandforth, R., Tripathi, P., Steiner-Mezzadri, A., Ninkovic, J., & Gotz, M. (2011). Prospective isolation of adult neural stem cells from the mouse subependymal zone. *Nat Protoc, 6*(12), 1981-1989. doi:10.1038/nprot.2011.412

Franco, R., & Fernandez-Suarez, D. (2015). Alternatively activated microglia and macrophages in the central nervous system. *Prog Neurobiol, 131*, 65-86. doi:10.1016/j.pneurobio.2015.05.003

Fukunaga, B. N., Probst, M. R., Reisz-Porszasz, S., & Hankinson, O. (1995). Identification of functional domains of the aryl hydrocarbon receptor. *J Biol Chem, 270*(49), 29270-29278.

Gadea, A., Schinelli, S., & Gallo, V. (2008). Endothelin-1 regulates astrocyte proliferation and reactive gliosis via a JNK/c-Jun signaling pathway. *J Neurosci, 28*(10), 2394-2408. doi:10.1523/JNEUROSCI.5652-07.2008

Gao, Z., Zhu, Q., Zhang, Y., Zhao, Y., Cai, L., Shields, C. B., & Cai, J. (2013). Reciprocal modulation between microglia and astrocyte in reactive gliosis following the CNS injury. *Mol Neurobiol, 48*(3), 690-701. doi:10.1007/s12035-013-8460-4

Garcia, A. D., Petrova, R., Eng, L., & Joyner, A. L. (2010). Sonic hedgehog regulates discrete populations of astrocytes in the adult mouse forebrain. *J Neurosci, 30*(41), 13597-13608. doi:10.1523/JNEUROSCI.0830-10.2010

Gasiewicz, T. A., Singh, K. P., & Bennett, J. A. (2014). The Ah receptor in stem cell cycling, regulation, and quiescence. *Ann N Y Acad Sci, 1310*, 44-50. doi:10.1111/nyas.12361

Gohlke, J. M., Stockton, P. S., Sieber, S., Foley, J., & Portier, C. J. (2009). AhR-mediated gene expression in the developing mouse telencephalon. *Reprod Toxicol, 28*(3), 321-328. doi:10.1016/j.reprotox.2009.05.067

Gordon, G. R., Mulligan, S. J., & MacVicar, B. A. (2007). Astrocyte control of the cerebrovasculature. *Glia, 55*(12), 1214-1221. doi:10.1002/glia.20543

Gotz, M., Sirko, S., Beckers, J., & Irmler, M. (2015). Reactive astrocytes as neural stem or progenitor cells: In vivo lineage, In vitro potential, and Genome-wide expression analysis. *Glia, 63*(8), 1452-1468. doi:10.1002/glia.22850

Haarmann-Stemmann, T., Bothe, H., & Abel, J. (2009). Growth factors, cytokines and their receptors as downstream targets of arylhydrocarbon receptor (AhR) signaling pathways. *Biochem Pharmacol, 77*(4), 508-520. doi:10.1016/j.bcp.2008.09.013

Hahn, M. E., Karchner, S. I., Shapiro, M. A., & Perera, S. A. (1997). Molecular evolution of two vertebrate aryl hydrocarbon (dioxin) receptors (AHR1 and AHR2) and the PAS family. *Proc Natl Acad Sci U S A, 94*(25), 13743-13748.

Hamby, M. E., Coppola, G., Ao, Y., Geschwind, D. H., Khakh, B. S., & Sofroniew, M. V. (2012). Inflammatory mediators alter the astrocyte transcriptome and calcium signaling elicited by multiple G-protein-coupled receptors. *J Neurosci, 32*(42), 14489-14510. doi:10.1523/JNEUROSCI.1256-12.2012

Hanisch, U. K., & Kettenmann, H. (2007). Microglia: active sensor and versatile effector cells in the normal and pathologic brain. *Nat Neurosci, 10*(11), 1387-1394. doi:10.1038/nn1997

Hankinson, O. (2005). Role of coactivators in transcriptional activation by the aryl hydrocarbon receptor. *Arch Biochem Biophys, 433*(2), 379-386. doi:10.1016/j.abb.2004.09.031

Hauck, S. M., Dietter, J., Kramer, R. L., Hofmaier, F., Zipplies, J. K., Amann, B., . . . Ueffing, M. (2010). Deciphering membrane-associated molecular processes in target tissue of autoimmune uveitis by label-free quantitative mass spectrometry. *Mol Cell Proteomics, 9*(10), 2292-2305. doi:10.1074/mcp.M110.001073

Heid, S. E., Pollenz, R. S., & Swanson, H. I. (2000). Role of heat shock protein 90 dissociation in mediating agonist-induced activation of the aryl hydrocarbon receptor. *Mol Pharmacol, 57*(1), 82-92.

Herrera, D. G., Garcia-Verdugo, J. M., & Alvarez-Buylla, A. (1999). Adult-derived neural precursors transplanted into multiple regions in the adult brain. *Ann Neurol, 46*(6), 867-877.

Herrmann, J. E., Imura, T., Song, B., Qi, J., Ao, Y., Nguyen, T. K., . . . Sofroniew, M. V. (2008). STAT3 is a critical regulator of astrogliosis and scar formation after spinal cord injury. *J Neurosci, 28*(28), 7231-7243. doi:10.1523/JNEUROSCI.1709-08.2008

Hestermann, E. V., & Brown, M. (2003). Agonist and chemopreventative ligands induce differential transcriptional cofactor recruitment by aryl hydrocarbon receptor. *Mol Cell Biol, 23*(21), 7920-7925.

Hu, X., Li, P., Guo, Y., Wang, H., Leak, R. K., Chen, S., . . . Chen, J. (2012). Microglia/macrophage polarization dynamics reveal novel mechanism of injury expansion after focal cerebral ischemia. *Stroke, 43*(11), 3063-3070. doi:10.1161/STROKEAHA.112.659656

Huai, W., Zhao, R., Song, H., Zhao, J., Zhang, L., Zhang, L., . . . Zhao, W. (2014). Aryl hydrocarbon receptor negatively regulates NLRP3 inflammasome activity by inhibiting NLRP3 transcription. *Nat Commun, 5*, 4738. doi:10.1038/ncomms5738

Huang, C., Sakry, D., Menzel, L., Dangel, L., Sebastiani, A., Kramer, T., . . . Schafer, M. K. (2016). Lack of NG2 exacerbates neurological outcome and modulates glial responses after traumatic brain injury. *Glia, 64*(4), 507-523. doi:10.1002/glia.22944

Huang da, W., Sherman, B. T., & Lempicki, R. A. (2009). Systematic and integrative analysis of large gene lists using DAVID bioinformatics resources. *Nat Protoc, 4*(1), 44-57. doi:10.1038/nprot.2008.211

Hughes, E. G., Kang, S. H., Fukaya, M., & Bergles, D. E. (2013). Oligodendrocyte progenitors balance growth with self-repulsion to achieve homeostasis in the adult brain. *Nat Neurosci, 16*(6), 668-676. doi:10.1038/nn.3390

Ikuta, T., Eguchi, H., Tachibana, T., Yoneda, Y., & Kawajiri, K. (1998). Nuclear localization and export signals of the human aryl hydrocarbon receptor. *J Biol Chem, 273*(5), 2895-2904.

Kettenmann, H., Hanisch, U. K., Noda, M., & Verkhratsky, A. (2011). Physiology of microglia. *Physiol Rev, 91*(2), 461-553. doi:10.1152/physrev.00011.2010

Kigerl, K. A., Gensel, J. C., Ankeny, D. P., Alexander, J. K., Donnelly, D. J., & Popovich, P. G. (2009). Identification of two distinct macrophage subsets with divergent effects causing either neurotoxicity or regeneration in the injured mouse spinal cord. *J Neurosci, 29*(43), 13435-13444. doi:10.1523/JNEUROSCI.3257-09.2009

Kimura, A., Naka, T., Nakahama, T., Chinen, I., Masuda, K., Nohara, K., . . . Kishimoto, T. (2009). Aryl hydrocarbon receptor in combination with Stat1 regulates LPS-induced inflammatory responses. *J Exp Med, 206*(9), 2027-2035. doi:10.1084/jem.20090560

Ko, H. P., Okino, S. T., Ma, Q., & Whitlock, J. P., Jr. (1996). Dioxin-induced CYP1A1 transcription in vivo: the aromatic hydrocarbon receptor mediates transactivation, enhancer-promoter communication, and changes in chromatin structure. *Mol Cell Biol, 16*(1), 430-436.

Kondo, T., & Raff, M. (2000). Oligodendrocyte precursor cells reprogrammed to become multipotential CNS stem cells. *Science, 289*(5485), 1754-1757.

Kumar, A., & Loane, D. J. (2012). Neuroinflammation after traumatic brain injury: opportunities for therapeutic intervention. *Brain Behav Immun, 26*(8), 1191-1201. doi:10.1016/j.bbi.2012.06.008

Kumar, M. B., & Perdew, G. H. (1999). Nuclear receptor coactivator SRC-1 interacts with the Q-rich subdomain of the AhR and modulates its transactivation potential. *Gene Expr, 8*(5-6), 273-286.

Laiosa, M. D., Wyman, A., Murante, F. G., Fiore, N. C., Staples, J. E., Gasiewicz, T. A., & Silverstone, A. E. (2003). Cell proliferation arrest within intrathymic lymphocyte progenitor cells causes thymic atrophy mediated by the aryl hydrocarbon receptor. *J Immunol, 171*(9), 4582-4591.

Latchney, S. E., Hein, A. M., O'Banion, M. K., DiCicco-Bloom, E., & Opanashuk, L. A. (2013). Deletion or activation of the aryl hydrocarbon receptor alters adult hippocampal neurogenesis and contextual fear memory. *J Neurochem, 125*(3), 430-445. doi:10.1111/jnc.12130

Latchney, S. E., Lioy, D. T., Henry, E. C., Gasiewicz, T. A., Strathmann, F. G., Mayer-Proschel, M., & Opanashuk, L. A. (2011). Neural precursor cell proliferation is disrupted through activation of the aryl hydrocarbon receptor by 2,3,7,8-tetrachlorodibenzo-p-dioxin. *Stem Cells Dev, 20*(2), 313-326. doi:10.1089/scd.2009.0529

Lawson, L. J., Perry, V. H., Dri, P., & Gordon, S. (1990). Heterogeneity in the distribution and morphology of microglia in the normal adult mouse brain. *Neuroscience, 39*(1), 151-170.

Lee, Y. H., Lin, C. H., Hsu, P. C., Sun, Y. Y., Huang, Y. J., Zhuo, J. H., . . . Shie, F. S. (2015). Aryl hydrocarbon receptor mediates both proinflammatory and anti-inflammatory effects in lipopolysaccharide-activated microglia. *Glia, 63*(7), 1138-1154. doi:10.1002/glia.22805

Li, Y., Innocentin, S., Withers, D. R., Roberts, N. A., Gallagher, A. R., Grigorieva, E. F., . . . Veldhoen, M. (2011). Exogenous stimuli maintain intraepithelial lymphocytes via aryl hydrocarbon receptor activation. *Cell, 147*(3), 629-640. doi:10.1016/j.cell.2011.09.025

Lois, C., & Alvarez-Buylla, A. (1994). Long-distance neuronal migration in the adult mammalian brain. *Science, 264*(5162), 1145-1148.

Luskin, M. B. (1993). Restricted proliferation and migration of postnatally generated neurons derived from the forebrain subventricular zone. *Neuron, 11*(1), 173-189.

Martin, P., & Leibovich, S. J. (2005). Inflammatory cells during wound repair: the good, the bad and the ugly. *Trends Cell Biol, 15*(11), 599-607. doi:10.1016/j.tcb.2005.09.002

Mascanfroni, I. D., Takenaka, M. C., Yeste, A., Patel, B., Wu, Y., Kenison, J. E., . . . Quintana, F. J. (2015). Metabolic control of type 1 regulatory T cell differentiation by AHR and HIF1-alpha. *Nat Med, 21*(6), 638-646. doi:10.1038/nm.3868

Mathew, A., Lindsley, T. A., Sheridan, A., Bhoiwala, D. L., Hushmendy, S. F., Yager, E. J., . . . Crawford, D. R. (2012). Degraded mitochondrial DNA is a newly identified subtype of the damage associated molecular pattern (DAMP) family and possible trigger of neurodegeneration. *J Alzheimers Dis, 30*(3), 617-627. doi:10.3233/JAD-2012-120145

Mimura, J., Yamashita, K., Nakamura, K., Morita, M., Takagi, T. N., Nakao, K., . . . Fujii-Kuriyama, Y. (1997). Loss of teratogenic response to 2,3,7,8-tetrachlorodibenzo-p-dioxin (TCDD) in mice lacking the Ah (dioxin) receptor. *Genes Cells, 2*(10), 645-654.

Mohinta, S., Kannan, A. K., Gowda, K., Amin, S. G., Perdew, G. H., & August, A. (2015). Differential regulation of Th17 and T regulatory cell differentiation by aryl hydrocarbon receptor dependent xenobiotic response element dependent and independent pathways. *Toxicol Sci, 145*(2), 233-243. doi:10.1093/toxsci/kfv046

Murray, I. A., Patterson, A. D., & Perdew, G. H. (2014). Aryl hydrocarbon receptor ligands in cancer: friend and foe. *Nat Rev Cancer, 14*(12), 801-814. doi:10.1038/nrc3846
Nimmerjahn, A., Kirchhoff, F., & Helmchen, F. (2005). Resting microglial cells are highly dynamic surveillants of brain parenchyma in vivo. *Science, 308*(5726), 1314-1318. doi:10.1126/science.1110647
Nishino, A., Suzuki, M., Ohtani, H., Motohashi, O., Umezawa, K., Nagura, H., & Yoshimoto, T. (1993). Thrombin may contribute to the pathophysiology of central nervous system injury. *J Neurotrauma, 10*(2), 167-179.
Norden, D. M., Fenn, A. M., Dugan, A., & Godbout, J. P. (2014). TGFbeta produced by IL-10 redirected astrocytes attenuates microglial activation. *Glia, 62*(6), 881-895. doi:10.1002/glia.22647
Obermeier, B., Daneman, R., & Ransohoff, R. M. (2013). Development, maintenance and disruption of the blood-brain barrier. *Nat Med, 19*(12), 1584-1596. doi:10.1038/nm.3407
Ohtake, F., Fujii-Kuriyama, Y., & Kato, S. (2009). AhR acts as an E3 ubiquitin ligase to modulate steroid receptor functions. *Biochem Pharmacol, 77*(4), 474-484. doi:10.1016/j.bcp.2008.08.034
Olsen, M. L., Khakh, B. S., Skatchkov, S. N., Zhou, M., Lee, C. J., & Rouach, N. (2015). New Insights on Astrocyte Ion Channels: Critical for Homeostasis and Neuron-Glia Signaling. *J Neurosci, 35*(41), 13827-13835. doi:10.1523/JNEUROSCI.2603-15.2015
Pekny, M., & Pekna, M. (2016). Reactive gliosis in the pathogenesis of CNS diseases. *Biochim Biophys Acta, 1862*(3), 483-491. doi:10.1016/j.bbadis.2015.11.014
Perea, G., Navarrete, M., & Araque, A. (2009). Tripartite synapses: astrocytes process and control synaptic information. *Trends Neurosci, 32*(8), 421-431. doi:10.1016/j.tins.2009.05.001
Petersen, S. L., Curran, M. A., Marconi, S. A., Carpenter, C. D., Lubbers, L. S., & McAbee, M. D. (2000). Distribution of mRNAs encoding the arylhydrocarbon receptor, arylhydrocarbon receptor nuclear translocator, and arylhydrocarbon receptor nuclear translocator-2 in the rat brain and brainstem. *J Comp Neurol, 427*(3), 428-439.
Petrulis, J. R., & Perdew, G. H. (2002). The role of chaperone proteins in the aryl hydrocarbon receptor core complex. *Chem Biol Interact, 141*(1-2), 25-40.
Poland, A., Glover, E., & Kende, A. S. (1976). Stereospecific, high affinity binding of 2,3,7,8-tetrachlorodibenzo-p-dioxin by hepatic cytosol. Evidence that the binding species is receptor for induction of aryl hydrocarbon hydroxylase. *J Biol Chem, 251*(16), 4936-4946.
Prochazkova, J., Kabatkova, M., Bryja, V., Umannova, L., Bernatik, O., Kozubik, A., . . . Vondracek, J. (2011). The interplay of the aryl hydrocarbon receptor and beta-catenin alters both AhR-dependent transcription and Wnt/beta-catenin signaling in liver progenitors. *Toxicol Sci, 122*(2), 349-360. doi:10.1093/toxsci/kfr129
Puga, A., Ma, C., & Marlowe, J. L. (2009). The aryl hydrocarbon receptor cross-talks with multiple signal transduction pathways. *Biochem Pharmacol, 77*(4), 713-722. doi:10.1016/j.bcp.2008.08.031
Quintana, F. J., Basso, A. S., Iglesias, A. H., Korn, T., Farez, M. F., Bettelli, E., . . . Weiner, H. L. (2008). Control of T(reg) and T(H)17 cell differentiation by the aryl hydrocarbon receptor. *Nature, 453*(7191), 65-71. doi:10.1038/nature06880
Rentas, S., Holzapfel, N. T., Belew, M. S., Pratt, G. A., Voisin, V., Wilhelm, B. T., . . . Hope, K. J. (2016). Musashi-2 attenuates AHR signalling to expand human haematopoietic stem cells. *Nature, 532*(7600), 508-511. doi:10.1038/nature17665

Richardson, W. D., Young, K. M., Tripathi, R. B., & McKenzie, I. (2011). NG2-glia as multipotent neural stem cells: fact or fantasy? *Neuron, 70*(4), 661-673. doi:10.1016/j.neuron.2011.05.013

Rier, S. E., Coe, C. L., Lemieux, A. M., Martin, D. C., Morris, R., Lucier, G. W., & Clark, G. C. (2001). Increased tumor necrosis factor-alpha production by peripheral blood leukocytes from TCDD-exposed rhesus monkeys. *Toxicol Sci, 60*(2), 327-337.

Robel, S., Berninger, B., & Gotz, M. (2011). The stem cell potential of glia: lessons from reactive gliosis. *Nat Rev Neurosci, 12*(2), 88-104. doi:10.1038/nrn2978

Rose, C. R., & Verkhratsky, A. (2016). Principles of sodium homeostasis and sodium signalling in astroglia. *Glia*. doi:10.1002/glia.22964

Rothhammer, V., Borucki, D. M., Tjon, E. C., Takenaka, M. C., Chao, C. C., Ardura-Fabregat, A., . . . Quintana, F. J. (2018). Microglial control of astrocytes in response to microbial metabolites. *Nature, 557*(7707), 724-728. doi:10.1038/s41586-018-0119-x

Rothhammer, V., Mascanfroni, I. D., Bunse, L., Takenaka, M. C., Kenison, J. E., Mayo, L., . . . Quintana, F. J. (2016). Type I interferons and microbial metabolites of tryptophan modulate astrocyte activity and central nervous system inflammation via the aryl hydrocarbon receptor. *Nat Med, 22*(6), 586-597. doi:10.1038/nm.4106

Ryu, J. K., Davalos, D., & Akassoglou, K. (2009). Fibrinogen signal transduction in the nervous system. *J Thromb Haemost, 7 Suppl 1*, 151-154. doi:10.1111/j.1538-7836.2009.03438.x

Schmidt, J. V., Su, G. H., Reddy, J. K., Simon, M. C., & Bradfield, C. A. (1996). Characterization of a murine Ahr null allele: involvement of the Ah receptor in hepatic growth and development. *Proc Natl Acad Sci U S A, 93*(13), 6731-6736.

Seidenfaden, R., Desoeuvre, A., Bosio, A., Virard, I., & Cremer, H. (2006). Glial conversion of SVZ-derived committed neuronal precursors after ectopic grafting into the adult brain. *Mol Cell Neurosci, 32*(1-2), 187-198. doi:10.1016/j.mcn.2006.04.003

Seri, B., Garcia-Verdugo, J. M., McEwen, B. S., & Alvarez-Buylla, A. (2001). Astrocytes give rise to new neurons in the adult mammalian hippocampus. *J Neurosci, 21*(18), 7153-7160.

Shirakawa, H., Sakimoto, S., Nakao, K., Sugishita, A., Konno, M., Iida, S., . . . Kaneko, S. (2010). Transient receptor potential canonical 3 (TRPC3) mediates thrombin-induced astrocyte activation and upregulates its own expression in cortical astrocytes. *J Neurosci, 30*(39), 13116-13129. doi:10.1523/JNEUROSCI.1890-10.2010

Simon, C., Gotz, M., & Dimou, L. (2011). Progenitors in the adult cerebral cortex: cell cycle properties and regulation by physiological stimuli and injury. *Glia, 59*(6), 869-881. doi:10.1002/glia.21156

Sirko, S., Behrendt, G., Johansson, P. A., Tripathi, P., Costa, M., Bek, S., . . . Gotz, M. (2013). Reactive glia in the injured brain acquire stem cell properties in response to sonic hedgehog. [corrected]. *Cell Stem Cell, 12*(4), 426-439. doi:10.1016/j.stem.2013.01.019

Smith, B. W., Rozelle, S. S., Leung, A., Ubellacker, J., Parks, A., Nah, S. K., . . . Murphy, G. J. (2013). The aryl hydrocarbon receptor directs hematopoietic progenitor cell expansion and differentiation. *Blood, 122*(3), 376-385. doi:10.1182/blood-2012-11-466722

Soares, L., Seroogy, C., Skrenta, H., Anandasabapathy, N., Lovelace, P., Chung, C. D., . . . Fathman, C. G. (2004). Two isoforms of otubain 1 regulate T cell anergy via GRAIL. *Nat Immunol, 5*(1), 45-54. doi:10.1038/ni1017

Stence, N., Waite, M., & Dailey, M. E. (2001). Dynamics of microglial activation: a confocal time-lapse analysis in hippocampal slices. *Glia, 33*(3), 256-266.
Stockinger, B., Di Meglio, P., Gialitakis, M., & Duarte, J. H. (2014). The aryl hydrocarbon receptor: multitasking in the immune system. *Annu Rev Immunol, 32*, 403-432. doi:10.1146/annurev-immunol-032713-120245
Sulentic, C. E., & Kaminski, N. E. (2011). The long winding road toward understanding the molecular mechanisms for B-cell suppression by 2,3,7,8-tetrachlorodibenzo-p-dioxin. *Toxicol Sci, 120 Suppl 1*, S171-191. doi:10.1093/toxsci/kfq324
Tan, A. M., Zhang, W., & Levine, J. M. (2005). NG2: a component of the glial scar that inhibits axon growth. *J Anat, 207*(6), 717-725. doi:10.1111/j.1469-7580.2005.00452.x
Tian, Y. (2009). Ah receptor and NF-kappaB interplay on the stage of epigenome. *Biochem Pharmacol, 77*(4), 670-680. doi:10.1016/j.bcp.2008.10.023
Veldhoen, M., Hirota, K., Westendorf, A. M., Buer, J., Dumoutier, L., Renauld, J. C., & Stockinger, B. (2008). The aryl hydrocarbon receptor links TH17-cell-mediated autoimmunity to environmental toxins. *Nature, 453*(7191), 106-109. doi:10.1038/nature06881
Walisser, J. A., Glover, E., Pande, K., Liss, A. L., & Bradfield, C. A. (2005). Aryl hydrocarbon receptor-dependent liver development and hepatotoxicity are mediated by different cell types. *Proc Natl Acad Sci U S A, 102*(49), 17858-17863. doi:10.1073/pnas.0504757102
Wang, Q., Chen, J., Ko, C. I., Fan, Y., Carreira, V., Chen, Y., . . . Puga, A. (2013). Disruption of aryl hydrocarbon receptor homeostatic levels during embryonic stem cell differentiation alters expression of homeobox transcription factors that control cardiomyogenesis. *Environ Health Perspect, 121*(11-12), 1334-1343. doi:10.1289/ehp.1307297
WorldHealthOrganization. (2006). Neurological Disorders: Public Health Challenges. *WHO Press*.
Wu, R., Zhang, L., Hoagland, M. S., & Swanson, H. I. (2007). Lack of the aryl hydrocarbon receptor leads to impaired activation of AKT/protein kinase B and enhanced sensitivity to apoptosis induced via the intrinsic pathway. *J Pharmacol Exp Ther, 320*(1), 448-457. doi:10.1124/jpet.106.111773
Xie, G., Peng, Z., & Raufman, J. P. (2012). Src-mediated aryl hydrocarbon and epidermal growth factor receptor cross talk stimulates colon cancer cell proliferation. *Am J Physiol Gastrointest Liver Physiol, 302*(9), G1006-1015. doi:10.1152/ajpgi.00427.2011
Xu, G., Li, Y., Yoshimoto, K., Wu, Q., Chen, G., Iwata, T., . . . Nie, X. (2014). 2,3,7,8-Tetrachlorodibenzo-p-dioxin stimulates proliferation of HAPI microglia by affecting the Akt/GSK-3beta/cyclin D1 signaling pathway. *Toxicol Lett, 224*(3), 362-370. doi:10.1016/j.toxlet.2013.11.003
Yeramian, A., Martin, L., Serrat, N., Arpa, L., Soler, C., Bertran, J., . . . Celada, A. (2006). Arginine transport via cationic amino acid transporter 2 plays a critical regulatory role in classical or alternative activation of macrophages. *J Immunol, 176*(10), 5918-5924.
Yu, J. S., & Cui, W. (2016). Proliferation, survival and metabolism: the role of PI3K/AKT/mTOR signalling in pluripotency and cell fate determination. *Development, 143*(17), 3050-3060. doi:10.1242/dev.137075
Zamanian, J. L., Xu, L., Foo, L. C., Nouri, N., Zhou, L., Giffard, R. G., & Barres, B. A. (2012). Genomic analysis of reactive astrogliosis. *J Neurosci, 32*(18), 6391-6410. doi:10.1523/JNEUROSCI.6221-11.2012

Zhang, Q., Raoof, M., Chen, Y., Sumi, Y., Sursal, T., Junger, W., . . . Hauser, C. J. (2010). Circulating mitochondrial DAMPs cause inflammatory responses to injury. *Nature, 464*(7285), 104-107. doi:10.1038/nature08780

Zhu, X., Bergles, D. E., & Nishiyama, A. (2008). NG2 cells generate both oligodendrocytes and gray matter astrocytes. *Development, 135*(1), 145-157. doi:10.1242/dev.004895

Zhu, X., Hill, R. A., Dietrich, D., Komitova, M., Suzuki, R., & Nishiyama, A. (2011). Age-dependent fate and lineage restriction of single NG2 cells. *Development, 138*(4), 745-753. doi:10.1242/dev.047951

7 Curriculum vitae

Ausbildung

Mai 2011	Allgemeine Hochschulreife am St.-Irmengard-Gymnasium Garmisch-Partenkirchen (1,0)
2011-2013	Vorklinischer Studienabschnitt im Fach Humanmedizin an der LMU München
August 2013	1. Staatsexamen
Seit Oktober 2013	Klinischer Studienabschnitt im Fach Humanmedizin an der TU München
April 2017	2. Staatsexamen
Mai 2017 – April 2018	Praktisches Jahr
	1. Tertial: Chirurgie am Kantonsspital Luzern 2. Tertial: Pathologie an der TU München 3. Tertial: Innere Medizin am Klinikum Landshut-Achdorf
Juli 2018	3. Staatsexamen und Erlangen der Approbation (Note 1,0)

Erfahrungen

Seit März 2014	Dissertation am Institut für Stammzellforschung des Helmholtz-Zentrums München unter Leitung von Frau Prof. Magdalena Götz
Oktober 2015 – März 2017	Arbeit als Studentische Hilfskraft am Institut für Humangenetik der TU München Betreuung der Biodatenbanken MitoNET und TIRCON
August – September 2016	Forschungspraktikum am Institute of basic medical sciences der Universität Oslo (Vervake Lab)
Februar / März 2013	Kursassistenz im Biologie-Praktikum für Mediziner an der LMU München, Teilgebiet Genetik
März 2015	Hausarzt-Famulatur bei Dr. med. Wolfgang Blank, Gemeinschaftspraxis im Bayerwald, Kirchberg im Wald
August 2015	Famulatur in der Chirurgie des Luzerner Kantonsspitals
September 2015	Famulatur in der plastischen Chirurgie der Unfallklinik Murnau
Februar 2016	Famulatur in der HNO des Klinikums Rechts der Isar, TU München

Förderung

Juni 2012 – Juni 2018	Studienstiftung des deutschen Volkes

8 Acknowledgements

My thanks go first and foremost to my supervisors Prof. Dr. Jovica Ninkovic and Prof. Dr. Magdalena Götz for leaving the topic of the dissertation, exchange of ideas, impulses and encouragement. I cannot thank them enough for their expertise and support!

In addition, many thanks to all the other laboratory members, especially to Andrea Steiner-Mezzadri, who introduced me with much patience to all the various methods, as well as to Prof. Dr. Svetlana Sirko, who taught me the art of neurosphere cultivation.

I would also like to thank all my fellow doctoral students for the great time in and around the lab life.

Last but not least, I thank all my friends, my family and my boyfriend Sebastian Remke for supporting me, for always being proud of my work and for reminding me, that there is also a life outside of animal facilities, cell cultures and confocal microscopes.

9 Eidesstattliche Versicherung

Reiser, Marianne

Ich erkläre hiermit an Eides statt, dass ich die vorliegende Dissertation mit dem Thema

Role of aryl hydrocarbon receptor signalling in reactive gliosis

selbständig verfasst, mich außer der angegebenen keiner weiteren Hilfsmittel bedient und alle Erkenntnisse, die aus dem Schrifttum ganz oder annähernd übernommen sind, als solche kenntlich gemacht und nach ihrer Herkunft unter Bezeichnung der Fundstelle einzeln nachgewiesen habe.

Ich erkläre des Weiteren, dass die hier vorgelegte Dissertation nicht in gleicher oder in ähnlicher Form bei einer anderen Stelle zur Erlangung eines akademischen Grades eingereicht wurde.

München, 20. Dezember 2019	Marianne Reiser
Ort, Datum	Unterschrift Doktorandin/Doktorand